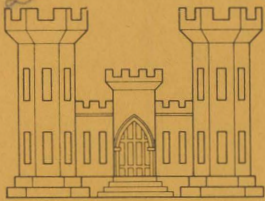
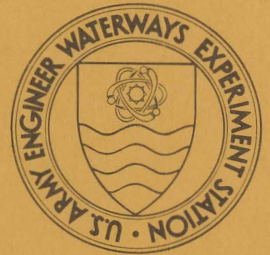


A 1  
W34  
NO. D-77-6  
APP. A  
COP. 22

US-CE-C Property of the United States Government



# DREDGED MATERIAL RESEARCH PROGRAM



TECHNICAL REPORT D-77-6

## AQUATIC DISPOSAL FIELD INVESTIGATIONS EATONS NECK DISPOSAL SITE LONG ISLAND SOUND

### APPENDIX A: INVESTIGATION OF THE HYDRAULIC REGIME AND THE PHYSICAL CHARACTERISTICS OF BOTTOM SEDIMENTATION

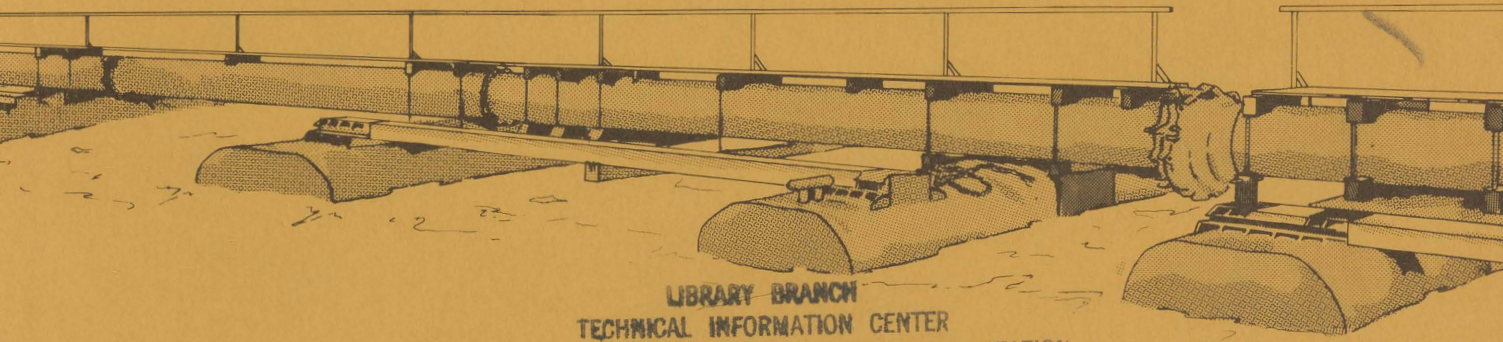
by

Henry Bokuniewicz, Michael Dowling, Jeffrey Gebert  
Robert Gordon, Peter Kaminsky, Carol Pilbeam, Catherine Tuttle

Department of Geology and Geophysics  
Yale University  
New Haven, Connecticut

September 1977  
Final Report

Approved For Public Release; Distribution Unlimited



LIBRARY BRANCH  
TECHNICAL INFORMATION CENTER  
U.S. ARMY ENGINEER WATERWAYS EXPERIMENT STATION  
VICKSBURG, MISSISSIPPI

Prepared for Office, Chief of Engineers, U. S. Army  
Washington, D. C. 20314

Monitored by Environmental Effects Laboratory  
U. S. Army Engineer Waterways Experiment Station  
P. O. Box 631, Vicksburg, Miss. 39180

Under Contract No. DACW51-75-C-0008  
(DMRP Work Unit 1A06A)

AQUATIC DISPOSAL FIELD INVESTIGATIONS  
EATONS NECK DISPOSAL SITE  
LONG ISLAND SOUND

- Appendix A: Investigation of the Hydraulic Regime and the Physical Characteristics of Bottom Sedimentation
- Appendix B: Water-Quality Parameters and Physicochemical Sediment Parameters
- Appendix C: Predisposal Baseline Conditions of Benthic Assemblages
- Appendix D: Predisposal Baseline Conditions of Demersal Fish Assemblages
- Appendix E: Predisposal Baseline Conditions of Zooplankton Assemblages
- Appendix F: Predisposal Baseline Conditions of Phytoplankton Assemblages

Destroy this report when no longer needed. Do not return  
it to the originator.



3 5925 00350 6349



DEPARTMENT OF THE ARMY  
WATERWAYS EXPERIMENT STATION, CORPS OF ENGINEERS  
P. O. BOX 631  
VICKSBURG, MISSISSIPPI 39180

IN REPLY REFER TO: WESYV

2 September 1977

SUBJECT: Transmittal of Technical Report D-77-6 (Appendix A)

TO: All Report Recipients

1. The technical report transmitted herewith represents the results of one of several research efforts (Work Units) undertaken as part of Task 1A, Aquatic Disposal Field Investigations of the Corps of Engineers' Dredged Material Research Program. Task 1A is a part of the Environmental Impacts and Criteria Development Project (EICDP), which has as a general objective determination of the magnitude and extent of effects of disposal sites on organisms and the quality of surrounding water, and the rate, diversity, and extent such sites are recolonized by benthic flora and fauna. The study reported on herein was an integral part of a series of research contracts jointly developed to achieve the EICDP general objective at the Eatons Neck Disposal Site, one of five sites located in several geographical regions of the United States. Consequently, this report presents results and interpretations of but one of several closely interrelated efforts and should be used only in conjunction with and consideration of the other related reports for this site.

2. This report, Appendix A: Investigation of the Hydraulic Regime and the Physical Characteristics of Bottom Sedimentation, is one of six contractor-prepared reports that are appended to the Waterways Experiment Station Technical Report D-77-6 entitled: Aquatic Disposal Field Investigations, Eatons Neck Disposal Site, Long Island Sound. The titles of all contractor-prepared appendices of this series are listed on the inside front cover of this report. The technical report provides additional results, interpretations, and conclusions not found in the individual contractor reports and provides a comprehensive summary and synthesis overview of the entire project.

3. The purpose of this study, conducted as Work Unit 1A06A, was to identify the baseline hydraulic regime, the meteorology, and the physical nature of bottom sedimentation in the Eatons Neck Disposal Site and the surrounding area. The report includes a discussion of the distribution of sediments and the distribution of currents that affect sediment erosion, transportation, and deposition within and in the vicinity of the site. The sediment distribution was determined through grab sampling, subbottom profiling, bottom photography, and coring of the area. Tidal and nontidal

WESYV

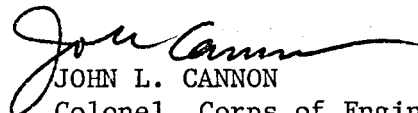
2 September 1977

SUBJECT: Transmittal of Technical Report D-77-6 (Appendix A)

circulation patterns were delineated with current meters, wave gages, and tide gages. Temperature-salinity profiles, suspended sediment sampling, and investigations of the interaction at the sediment-water interface were also made to obtain data needed to determine the movement of sediment within the site.

4. A conclusion of this report, based on the data presented, was that the Eatons Neck Disposal Site was an acceptable site for use as a dredged material repository where physical environmental effects were negligible, resulting in minimal loss of material from the site.

5. The baseline evaluations at all of the EICDP field sites were developed to determine the base or ambient physical, chemical, and biological conditions at the respective sites from which to determine impacts due to the subsequent disposal operations. Where the dump sites had historical usage, the long-term impacts of dumping at these sites could also be ascertained. Controlled disposal operations at the Eatons Neck site, however, did not occur due to local opposition to research activities and even though the Eatons Neck project was terminated after completion of the baseline, this information will be useful in evaluating the impacts of past disposal at this site. The results of this study are important in determining placement of dredged material for open-water disposal. Referenced studies, as well as the ones summarized in this report, will aid in determining the optimum disposal conditions and site selection for either the dispersion of the material from the dump site or for its retention within the confines of the site, whichever is preferred for maximum environmental protection at a given site.



JOHN L. CANNON  
Colonel, Corps of Engineers  
Commander and Director

1944

...

...

...

...

...

Unclassified

SECURITY CLASSIFICATION OF THIS PAGE (When Data Entered)

REPORT DOCUMENTATION PAGE		READ INSTRUCTIONS BEFORE COMPLETING FORM	
1. REPORT NUMBER Technical Report D-77-6	2. GOVT ACCESSION NO.	3. RECIPIENT'S CATALOG NUMBER	
4. TITLE (and Subtitle) AQUATIC DISPOSAL FIELD INVESTIGATIONS, EATONS NECK DISPOSAL SITE, LONG ISLAND SOUND; APP A: INVESTIGATION OF THE HYDRAULIC REGIME AND THE PHYSICAL CHARACTERISTICS OF BOTTOM SEDIMENTATION		5. TYPE OF REPORT & PERIOD COVERED Final report	
		6. PERFORMING ORG. REPORT NUMBER	
7. AUTHOR(s) Henry Bokuniewicz, Catherine Bultman, Michael Dowling, Jeffrey Gebert, Robert Gordon, Peter Kaminsky, Carol Pilbeam		8. CONTRACT OR GRANT NUMBER(s) Contract No. DACW51-75-C-0008	
9. PERFORMING ORGANIZATION NAME AND ADDRESS Yale University Department of Geology and Geophysics New Haven, Connecticut 06520		10. PROGRAM ELEMENT, PROJECT, TASK AREA & WORK UNIT NUMBERS DMRP Work Unit 1A06A	
11. CONTROLLING OFFICE NAME AND ADDRESS Office, Chief of Engineers, U. S. Army Washington, D. C. 20314		12. REPORT DATE September 1977	
		13. NUMBER OF PAGES 195	
14. MONITORING AGENCY NAME & ADDRESS (if different from Controlling Office) U. S. Army Engineer Waterways Experiment Station Environmental Effects Laboratory P. O. Box 631, Vicksburg, Mississippi 39180		15. SECURITY CLASS. (of this report) Unclassified	
		15a. DECLASSIFICATION/DOWNGRADING SCHEDULE	
16. DISTRIBUTION STATEMENT (of this Report)  Approved for public release; distribution unlimited.			
17. DISTRIBUTION STATEMENT (of the abstract entered in Block 20, if different from Report)			
18. SUPPLEMENTARY NOTES  Appendixes A-E were prepared on microfiche and are enclosed in an envelope in the back cover of this report.			
19. KEY WORDS (Continue on reverse side if necessary and identify by block number)			
Benthic fauna		Sediment sampling	
Disposal areas		Sediment transport	
Dredged material disposal		Sedimentation	
Eatons Neck disposal area		Waste water disposal	
Field Investigations		Water quality	
20. ABSTRACT (Continue on reverse side if necessary and identify by block number)			
<p>The major goal of the Eatons Neck disposal site field investigation was to evaluate the effects of aquatic disposal of dredged material on organisms and water quality, including the significance of physical, chemical, and biological factors that influence the rate of disposal site recolonization by benthic animals.</p> <p>A comprehensive research program was planned and conducted at Eatons</p>			
(Continued)			

20. ABSTRACT (Continued).

Neck in order to evaluate cause and effect relationships associated with the impacts of open-water disposal.

This volume of the study presents the investigation of the hydraulic regime and the physical characteristics of bottom sedimentation.

Acoustic-reflection profiles and mechanical analysis of core and grab samples of the bottom were used to define the sediment-type distribution of the area. Results were confirmed by penetrometer tests and bottom and profile photographs.

Since the study was made to determine the possible movement of dredged material placed on the bottom, the currents were studied using both averaging and instantaneous recording current meters.

The study concluded that there was no physical evidence of significant dispersion of dredged material from the Eatons Neck disposal site; no previously deposited material was detected outside the designated disposal area.

Appendix A details navigation procedures and permanent buoy construction used in the study. Appendix B are the 16 reflection-profile photos. Sediment analysis data are presented in Appendix C. Appendix D shows the profile camera photos and Appendix E shows the bottom photos. Appendixes A-E were prepared on microfiche and are enclosed in an envelope in the back cover of this report.

THE CONTENTS OF THIS REPORT ARE NOT TO  
BE USED FOR ADVERTISING, PUBLICATION,  
OR PROMOTIONAL PURPOSES. CITATION OF  
TRADE NAMES DOES NOT CONSTITUTE AN  
OFFICIAL ENDORSEMENT OR APPROVAL OF  
THE USE OF SUCH COMMERCIAL PRODUCTS.





## EXECUTIVE SUMMARY

The hydraulic and sedimentological regimes at the Eatons Neck disposal site were studied from 1 July 1974 to 30 September 1975.

Acoustic-reflection profiles and mechanical analysis of core and grab samples of the bottom were used to define the sediment-type distribution of the area. The disposal site was found to be predominantly silty sand with a sand and gravel shoal to the northeast. This was confirmed by penetrometer tests and bottom and profile photographs. Bottom and profile photographs also show an abundance of fecal pellets and marine life. The southern part of the disposal area was found to contain large amounts of material of anthropogenic origin.

The currents were studied using both averaging and instantaneous recording current meters. Since the study was made to determine the possible movement of dredged material placed on the bottom, most meters were placed 2 m above the bottom. Within the disposal area, a vertical array of four current meters was established. These meters operated simultaneously to examine the vertical current structure.

The tidal currents are rotary, counterclockwise. This is a consequence of the Coriolis force acting on the resonant co-oscillating tide of the embayment. The semi-major axis of the tidal ellipse is oriented in approximately the east-west direction. The semi-minor axis is about 2/10 of the semi-major axis. The maximum tidal velocity is about 40 cm/sec at 2 m above the bottom. The current flow is generally faster at the surface than near the bottom. The tidal currents are significantly influenced by shallow-water harmonics in the

study area.

The flow of the tidal stream is not steady, but is subject to appreciable fluctuations. The intensity of the velocity fluctuations becomes greater during periods of high wind stress. A correspondingly greater resuspension of bottom sediment was observed to occur during these periods. However, transmissometer measurements show that the resuspension of bottom sediment was limited to a thin, about 1 mm, layer at the sediment-water interface.

Two meters above the bottom, the current flow was generally to the west or southwest, parallel to the shore. This flow was identified as estuarine circulation. Salinity measurements confirm that density differences drive this circulation: outward flow of less saline top water and inward (westward) flow of more saline bottom water. The speed of the mean current was found to be less than 6 cm/sec. None of the current meter records from the study area show shoreward drift. Results from the vertical array show that the wind has a strong influence on the direction of the current in only the upper few meters of water.

A wave recorder was placed on the bottom on a gravel shoal in the northeast corner of the study area for 38 days during the stormiest part of the year. From the analysis of the resultant wave record it was concluded that only very strong winds from the east generate waves of sufficiently long wavelength to cause wave-induced movement of water over the bottom in the study area. Disturbance of the bottom by waves was shown to be small in comparison to that caused by the tidal stream.

In conclusion, there is no physical evidence of significant dispersion of dredged material from the Eatons Neck disposal site; no previously disposed material was detected outside the designated disposal area. Transmissometer measurements indicate that the exchange of sediments with the surrounding sea floor occurs only for silt and clay-sized particles found in a thin layer at the sediment-water interface. The mean currents were found to be predominantly westward and not toward either the Connecticut or Long Island shore. The dominant energy source for sediment transport was found to be the tide; wind driven waves were found to have little appreciable effect on the bottom. The Eatons Neck disposal site was found to be well chosen to be a dredged material repository where sediment dispersion will be minimal.

## PREFACE

A study of the sedimentary and hydraulic processes in Long Island Sound near Greens Ledge, Connecticut, and Eatons Neck, New York, was made as part of the aquatic disposal study in the Office, Chief of Engineers, Dredged Material Research Program (DMRP) of the U. S. Army Engineer Waterways Experiment Station (WES) in Vicksburg, Mississippi. This study was performed under Contract No. DACW51-75-C-0008 to Yale University, Work Unit 1A06A. The Contracting Office was COL Thomas C. Hunter, CE, U. S. Army Engineer District, New York.

This report was written by Henry Bokuniewicz, Michael Dowling, Jeffrey Gebert, Robert Gordon, Peter Kaminsky, Carol Pilbeam, and Catherine Tuttle, all of the Department of Geology and Geophysics, Yale University. Many of the measurements reported were made by Matthew Reed and Robert Kerley, profile photographs were taken by Robert Wells, and the typing of this report was done by Wanda Stark, all of the Department of Geology and Geophysics, Yale University. Barry Holliday, of the Environmental Resources Division, EEL, WES, and William Sacco, of the Audio-Visual Department, Yale University, made underwater photographs of the study site. Barbara Ford, of Branford, Connecticut, read current meter records. William F. Muszak, of the U. S. Army Corps of Engineers, New York District, supplied survey and tidal data.

The study was conducted under the direction of the following EEL personnel: The contract was managed by Mr. J. R. Reese,

Environmental Monitoring and Assessment Branch, under the supervision of Mr. R. C. Solomon, Branch Chief, and Dr. C. J. Kirby, Chief, Environmental Resources Division. The study was under the general supervision of Dr. R. M. Engler, Environmental Impacts and Criteria Development Project Manager, and Dr. John Harrison, Chief, EEL.

The Directors of WES during the conduct of the study and preparation of the report were COL G. H. Hilt, CE, and COL J. L. Cannon, CE. Technical Director was Mr. F. R. Brown.

## CONTENTS

	<u>Page</u>
EXECUTIVE SUMMARY.....	1
PREFACE.....	4
PART I: INTRODUCTION.....	8
PART II: METHODS USED.....	13
Navigation Procedures.....	13
Sediments and Bottom Structure.....	13
Hydraulic Regime.....	22
Sediment Resuspension.....	29
Disturbance of the Bottom by Waves.....	30
Salinity Observations.....	32
PART III: RESULTS AND DISCUSSION.....	33
Literature Review.....	33
Sediments and Bottom Structure.....	34
Hydraulic Regime.....	42
Sediment Resuspension.....	63
Disturbance of the Bottom by Waves.....	69
PART IV: CONCLUSIONS.....	72
REFERENCES.....	74
TABLES 1-9.....	78
PLATES 1-32.....	92
APPENDIX A: NAVIGATION*	
APPENDIX B: REFLECTION-PROFILE PHOTOS	
APPENDIX C: CORE AND GRAM SAMPLE DATA	
APPENDIX D: PROFILE CAMERA PHOTOS	
APPENDIX E: BOTTOM PHOTOS	

---

\* Appendixes A-E were prepared on microfiche and are enclosed in an envelope in the back cover of this report.

CONVERSION FACTORS, U. S. CUSTOMARY TO METRIC (SI)

UNITS OF MEASUREMENT

U. S. customary units of measurement used in this report can be converted to metric (SI) units as follows:

<u>Multiply</u>	<u>By</u>	<u>To Obtain</u>
inches	2.54	centimetres
feet	0.3048	metres
miles (U. S. statute)	1.609344	kilometres
fathoms	1.8288	metres
pounds (force) per square inch	68.9476	millibars
pounds (mass) per cubic foot	16.0185	kilograms per cubic metre
knots (international)	0.514444	metres per second



INVESTIGATION OF THE HYDRAULIC REGIME AND THE PHYSICAL  
CHARACTERISTICS OF BOTTOM SEDIMENTATION IN THE EATONS NECK DISPOSAL SITE

PART I: INTRODUCTION

1. This report deals with the physical factors relevant to the use of a site near Eatons Neck in Long Island Sound as a repository for dredged material. It presents results obtained during the period 1 July 1974 to 30 September 1975. The Eatons Neck disposal site, centered near  $41^{\circ}00'N$ ,  $73^{\circ}26'W$ , has been used for the disposal of a wide range of waste materials over a period of a great many years. Examination of the site and its surrounding area was relied upon to define the consequences of past disposal operations and to indicate the consequences of future use.

2. At the start of this study, the area of specific interest was defined to be the designated Eatons Neck disposal site plus an extension running approximately one-half mile\* to the east. Later, this area was redefined to include the Eatons Neck disposal site plus an extension one mile to the north. In March 1975 two sites, Eatons Neck North (EN-N) and South (EN-S) Experimental Sites, were designated as possible locations for future disposal operations and, in anticipation of these, were studied in detail. Figures 1a and 1b show the location of the study area, the bounds of the Eatons Neck disposal site

---

\* A table of factors for converting from U. S. customary units of measurement to Metric (SI) units of measurements can be found on page 7.

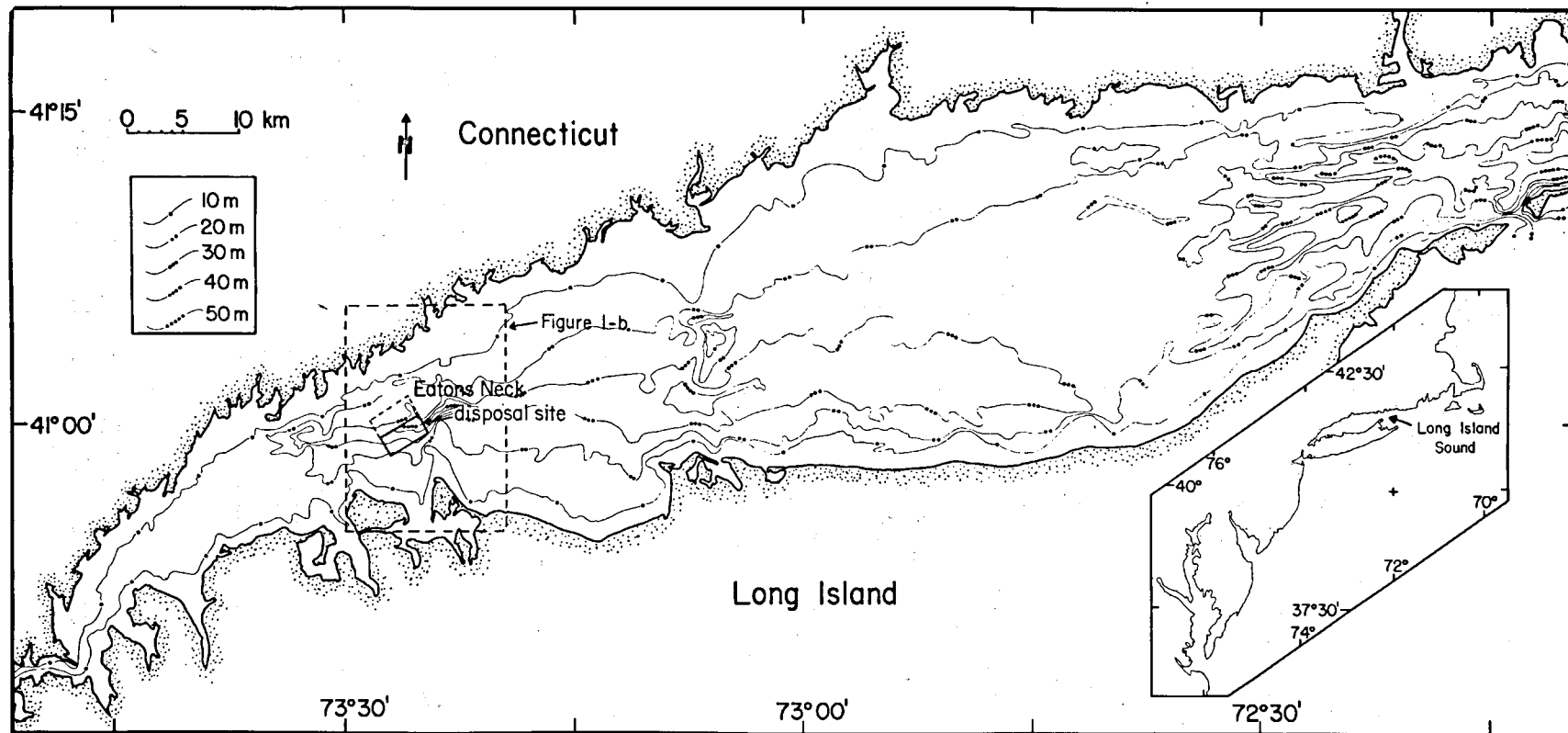


Figure 1a. Location of the study area in Long Island Sound

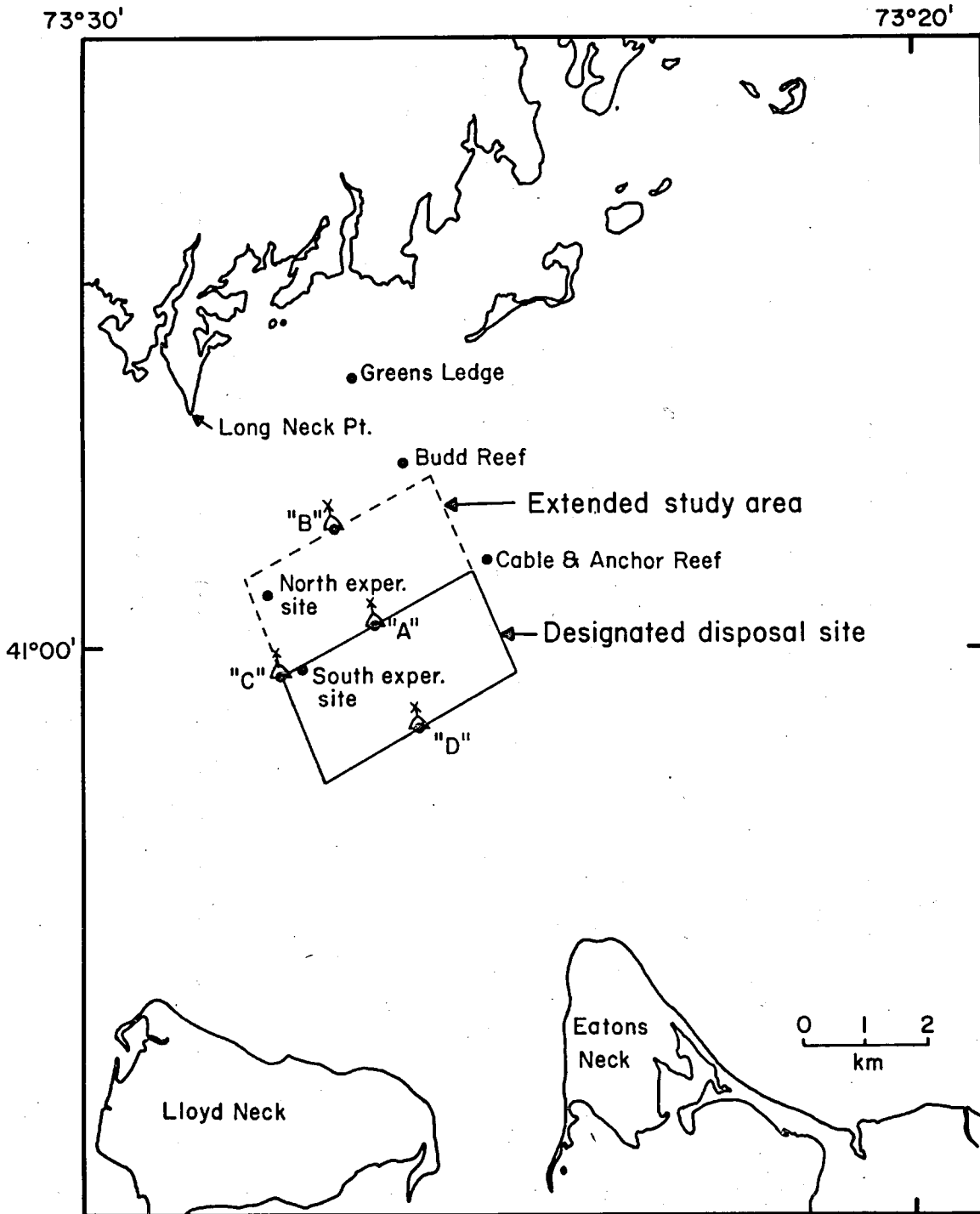


Figure 1b. Location map of Eatons Neck study area showing instrument stations and local landmarks

as indicated on navigational charts, and the extent of the area covered in the studies reported herein.

3. The overall objectives of this study included the following:

- a. To define the character and distribution of the natural sediments occurring at the Eatons Neck disposal site and its surrounding area and to relate these to the previously identified processes of sedimentation in Long Island Sound.
- b. To locate the area of the bottom that can be identified as now covered with material of anthropogenic origin and, if possible, estimate its volume.
- c. To examine the sediment-water interface at the disposal site and compare its constitution and structure with that of the surrounding sea floor.
- d. To determine the hydraulic characteristics of the water flow through the study area, including the effects of storms.
- e. To relate these flow characteristics to the active processes of sediment transport and to evaluate the stability of material placed on the bottom at the disposal site.

4. Both the plan of the research and the methods of observation used in this research were developed on the basis of recent experience with studies of the environmental consequences of the open-water disposal of dredged material. Such studies have been performed by Saila and his colleagues for a site in Rhode Island Sound (results mainly in unpublished reports to the U. S. Army Engineer Division, New England), by Nittrouer and Sternberg<sup>1</sup> in Washington, and Mauer et al.<sup>2</sup> in Delaware Bay. Most directly relevant to the present project are the studies of the New Haven disposal site now being completed by groups at the University of Connecticut and at Yale University. These are documented in an extensive series of unpublished reports to the

New England Division.

5. In the first part of this study, acoustic-reflection profiling and mechanical analyses of bottom samples were used both to define the physical character of the sediments in the study area and to define those areas where material of anthropogenic origin had been placed in the past. Areas of the disposal site were then selected for detailed examination by underwater photography. The movement of water through the study area was measured with both horizontal and vertical arrays of current meters. An attempt was made to maintain a nearly continuous record of the current at one station throughout the study period. All current meter records were analyzed to show the tidal, net drift, and fluctuating components of the flow. Response of the study area to storms was studied with a wave recorder as well as with the current meters. The interaction between the sediments on the bottom and the water flow was shown by turbidity observations.

## PART II: METHODS USED

### Navigation Procedures

6. Although disposal of dredged material has occurred over a considerable area of the study site, individual features of interest on the bottom are often quite small. Furthermore, changes in the character of naturally occurring sediments are found over very small distances. Consequently, a high standard of navigational accuracy was required for all field work in this study. There were many shoreside landmarks available at the site making it possible to fix navigational positions to an accuracy of a few feet with horizontal angles measured with a sextant or surveying quintant from the boat. All observations were made according to the procedures defined in the Admiralty Manual of Hydrographic Surveying<sup>3</sup>. To attain the full accuracy of the observations, positions must be calculated from the measured angles. To save this labor, precomputed plotting sheets were prepared according to the method described in Appendix A. Where a lesser degree of accuracy was required, as in the placement of current meters, positions were plotted directly on published charts with the aid of a station pointer.

### Sediments and Bottom Structure

#### Identification of sediment type

7. First phase. The examination of sediments of the Eatons Neck disposal site was conducted in order to identify the principal sediment

types and to define their distribution in the study area. In the initial phase of the sediment study, 16 north-south acoustic-reflection profiles (Figure 2) totalling 80 nautical miles, were run between the longitude of  $73^{\circ}20'W$  and  $72^{\circ}32'W$ . Table 1 gives the start and end points for each profile. A Raytheon RTT 1000 profiling system was used. This unit generates two types of acoustic pulse, one of 200 kHz frequency to provide high resolution of the bottom topography and one of 7 kHz, which penetrates the sediments to detect sub-bottom structures.

8. The sediments of the disposal site and surrounding area were broadly classified on the basis of reflection profiles as (a) sand and/or gravel, (b) silt with varying sand content, or (c) disposed material using the interpretations given in Bokuniewicz, Gebert, and Gordon<sup>4</sup>. This classification is possible because reflection of the acoustic signals from the bottom varies with the percentage of sand in the sediment; sediment with 80% or higher sand content is acoustically opaque.

9. Photos of the 16 acoustic-reflection profiles are presented in Appendix B. Subsequent to the decision to move the experimental site center to  $41^{\circ}00'30"N$ ,  $73^{\circ}29'00"W$ , three additional profiles were made in that area to improve the density of bathymetric and sub-bottom data. These profiles are shown as 17-19 on Figure 2. (Profiles 1, 15, and 16 are off the chart, Figure 2.)

10. Second phase. The second phase of the study involved the collection of 108 sediment samples within this same area (Figure 3) by

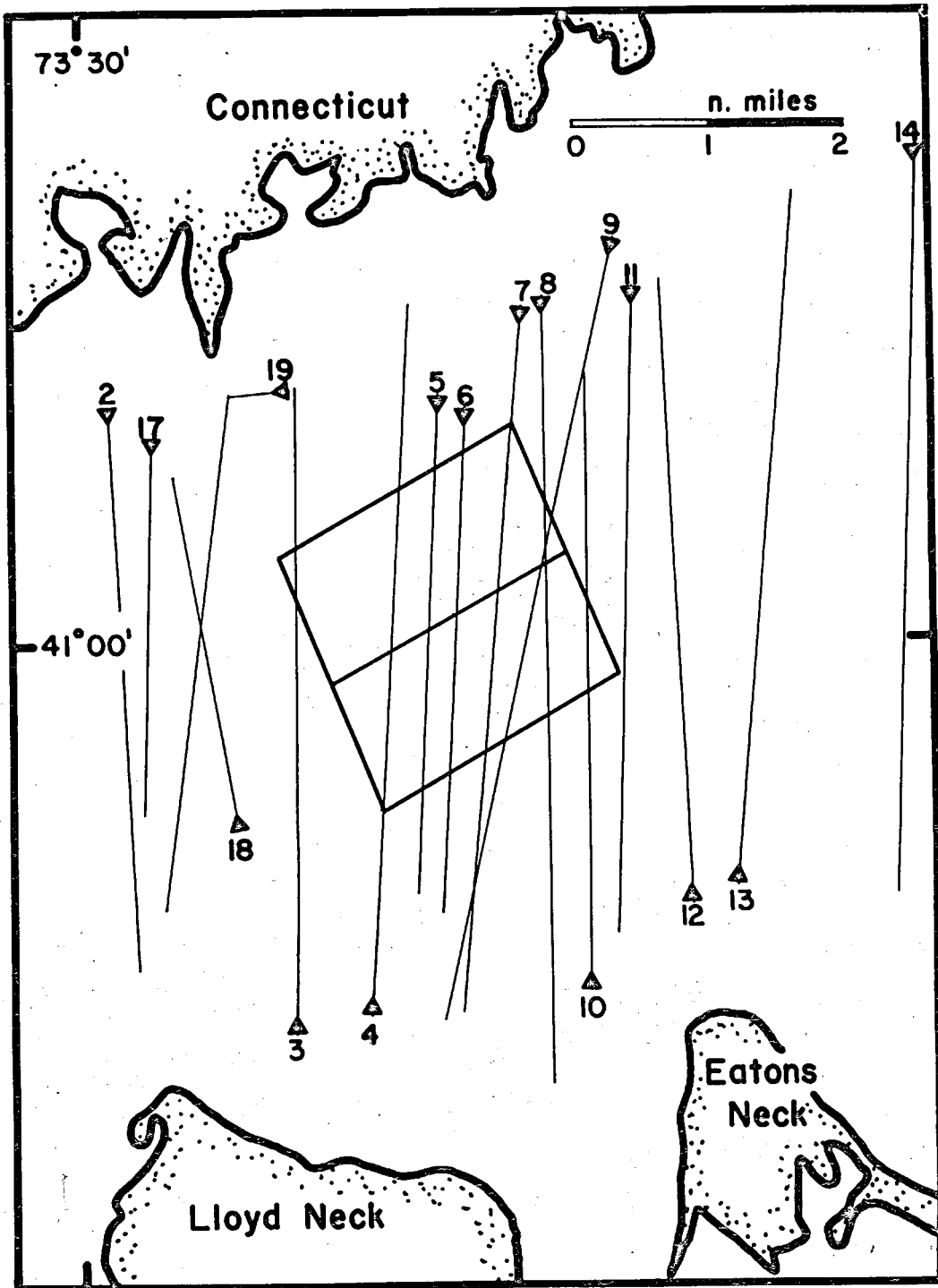


Figure 2. Tracks through the Eatons Neck study area along which acoustic-reflection profiles were made (Arrows indicate the direction in which the tracks were run and the track numbers refer to Table 1 and Appendix B)



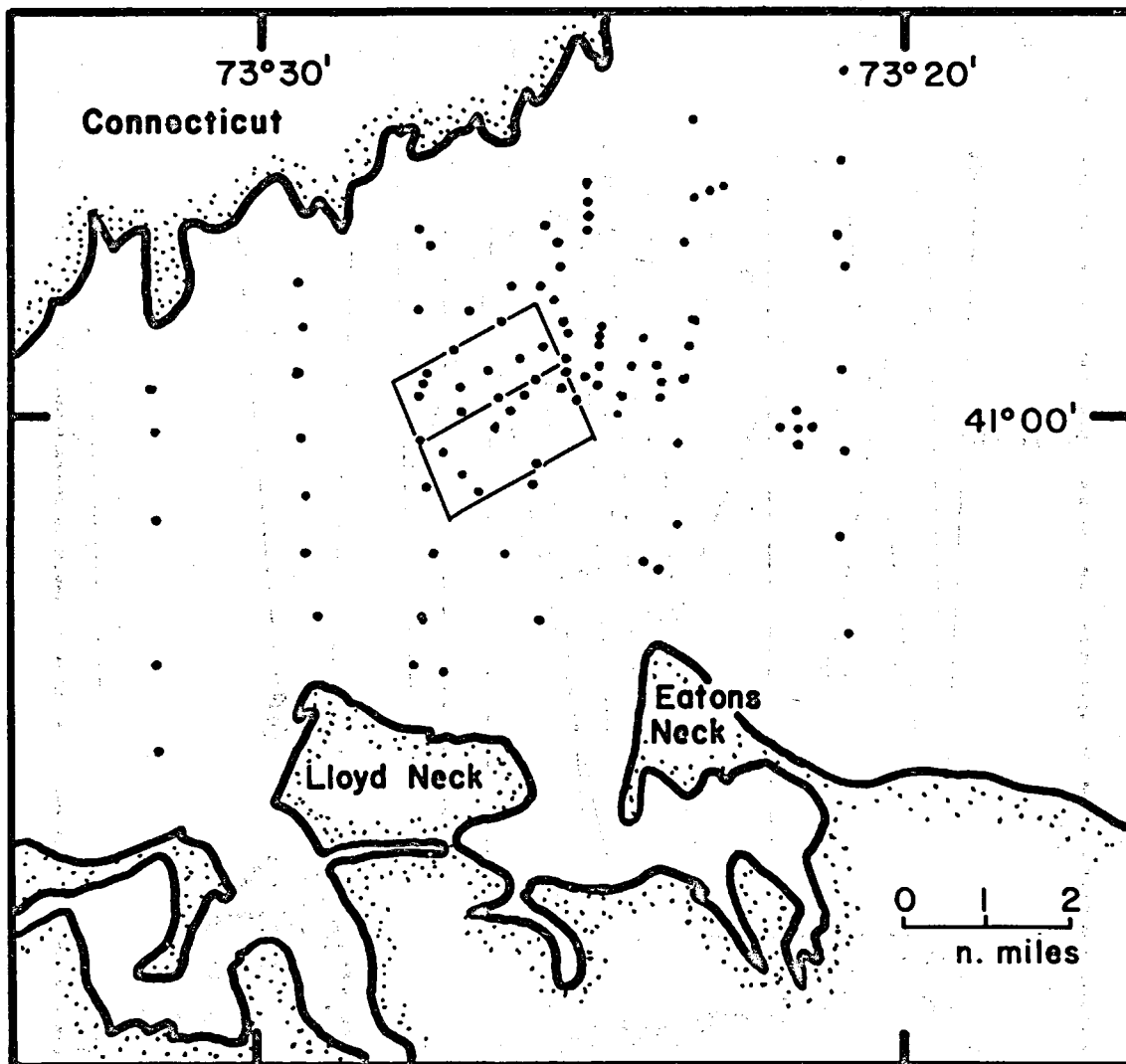


Figure 3. Location of sediment samples used to define the sediment distribution

either van-Veen grab or gravity corer. Additional acoustic-reflection profiles were made at each sample site to aid in the correlation of sediment type with the acoustic record. Thirty-eight of the samples were visually identified as 100% sand and/or gravel. Combined sieve and hydrometer tests were performed on the remaining 70 samples to obtain grain-size distribution curves. In addition, four specific gravity and eight Atterberg limits tests were performed. (The sediment analyses were performed by Haley & Aldrich, Consulting Soil Engineers, Cambridge, Massachusetts.) The sediment analysis data are presented in Appendix C.

#### Bottom photographs

11. Bottom photographs were taken and penetration tests were performed to confirm the sediment distribution information from the acoustic-reflection profiles and grab sampling and to provide for detailed examination of selected areas of the bottom.

12. Profile camera photographs. Profile photographs of the bottom were taken from the RV A. E. Verrill on 24 and 25 March 1975. Photographs were taken on Kodak "Plus-X" film at f-11 using electronic flash illumination with the profile camera designed by Rhoads and Cande<sup>5</sup>. The effective exposure time is about 1/1000 sec. A 10-sec delay time is used so that the picture is taken 10 sec after camera assembly has completed its penetration of the bottom. One picture is taken of each lowering of the camera from the ship. The magnification on the prints is 1 to 1. The photograph station positions for 24 March are shown in Figure 4, identified by photograph number. Photo D1 was

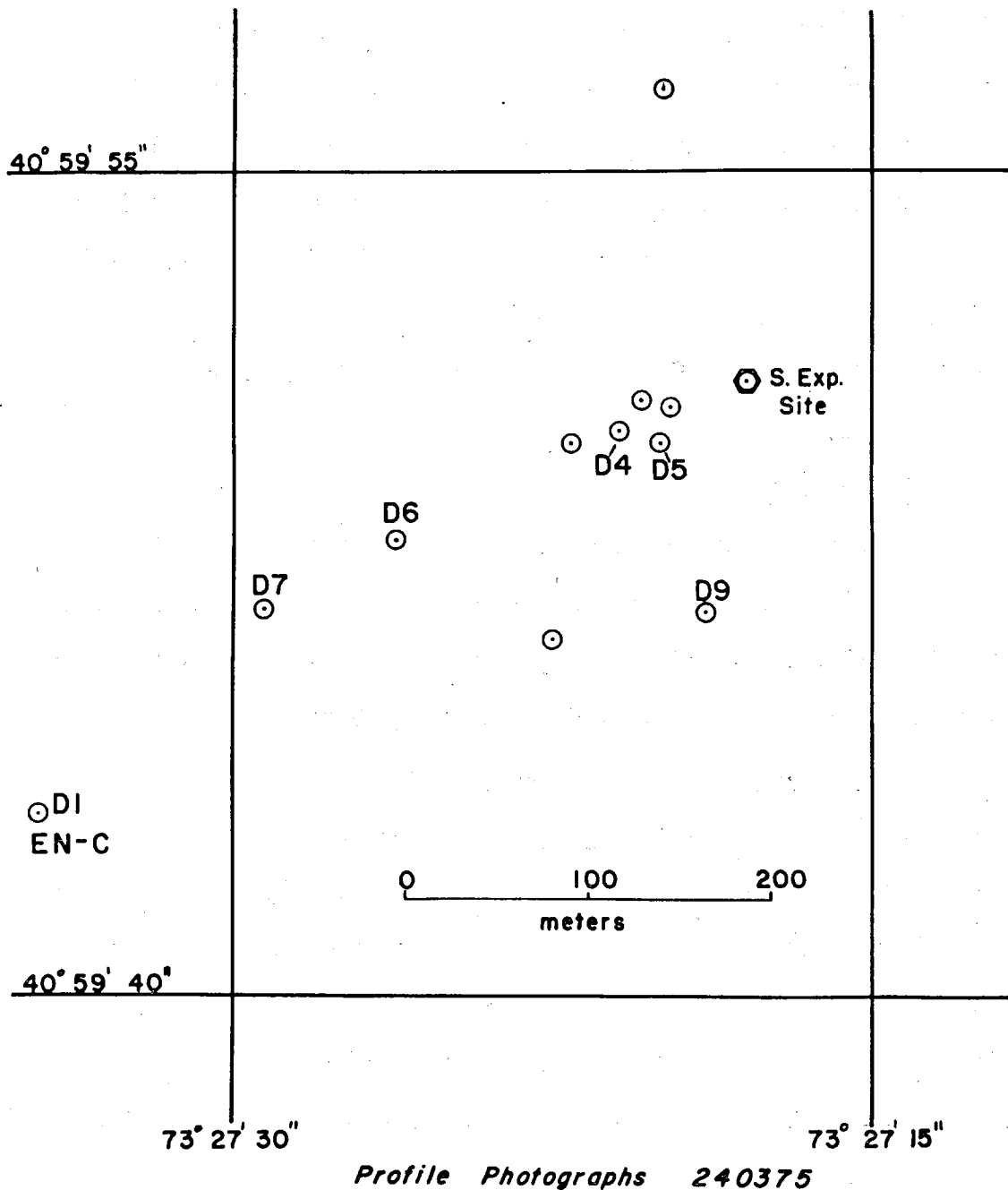


Figure 4. Locations of profile photographs (Appendix D) at EN-C taken on 24 March 1975

taken with the lighted Eatons Neck Disposal Ground buoy "C" (EN-C) close aboard. The circles are generous estimates of the position error. On 25 March only radar positions could be obtained because of fog. A diagram showing the approximate camera locations on this day is included (Figure 5). The profile photos are shown in Appendix D.

13. Note that in photographs D2 and D3, one of the two flash units failed to fire, resulting in nonuniform illumination. There is a slight optical distortion around the edges of the pictures, due to imperfections in the optical system.

14. Diver photographs. Diver photographs of the bottom were taken at two stations on 27 September 1975. Table 2 gives the depths and locations of the stations. Station 1 was located on top of a mound of disposed material (located by acoustic-reflection profiles) that rises to about 15 ft above the surrounding bottom. Station 2 was on Cable and Anchor Reef, in the northeast corner of the original disposal site. The photos were made to document the nature of the bottom sediments and associated fauna on this reef, which is presumed to be a partly eroded glacial lag deposit. The diver photographs are shown in Appendix E.

#### Mechanical properties of the bottom

15. In situ penetration tests were performed to determine the mechanical properties of the bottom in the study area (Figure 6). A description of the instrument used for this test and the interpretation of the test results in general are given by Gordon<sup>6</sup> and Bokuniewicz, Gordon, and Rhoads<sup>7</sup>. Briefly, the test consists of driving a cylindri-

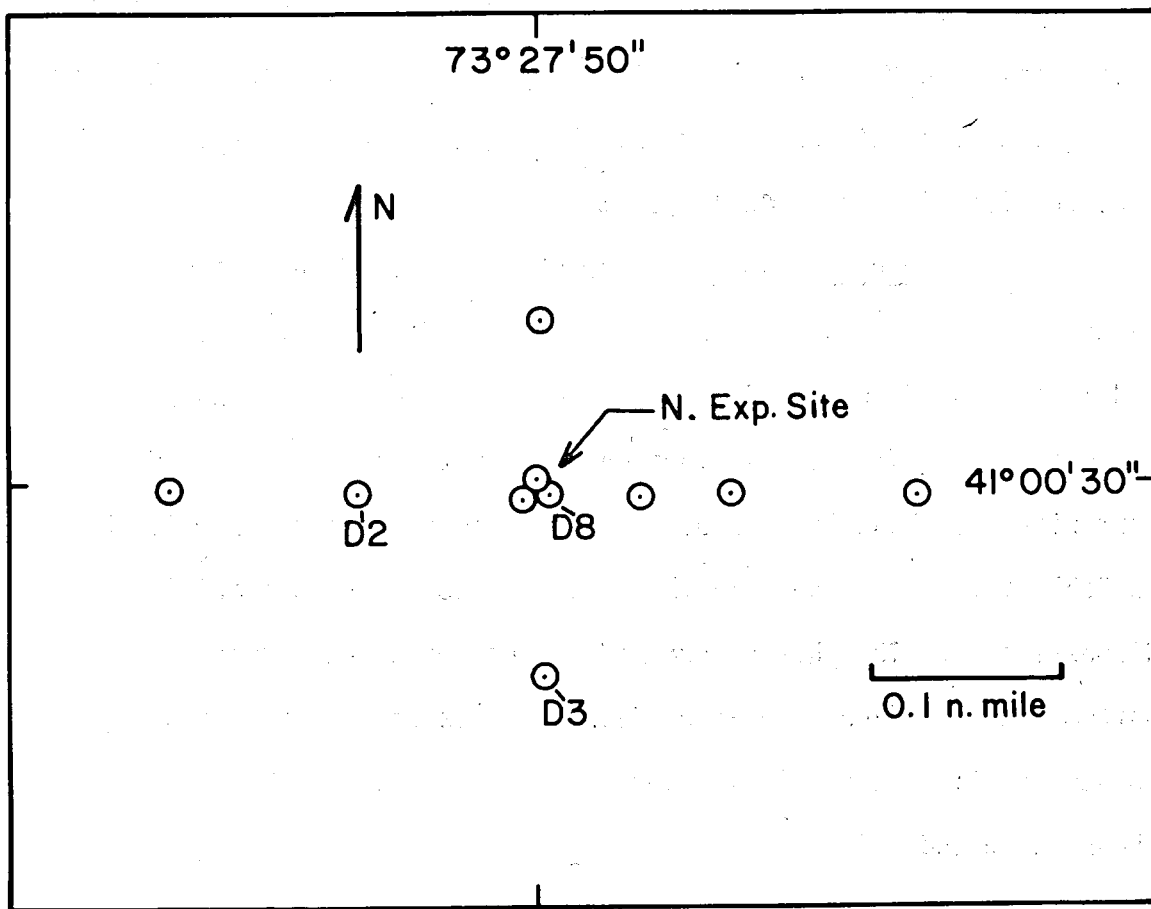


Figure 5. Locations of profile photographs (Appendix D) at EN-N taken on 25 March 1975

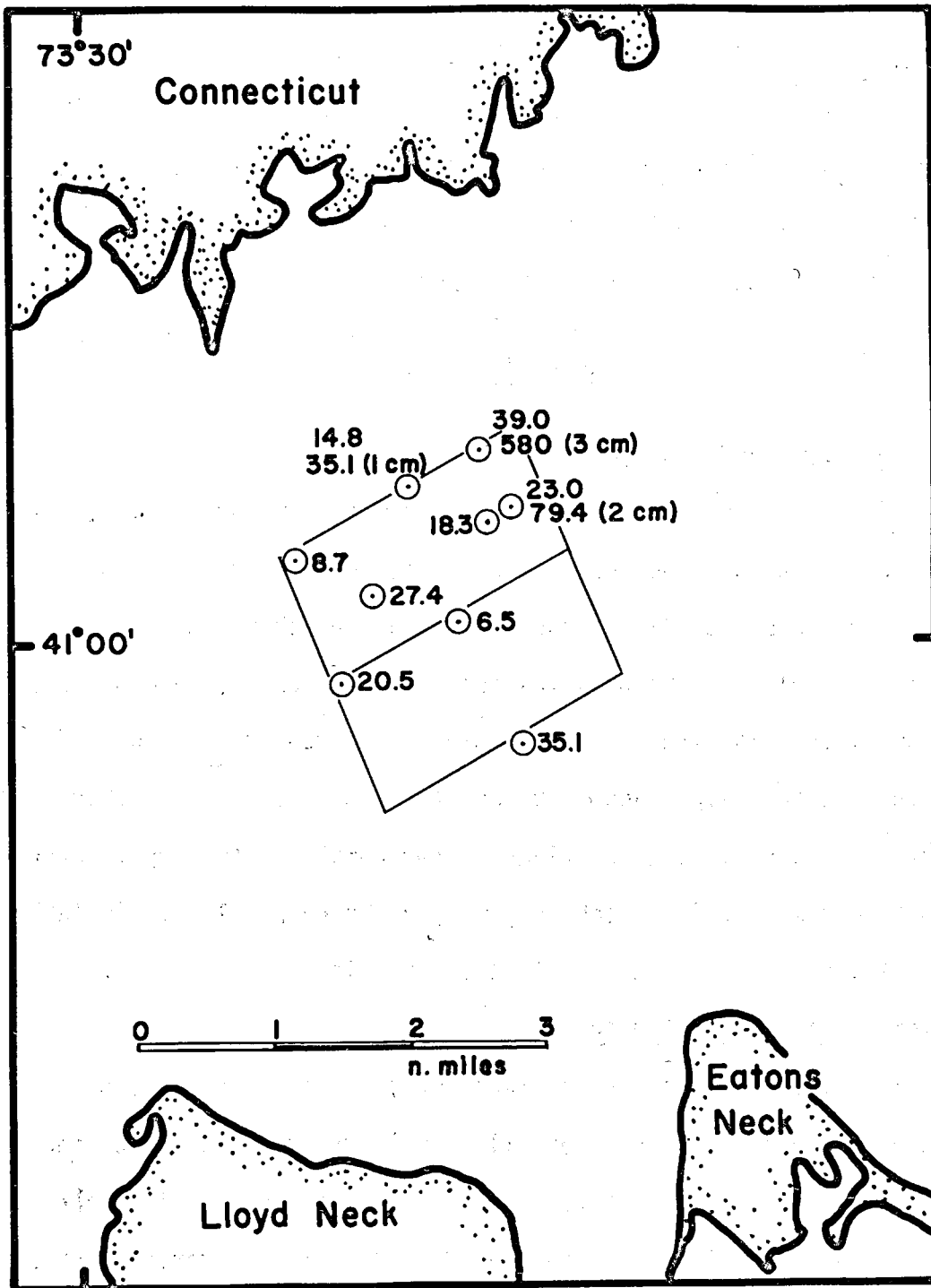


Figure 6. Location of penetrometer stations. The bottom hardness (mb/cm, see paragraph 12) is given for each station. At stations where the hardness changed with depth in the sediment, the surficial hardness is listed above the value deeper in the sediment and the depth at which the hardness changes (in cm) is recorded

cal piston (13.6 cm in diameter) into the bottom to a depth of 30 cm and measuring the pressure on the face of the piston as a function of depth. In Long Island Sound, the measured pressure is nearly a linear function of depth, and the slope of the pressure-depth curve is defined to be the sediment hardness  $H$  in  $\text{mb/cm}^6$ .

### Hydraulic Regime

#### Instrument type and deployment

16. Two types of recording current meters were used in the study. One type (Braincon, type 381) records average current speed and direction over successive 20-min intervals, and the other type (General Oceanics, model 2010) records instantaneous current speed and direction at fixed intervals (from 0.5 to 30 min). The meters were suspended between a bottom weight and an underwater float immediately above the meter. The current meter stations, meter height, meter type, water depth, and times during which they were occupied are listed in Table 3. A map of the station locations is given in Figure 7.

#### Analysis of the current data

17. The instantaneous current  $v(t)$  at any station can be written as the sum of a sinusoidally varying term (or group of terms)  $U(t)$ , a steady or constant term  $U_0(t)$ , and a term  $u'(t)$  representing the residual. The time scale used to delimit the terms is chosen both for operational convenience and according to the physical interpretation of the terms.  $U(t)$  is equated with the tidal stream flow and can be represented by a sum of sines and cosines with appropriate,

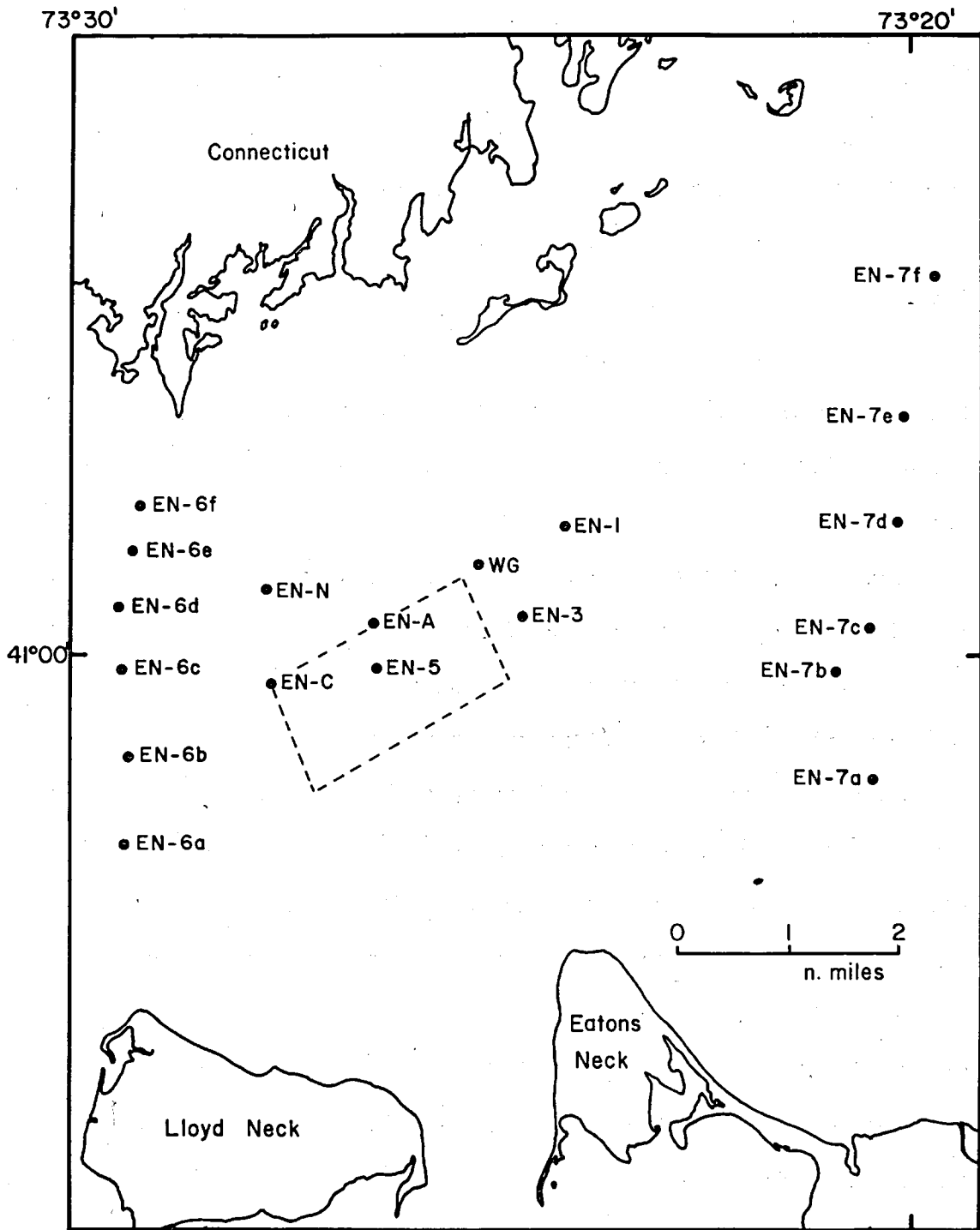


Figure 7. Index map of current meter stations (see Table 3)

EN = current meter stations  
 WG = wave gage stations  
 TG = tide gage stations



known tidal frequencies and with amplitudes and phases determined from the current observations at a particular station. (Although the periodic flow normal to the Sound axis is not strictly tidal flow, the same form and frequencies are applicable.) Together  $U_0(t)$  and  $u'(t)$  constitute the nontidal flow at a station.  $U_0(t)$  is operationally defined as the net displacement or the average velocity over one or more complete tidal cycles (cycle being defined by the period of the major tidal constituent present); and hence  $u'(t)$ , the fluctuating velocity, is simply the deviation of  $U(t) + U_0(t)$  from  $v(t)$ .

18. Although the physical interpretation of  $U(t)$  is straightforward, the complete separation of this component from the observed data is usually impracticable due to nonlinearities introduced by shallow water waves and to tidal constituents that cannot be characterized from the available length of record. Thus, in practice, the tidal and nontidal components may not be completely separable. The usual physical interpretation of the nontidal terms is to equate  $U_0(t)$  with estuarine circulation and  $u'(t)$  with tidal stream turbulence. However, there are problems in choosing an averaging time for  $U_0(t)$  that will satisfactorily separate these two components in accordance with their physical definitions. These problems will become clearer in the following discussion.

#### Tidal stream flow

19. The tidal stream flow is separated using a computer program for linear regression analysis<sup>8</sup> on the E-W and N-S components of the

total current. Records to be analyzed that have a variable sampling interval are interpolated, using a computer program, to give an equi-spaced data set. At each time  $t_i = i\Delta t$ , the regression program predicts a velocity

$$\hat{y}_i = A_0 + \sum_{j=1}^M (A_j \sin \omega_j t_i + B_j \cos \omega_j t_i) \quad (1)$$

where the  $\omega_j$  values are specified initially as appropriate tidal frequencies. The A's and B's are calculated so as to minimize the expression

$$\sum_{i=1}^N (\hat{y}_i - y_i)^2 \quad (2)$$

where  $y_i$  is the observed velocity at  $t_i$ .

20. The choice of tidal frequencies to be used in the analysis depends on the span of continuous observations available. Only those constituents whose phases separate by a sufficient amount during the record span can be distinguished. This problem is discussed in detail in Chapter 13 of Admiralty Manual of Tides by Doodson and Warburg<sup>9</sup>. Observation spans of 15, 29, and 365 days are recommended. A record length of 29 days is sufficient to separate the phases of the most significant constituents by approximately  $360^\circ$ . For such records, as many as 18 different constituents were determined. The same constituents could be separated from 15 days of data but with less accuracy. For records of only 24 hr or so, it is only possible to separate the species of tide (i.e., diurnal versus semi-diurnal). Constituents that cannot be separated can often be approximated, if necessary,

according to the equilibrium tidal relations.

21. The accurate prediction of shallow water constituents is difficult. The amplitudes of the shallow water waves vary nonlinearly with the amplitudes of the primary tides and this variation is not accounted for in the linear regression analysis. Consequently, as pointed out in Reference 9 (p. 69), it is generally inadequate to take only one term of a shallow water species as representative.

22. The result of the regression analysis is to give, for each frequency, the quantities  $A$  and  $B$  that specify a tidal constituent of frequency  $n$  as  $A \cos nt + B \sin nt$  or, alternatively, as  $R \cos (nt - k)$ , where  $R = (A^2 + B^2)^{1/2}$  and  $k = \arctan B/A$ . Both the amplitude  $R$  and the phase lag  $k$  are slowly varying due to the changing orbit of the moon with a period of about 19 yr. The  $R$  and  $k$  calculated for each constituent are corrected for this variation by multiplying  $R$  by  $f$  (nodal factor) and adding  $u$  (nodal angle) to  $k$ . Monthly values of  $f$  for the middle of the month are listed for a number of constituents in the Admiralty Tide Tables<sup>10</sup>. In addition to the nodal correction,  $k$  must also be converted to a standard reference frame. The measured phase lag  $k$  is relative to the time origin used in each regression analysis which is, in this case, the midpoint  $t_s$  of the length of data analyzed. The argument of the cosine can be rewritten as  $(nt - k - nt_s)$ , where  $t$  is time measured from 0000 EST on the same day as  $t_s$ . Then, following Reference 9 (p. 16),

$$nt - (k + nt_s) = V + u - \kappa \quad (3)$$

$$\text{or } nt - k - nt_s = (nt + V_0) + u - \kappa \quad (4)$$

where  $V$  is the phase of the equilibrium tide at the current meter station (and  $V_0$  is its value at 0000 EST);  $u$  is the nodal correction, and  $\kappa$  is the lag of the observed tide behind the equilibrium tide at the station. It is now customary to convert  $V_0$  and  $\kappa$  to the equivalent values at Greenwich, called  $E$  ( $E_0$  = the value of  $E$  at 0000 GMT) and  $g$ , and the above expression becomes

$$-k - nt_s = E_0 + u - g \quad (5)$$

$$\text{or } g = (E_0 + u) + k + nt_s \quad (6)$$

The conversion from  $V$  to  $E$  is as follows:

$$V \left( \begin{matrix} x = \text{station} \\ t > 0000 \text{ EST} \end{matrix} \right) = nt + V \left( \begin{matrix} x = \text{station} \\ t = 0000 \text{ EST} \end{matrix} \right) \quad (7)$$

$$\text{then } V \left( \begin{matrix} x = \text{station} \\ t = 1900 \text{ EST or } 0000 \text{ GMT} \end{matrix} \right) = -5n + V \left( \begin{matrix} x = \text{station} \\ t = 0000 \text{ EST} \end{matrix} \right) \quad (8)$$

$$\text{and } E_0 \equiv V \left( \begin{matrix} x = \text{Greenwich} \\ t = 0000 \text{ GMT} \end{matrix} \right) = -5n + jL + V \left( \begin{matrix} x = \text{station} \\ t = 0000 \text{ EST} \end{matrix} \right) \quad (9)$$

where  $j$  = the species number (Diurnal = 1, semidiurnal = 2) and  $L$  = longitude of station in degrees west of Greenwich. Similarly,  $g$  is related to  $\kappa$  by

$$g = \kappa + jL - 5n \quad (10)$$

$H$ , defined as  $R/f$ , and  $g$  are called the harmonic constants for the station. Daily values of  $E_0 + u$  are tabulated in Reference 10 for a number of primary constituents. Values of  $f$  and  $E_0 + u$  not tabulated for the primary constituents can be calculated from equations in Reference 9 (p. 50-52). Values of  $f$  and  $(E_0 + u)$  for the shallow water waves are calculated from the corresponding values for

the primary tides according to the rules  $f_{ixy} = f_x^i \cdot f_y$  and  $(E_0 + u)_{ixy} = i(E_0 + u)_x + (E_0 + u)_y$  as described in Reference 9 (p. 68). For example,  $f_{M_4} = (f_{M_2})^2$ ,  $f_{2MN_6} = (f_{M_2})^2 \cdot f_{N_2}$  and  $(E_0 + u)_{M_4} = 2(E_0 + u)_{M_2}$ ,  $(E_0 + u)_{2MN_6} = 2(E_0 + u)_{M_2} + (E_0 + u)_{N_2}$ .

23. Given  $g$  and  $H$  for a station, then, the tidal stream (or tide height if  $g$  and  $H$  were obtained from a tide record) can be predicted at that station as a sum over all the important tidal constituents:

$$y(t) = \sum_{i=1}^S f_i H_i \cos(n_i t + (E_0 + u)_i - g_i), \quad (11)$$

where  $t$  is EST. The value of  $t$  can be restarted at 0000 EST on each day (corresponding to the tabulated daily values of  $E_0 + u$ ) for which the prediction is wanted; however, the correction necessary is small if  $(E_0 + u)$  is specified only on the first day and time is allowed to increase continuously for up to a month.

24. Estuarine circulation. There are several ways to separate the long-term flow from the total current. One way is to average, over a suitable interval, the velocity deviations found by subtracting the tidal stream velocity predicted by regression analysis from the observed velocity. A second way is to pass the total current time series through an appropriate low-pass digital filter. A third method, progressive vector summation or the successive addition over 12.42 hr of the displacement vectors calculated for each sampling interval, requires much less calculation and is sufficiently accurate for most purposes. The resultant flow vector is defined to be the net displace-

ment per tidal cycle at the current meter station. Progressive vector summation is done routinely for all the stations. Diagrams of net displacement/tidal cycle over many tidal cycles are shown in Plates 1-16.

25. Tidal stream turbulence. The fluctuating velocity component is found by subtracting the tidal stream flow predicted by the regression program, plus an average flow over some appropriate interval, from the total current.

#### Sediment Resuspension

26. The distribution of suspended sediment through the water column is measured with a white light transmissometer having a 10-cm path length. This instrument also contains a pressure sensor, which serves to indicate its depth. Transmittance vs depth is traced on an X-Y recorder as the transmissometer is lowered through the water column. The relationship between transmittance and the concentration of sediment depends on the grain size of the particles<sup>11</sup>. The transmissometer is, therefore, calibrated by resuspending weighed quantities of sediment collected from the study area. Eleven calibration tests were performed spanning concentrations of suspended sediment ranging from 0 to 450 mg/l. The relationship between the suspended sediment concentrations (c in milligrams/liter) and the percent transmittance of light, %t, is

$$c = 6.2 \times 10^2 (2.0 - \log_{10} (\%t)) \quad (12)$$

Only in one case did the calculated concentration differ from the

measured concentration by as much as 20%.

27. To document the variation in turbidity over a tidal cycle, vertical turbidity profiles were recorded with the transmissometer at EN-N every 30 min beginning at 1800 hr on 24 March 1975 until 1600 hr on 25 March 1975, a total of 22 hr. Minor calibration adjustments were made throughout the experiment by submerging the instrument in clean, fresh water. Wind velocity was also measured every 30 min during the experiment with a shipboard anemometer. A General Oceanics current meter was established 2 m above the bottom at EN-N sampling the flow every 0.94 min for the duration of the experiment (i.e. from 24 March 1975, 1412 hr until 25 March 1975, 1230 hr). The tidal velocities were removed from the current meter record with a least-square regression of sinusoid with four tidal periods (see paragraph 19), and the fluctuating current velocity examined directly.

#### Disturbance of the Bottom by Waves

28. While the tidal stream dominates water movement at EN-N, there is the possibility that storm-generated waves might contribute to the erosion or transport of dredged material placed on the bottom. To test this possibility, a wave recorder was deployed in the study area during February and March, 1975 which are normally the stormiest months in this area. The experiment was designed not to record all aspects of the sea state but to detect only those waves that would influence the bottom. Hence, the wave recorder was placed at a depth such that short-wavelength waves were not recorded, and a search was

made for waves of sufficient wavelength to produce an appreciable particle velocity on the bottom at the experimental site.

29. A Bass model WG100 wave recorder was placed on the top of Cable and Anchor Reef ( $L = 41^{\circ}00'36''$   $\lambda = 73^{\circ}25'12''$ ) in a mean water depth of 45 ft. (Station WG in Figure 7). The instrument was set to record water pressure continuously for 3 min of each hour. Thus a tide height as well as a wave record is obtained. The record obtained runs from 19 February 1975 to 27 March 1975. A representative photograph of the wave record, for the time period, is shown in Plate 17. The pressure sensitivity of the instrument is 0.05 ft of water. All nontidal pressure fluctuations greater than this were read from the chart record and analyzed. The period of the pressure fluctuations was determined by measuring the spacing of oscillation recorded on the chart with a measuring microscope; pressure amplitude was read from the chart graduations.

30. The analysis of the recorded pressure fluctuations involves two steps: first, determination of the surface sea state responsible for the fluctuations; and second, determination of the resultant particle velocities on the bottom. All calculations are based on the equations of small amplitude wave theory; departures from these relations for the waves studied are expected to be small. The first step is the determination of the wavelength  $\lambda$  from the measured period of the waves  $P$  by graphical solution of the relation

$$\frac{gP^2}{2\pi} = \frac{\lambda}{\tanh 2\pi \frac{d}{\lambda}} \quad (13)$$



where  $d$ , the water depth, is 45 ft. These solutions are recorded in Table 4. The height of the wave on the surface  $H$  responsible for a pressure fluctuation  $\delta p$  at depth  $d$  is then found from

$$H = 2 \frac{\delta p}{\rho g} \cosh 2\pi \frac{d}{\lambda} \quad (14)$$

The attenuation of  $\delta p$  with depth is rapid unless the wavelength is long.

### Salinity Observations

31. Salinity data are useful for two reasons: to help identify water masses and to define the density gradient through the water column. The latter is important in analysis of the transport of dredged material to the bottom since an increase of density with depth means increased buoyancy forces on the descending material. Salinity was measured with a Hydroproducts model 645 salinometer modified so that its output signal can be recorded. The sensor unit of the salinometer is attached to a pressure indicator so that a continuous trace of salinity vs. depth can be made with an X-Y recorder. Salinity profiles were made along a series of short transects extending outwards from the Connecticut shore to detect the width of the zone in which high salinity bottom water mixes with less saline surface water. The technique is the same as that described by Gordon and Pilbeam<sup>12</sup>.

## PART III: RESULTS AND DISCUSSION

### Literature Review

32. There are few published papers dealing with the oceanography and geology of Long Island Sound. Those papers containing background information helpful in the interpretation of the observations at the Eatons Neck study area are mentioned herein.

33. The movement of water through Long Island Sound has been the subject of a number of published papers beginning with the monograph on tides and currents by LeLacheur and Sammons<sup>13</sup>. An analysis of the tides in the Sound based on a damped resonance model was presented by Redfield<sup>14</sup> and further developed by Ippen and Harleman<sup>15</sup>. A comprehensive discussion of circulation and mixing processes is given in a series of papers by Riley,<sup>16, 17, 18</sup> more recent results for the central Sound are given by Gordon and Pilbeam<sup>12</sup>. Summaries of recently obtained hydrographic data are available in the Technical Report Series of the Marine Sciences Research Center of the State University of New York at Stony Brook.

34. Interest in the submarine geology of Long Island Sound dates back to the early work of J. D. Dana.<sup>19, 20, 21</sup> More recently, seismic surveys have shown the bottom of the Sound to be typically bedrock covered by thick blanket deposits of glacial drift and relatively thin layers of lacustrine and marine sediments.<sup>22, 23, 24</sup> Acoustic-reflection profiling has been used to define submerged, glacially-formed structures<sup>25</sup>, to measure the volume and distribution of marine sediment<sup>4</sup>.

and to determine the rate of transport of sand<sup>26</sup> in Long Island Sound. The general character of the marine sediments is known from the published data of McCrone et al.<sup>27</sup> and Buzas<sup>28</sup>.

### Sediments and Bottom Structure

#### Identification of sediment type

35. The Eatons Neck disposal site is located approximately midway between the irregular, east northeast trending shorelines of Connecticut on the north and Long Island on the south. From the center of the disposal site, the shortest distance to the northern shore is 3.1 nautical miles to Long Neck Point; whereas to the southern shore it is 2.9 nautical miles to Eatons Neck Point (see Figure 1b).

36. A simplified geological cross section through this region of Long Island Sound can be represented by the following sequence: a pre-glacial bedrock basin, covered by as much as 100 ft of glacial drift, and that covered by as much as 100 ft of Recent sediment. In places, shoals of either bedrock (for example, Budd Reef) or partially eroded glacial drift (for example, Cable and Anchor Reef) crop out of the surrounding Recent sediment cover.

37. The Connecticut shoreline consists of exposed bedrock and bedrock covered with a thin veneer of glacial drift, primarily till and sand and gravel; the Long Island shoreline consists of beach sand and glacial till over outwash sand and gravel.

38. Most of the bottom at the disposal site is at depths of 100 ft or greater. The north-central, northwest, and central portions

slope gradually to the south. A trough, in places as deep as 200 ft, trends east-west along the southern edge of the disposal site. At the northeast corner of the disposal site is Cable and Anchor Reef, which shoals to 25 ft. There are also several shoals in the vicinity of the disposal site that exhibit relief greater than 50 ft above the surrounding bottom.

39. From the grain-size analyses performed on the sediment samples, it appears that a useful parameter for representing sediment type is the percent (by weight) of sediment coarser than 0.074 mm, the division between sand and silt in the Unified Soil Classification System<sup>29</sup>. Many of the grain-size analysis curves show a distinct change in slope at approximately that division (Appendix C). The percent by weight of sand in the sediment samples was plotted and contoured at 10% intervals (Figure 8).

40. In addition, a map of the area depicting the principal sediment types based on the Unified Soil Classification System<sup>29</sup> was drawn (Figure 9). This map shows that the bottom in the central part of the Sound is predominantly silt with varying amounts of sand. Silty sand, sand, and gravel are found near the shorelines, particularly around the sandy headlands of Long Island and at the shoals in the central part of the Sound.

41. The portion of the bottom on which extensive waste disposal has taken place is delineated as the gray area of Figure 8. The identification of this material as "disposed" is based on the presence of numerous artifacts (brick, cinder block, etc.) in sediment samples

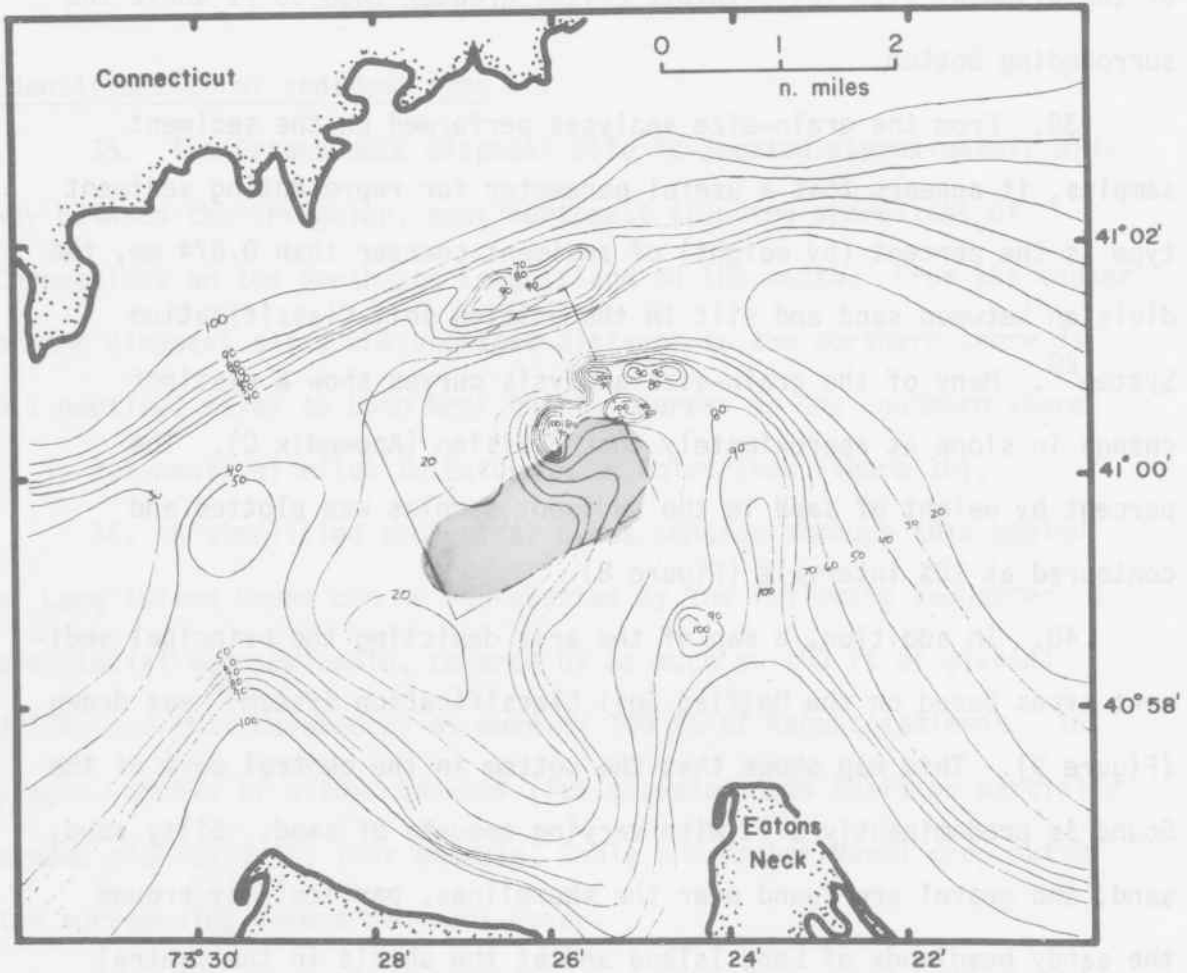


Figure 8. Contour map of percent sand content (10% contour intervals) in the surficial sediment in the Eatons Neck study area. The shaded area indicates portion of the bottom where extensive disposal has taken place

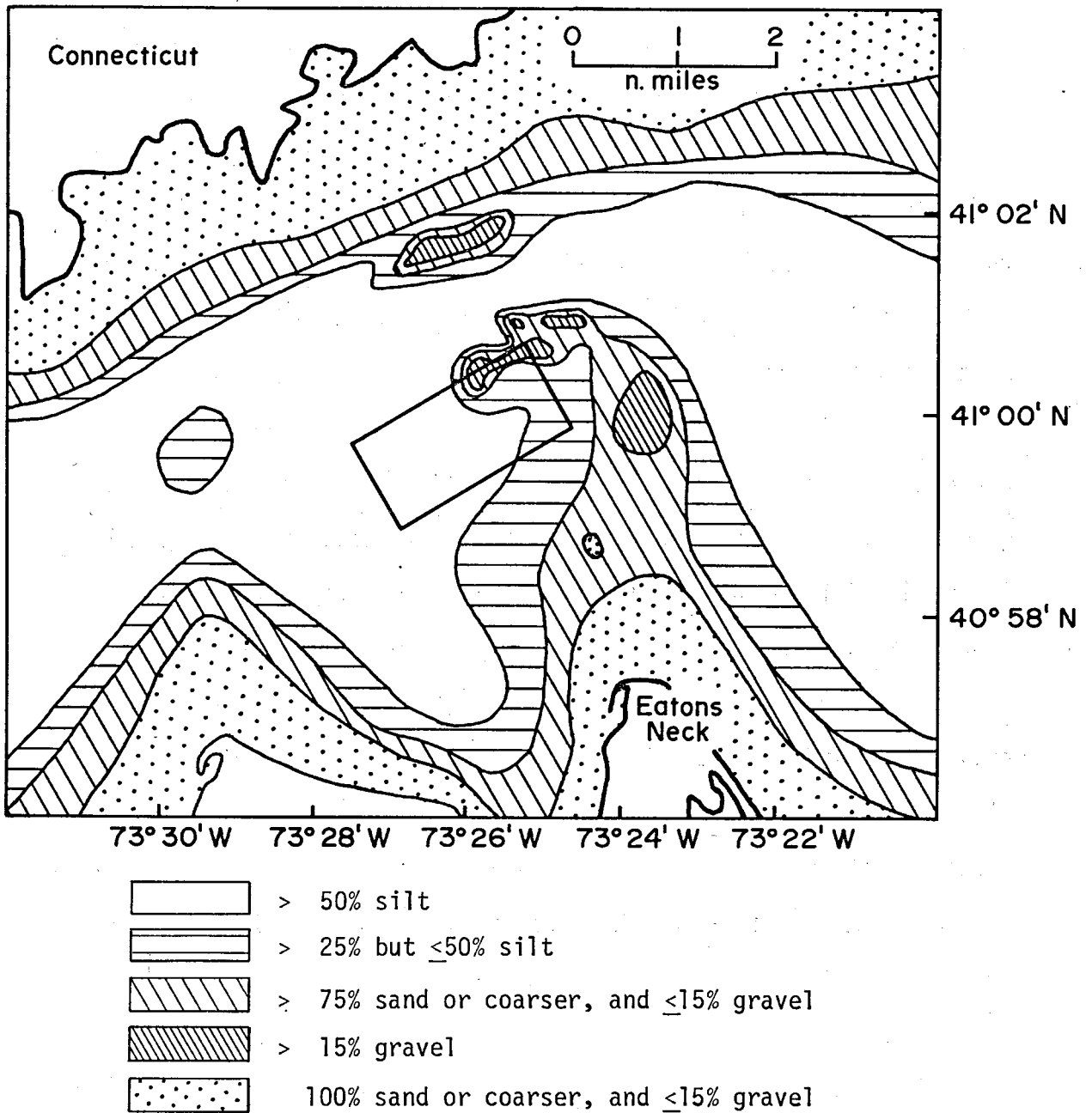


Figure 9. Predominant sediment types of Eatons Neck Area

and on diver identification of sunken pilings, cables, etc. Acoustic-reflection profiles 4 through 10 (Appendix B), which pass through the designated disposal area, also indicate the presence of disposed material. (On profiles 4-10, the bounds of the disposal area are indicated by double vertical lines.) For example, on profiles 6, 7, 9, and 10, individual piles of material as high as 18 ft are present, and most profiles over the disposal area exhibit a characteristic rough microtopography and irregularities of the bottom on the order of 2 ft (which are correlated by sediment samples to be disposed material intermixed with naturally occurring silt). Essentially all of this material is within the designated bounds of the disposal ground; at some other sites in Long Island Sound evidence of "short dumping", i.e., disposal outside of the designated disposal site bounds, is found. This may be because the Eatons Neck disposal area is close enough to shore that visual positioning is relatively easy.

42. The results of the bottom sampling and reflection profiling study show that the naturally occurring sediment over most of the disposal site is silt with as much as 50% sand by weight. The exceptions to this are the shoal at Cable and Anchor Reef and the deep hole on the southeast corner of the disposal site, where muddy sand and gravel predominate.

#### Bottom photographs

43. Additional information, particularly about the fine-scale structure of the sediment-water interface, is obtained from the underwater photographs (Appendix E). On the side of Cable and Anchor Reef

(Photo E1), pebbles and coarse sand characteristic of a glacial lag deposit are seen. Much of this material is bound together by algae, as shown in Photo E2. The photographs taken by divers on the top of a large mound of disposed material show that fine sediment from the surrounding sea floor has been deposited here, forming a surface suitable for recolonization by benthic animals. This cover of fine sediment is evident in Photo E3, in which an abundance of casts of deposit-feeding, benthic animals is evident on the sediment surface. Photo E4 shows this fine sediment at greater magnification; polychaete tubes are seen emerging from the sediment and bryozoans may be seen growing on the shell debris. The Eatons Neck disposal site has not been used for the last few years; the transport and deposition of suspended sediment from surrounding areas establishes a benthic habitat suitable for recolonization in a relatively short time.

44. EN-N and EN-S are located off the designated disposal area; the interface photographs taken there show the texture of the fine silt bottom of this area of the Sound and information on the biological, chemical, and physical processes that occur at the sediment-water interface (Appendix D). Because of the accurate positioning attained in the interface photography at EN-S, the pictures may be used to estimate the scale of lateral heterogeneity in the sediment. There is little discernible difference in the grain size or depths of the oxidized zone of the bottom in D4-D7 (Appendix D). This shows that the scale of heterogeneity is greater than 50 m. Over distances of 100 m or more, significant differences in sediment texture and in the



depth of the oxidized zone can be seen.

45. Oxidized sediment is distinguished by its light color in the interface photographs<sup>7</sup>. At both of the experimental sites the depth of oxidized sediment is about 3 cm, as may be seen in Photos D4-D7. At the lighted buoy "C" it is significantly deeper, probably because of higher bottom permeability due to the increased sand content at this location (Photo D1). In those areas where the oxidized layer is particularly thin, evidence of a relic, deeper zone may be seen (Photos D2, D3, and D8). This is probably indicative of a reduced intensity of bioturbation\* at the time the photographs were taken.

46. A large amount of suspended sediment is evident in the water in both the profile camera photographs and in diver photographs E2, E5, E6, and E7. The particle densities are much greater in the profile photos taken on 25 March (Photos D2, D3, and D8) than 24 March (Photos D1, D4-D7, and D9). This is attributed to the eastern storm which occurred during the evening of the 24th (see Appendix D).

47. Close examination of the photographs will show that the sediment-water interface is composed of granules, presumably fecal pellets, on the order of 0.25 mm in diameter. The interpretation of these structures is discussed in Bokuniewicz, Gordon, and Rhoads<sup>7</sup>. These form a layer 2 to 3 mm thick, except in the feeding burrows. It is this material that is regularly resuspended in the tidal stream<sup>30</sup>.

48. Evidence of sediment resuspension can be seen in several of

---

\* Bioturbation - disturbance by organisms.

the photographs but is best shown in Photo D9. Here pellets are being swept out of one of the feeding burrows. This photograph shows wisps of particles too fine to be resolved by the camera. These particles are evident at a number of places along the bottom; and they are thought to be the silt component of the sediment and are mostly confined to a boundary layer a few millimeters thick. In two places the transfer of this fine material from the boundary layer to the stream above can be seen to be in progress.

49. The most abundant animal seen in the profile camera photos is the polychaete Owenia fusiformis, characterized by a small flexible tube (see Photo D7, Appendix D). Owenia is considered to be a pioneer species and is expected to occur in a heavily stressed environment<sup>31</sup>. Hydroids, common on the Sound bottom in winter, occurred in both the profile camera photographs and the diver photographs (e.g., Photos D6, Appendix D and E7, Appendix E). Other benthic fauna that can be seen in the diver photographs include cup corals (E8, E9, and E10 where the polyps are extended) sponges (E2, E6, E7) demersal fish (E11), and starfish (E12). Evidence of small burrowing animals can be seen in most of the profile camera photographs; a particularly large burrow is seen in Photo D7. These burrows, being filled with loose material, may act as paths for the rapid diffusive exchange of chemical species between sediment and water. Their preservation would be important in any laboratory experiment on chemical exchange between sediment and water.

### Mechanical properties of the bottom

50. Penetrometer tests were used to measure bottom hardness. This quantity is useful in evaluating deflection of the bottom under a superimposed surficial load<sup>32</sup>. A penetration test into a hard, sand bottom would yield a sediment hardness value  $H$  of about 500 mb/cm; whereas a soft, silt bottom has a hardness around 15 mb/cm. Throughout most of the study area, the penetration data suggests that the bottom is silt but that the mechanical characteristics are heterogeneous and locally very soft ( $H = 6.4$  mb/cm, for example). Figure 6 depicts the sediment hardness  $H$  (in mb/cm) as determined by in situ penetration tests. Where a change in  $H$  occurred, the surficial value is written above the deeper value and the depth in the sediment at which the transition occurs is recorded in parenthesis. In the northeast corner of the study area, between Cable and Anchor Reef and Budd Reef, a soft layer a few centimeters thick overlies a much harder, probably sandy, substrate. An estimate of the initial deflection of the sediment surface,  $d$  under a load  $L$  applied over area  $A$  would be given by  $d = \frac{L}{AH}$ .

### Hydraulic Regime

#### Currents

51. An objective of this study was to determine those characteristics of the flow in the Eatons Neck region that are necessary for predicting the transport of sediment in suspension and as bed load. In general, all stations exhibit similar hydraulic characteristics (Figure 7, Table 3):

- a. The tidal currents are predominantly along the axis of the Sound with maximum speeds (observed 2 m above the

- bottom) of less than 30 cm/sec (e.g. Plates 26, 27).
- b. Isotropic fluctuating velocities about 3 cm/sec in magnitude are present (e.g. Plates 25, 27, and 30).
  - c. There is a net drift velocity to the west southwest, (e.g. Plate 23) or the south (e.g. Plate 30).

### Tidal currents

52. Major tidal flow is along the east-west axis of the Sound with a small component normal to the axis. A current ellipse calculated for station EN-3 (Figure 10) progresses in a counterclockwise direction, suggesting that the periodic component normal to the axis is the result of Coriolis force on a resonant co-oscillating tide. The variation of velocity with depth over several tidal cycles is shown in Figure 11. The magnitude of the maximum tidal velocity increases by a factor of three at the surface. The data in this figure are from the vertical meter array established at EN-A from 10 January 1975 to 22 January 1975 (see Table 3).

53. Values of the tidal constants  $g$  and  $H$  calculated for Eatons Neck Stations A and C are listed in Table 5. The semidiurnal constituent  $M_2$  is dominant, with a period of 12.42 hr, and could be used by itself to approximate the tidal stream. The importance of the shallow-water constituents (subscript 3 and greater), however, is evident from the table and can also be seen in the periodograms in Figure 12 and 13, which were calculated from data from station A and C. It is this shallow-water component of the tidal stream that distorts (from simple sinusoidal form) the shape of the current versus time curves shown in the computer printouts. The presence of the

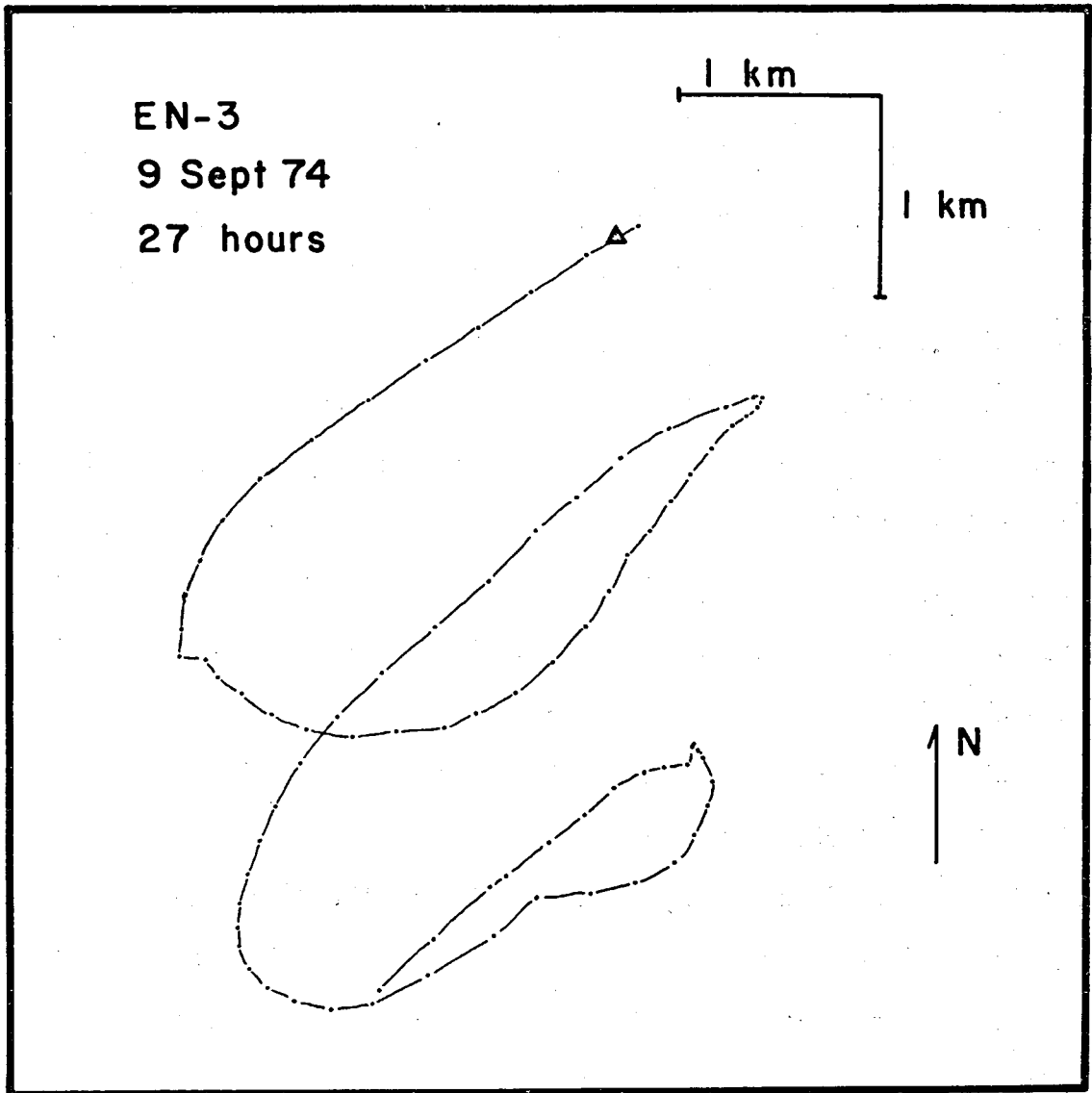


Figure 10. Progressive vector diagram of the recorded current velocity 2 m above the bottom at EN-3 over 27 hr showing a counterclockwise tidal rotation

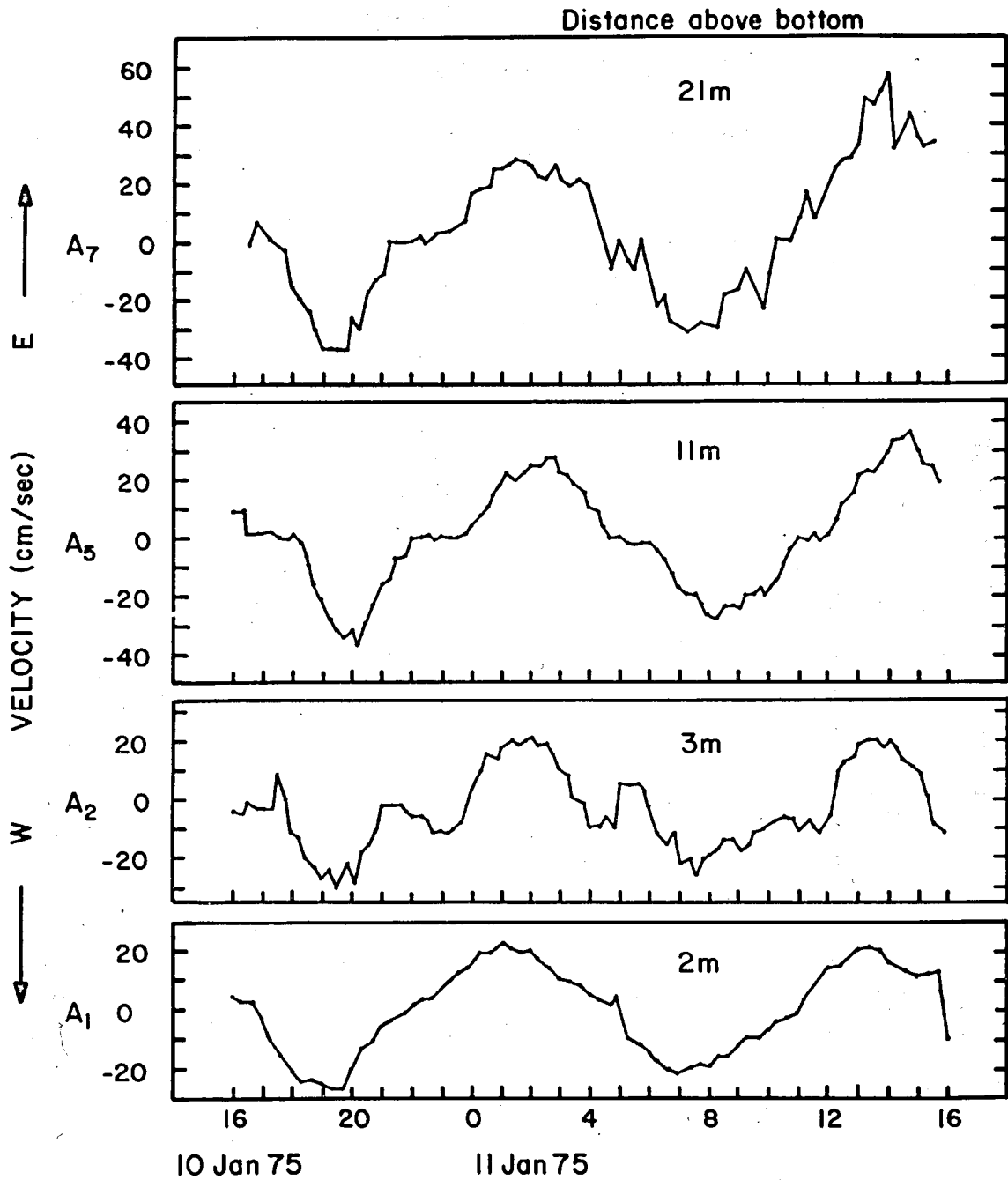


Figure 11. The east-west component of the current recorded at four depths at EN-A over 24 hr 10 Jan 75. The water depth is 24 m

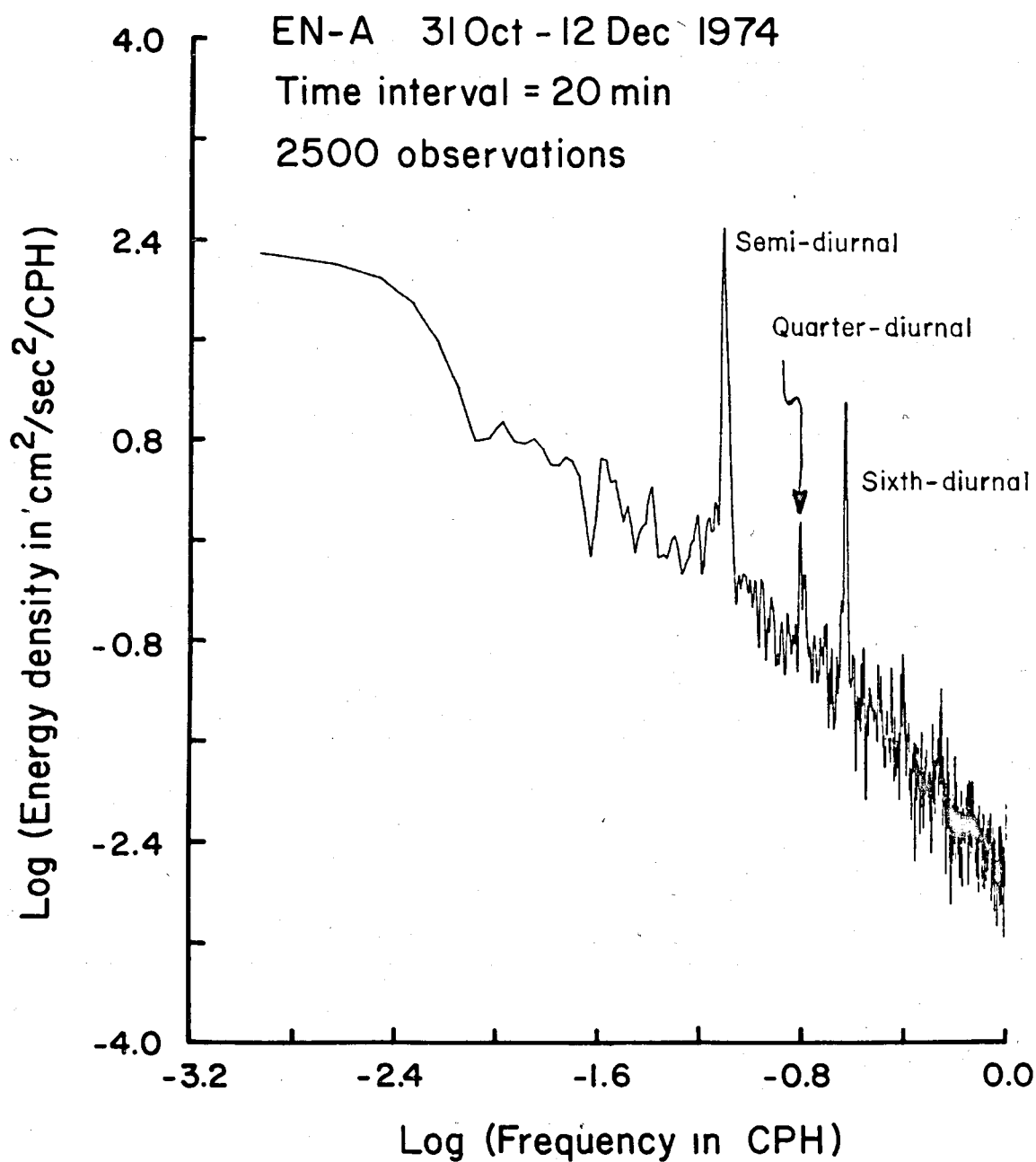


Figure 12. Energy density for current velocities at EN-A from a current meter record taken 2 m above the bottom, 31 October to 12 December 1974. The peaks due to the primary tidal components in the area are labeled

EN-C 31 Oct - 25 Nov 1974

Time interval = 20 min

1024 observations

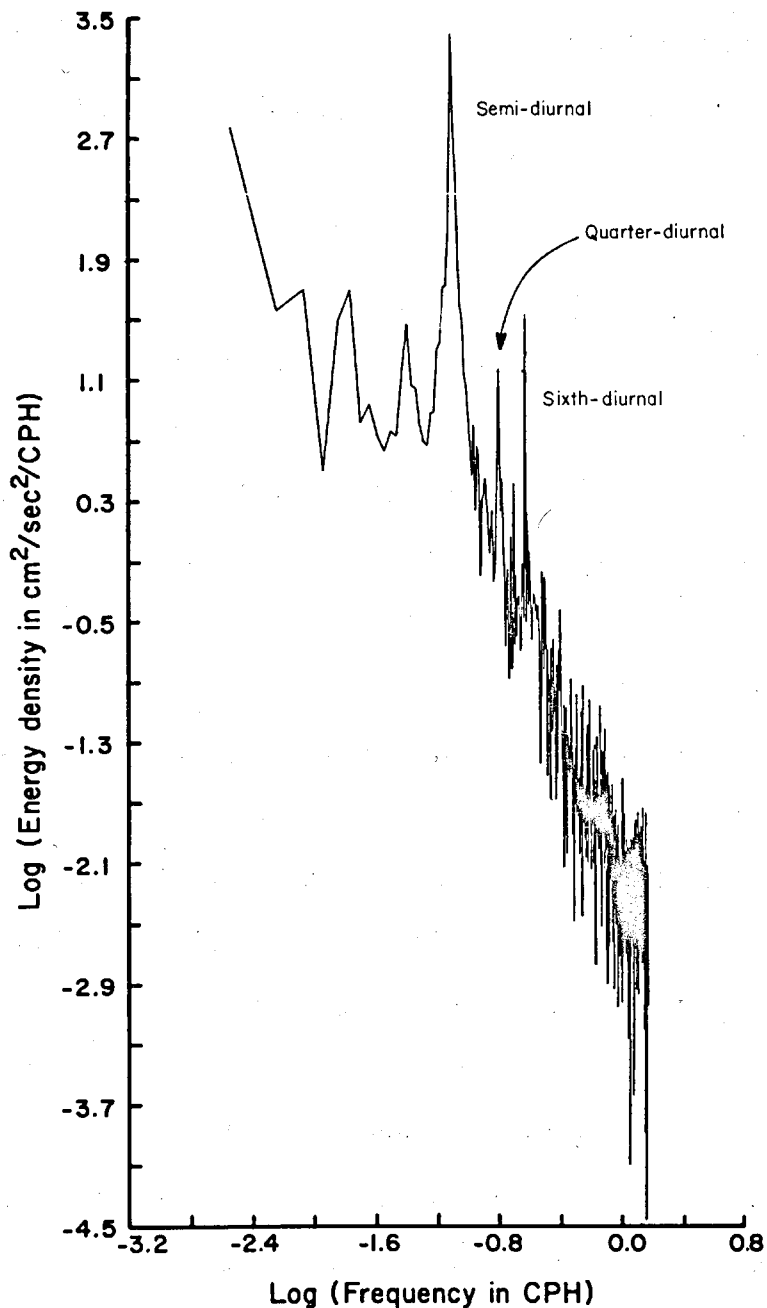


Figure 13. Energy density for current velocities at EN-C from a current meter record taken 2 m above the bottom, 31 October to 25 November 1974. The peaks due to the primary tidal components in the area are labeled



shallow-water constituents in the tides tends to decrease the mean squared flow velocity. In the histogram representation, this causes an unusual number of low velocities to be observed. The effect is most pronounced at EN-C and EN-A where the typical velocities are only  $\sim 10$  cm/sec.

#### Nontidal flow

54. Estuarine circulation. Superimposed on the oscillating tidal stream flow is a smaller, generally unidirectional flow identified as the estuarine circulation of Long Island Sound. The flow is out of the Sound in the less saline surface layer and inwards in the more saline bottom layer. Density gradients due to salinity differences drive the circulation. The resultant flow vectors at all current meter stations indicate a net westward movement of bottom water ranging from 1.5 to 5.5 cm/sec (Figure 14). In central Long Island Sound, net shoreward flow of bottom water is found only close to the shore, where bottom water moves into the shoreside mixing zones<sup>12</sup>. The boundary of the mixing zone along the Connecticut shore is shown in Figure 15. It generally follows the 10-fathom depth contour. Because of the rapid increase of water depth south from the Connecticut shore, the mixing zone is relatively narrow in this part of the Sound, and shoreward flow would not be expected to occur anywhere near the disposal area. This is confirmed by the current meter results; shoreward flow is not found at any of the stations.

55. The variation of the resultant flow vectors with depth is shown in Figure 16. The data are from the vertical array at EN-A from

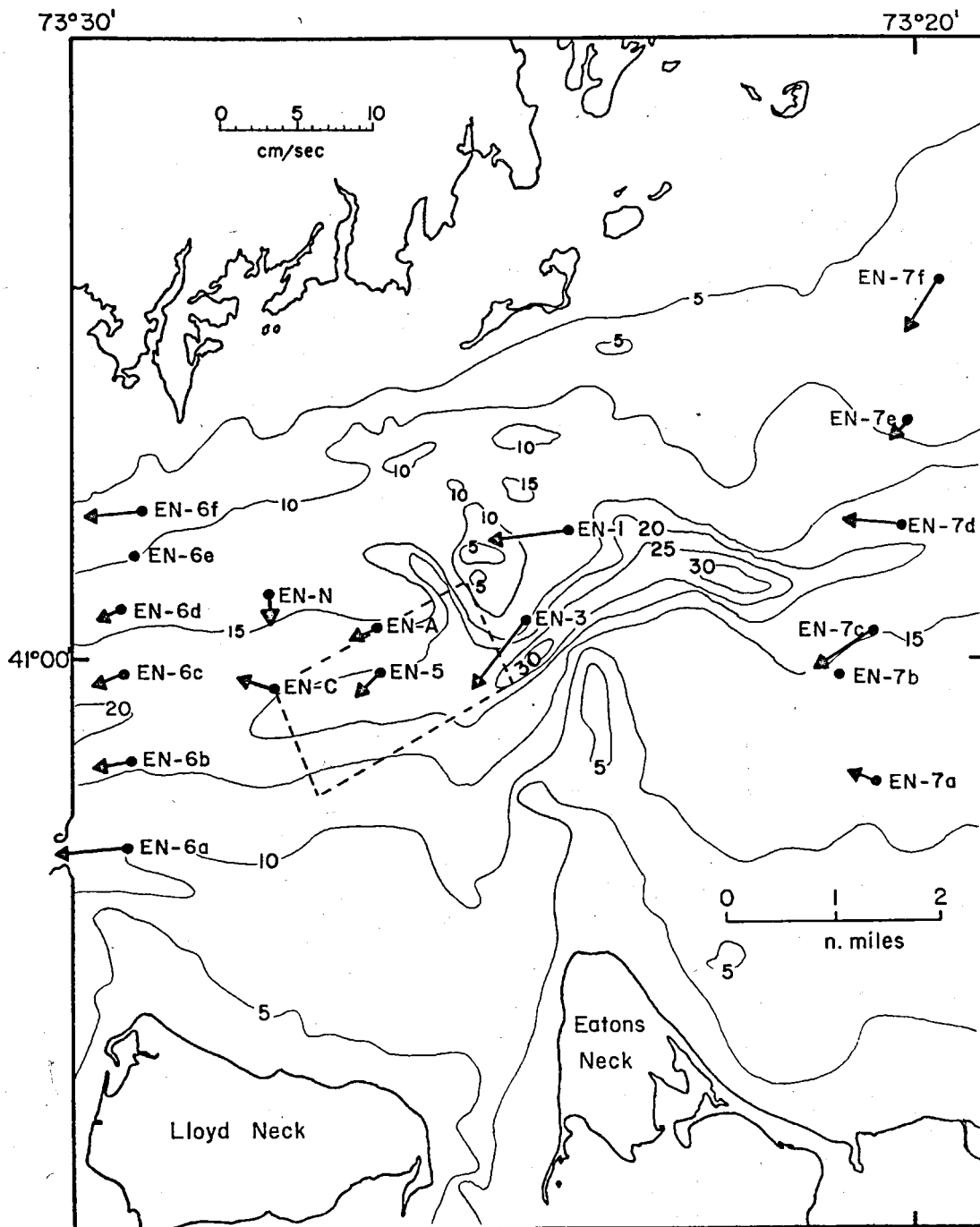


Figure 14. The net bottom current velocities recorded 2 m above the bottom

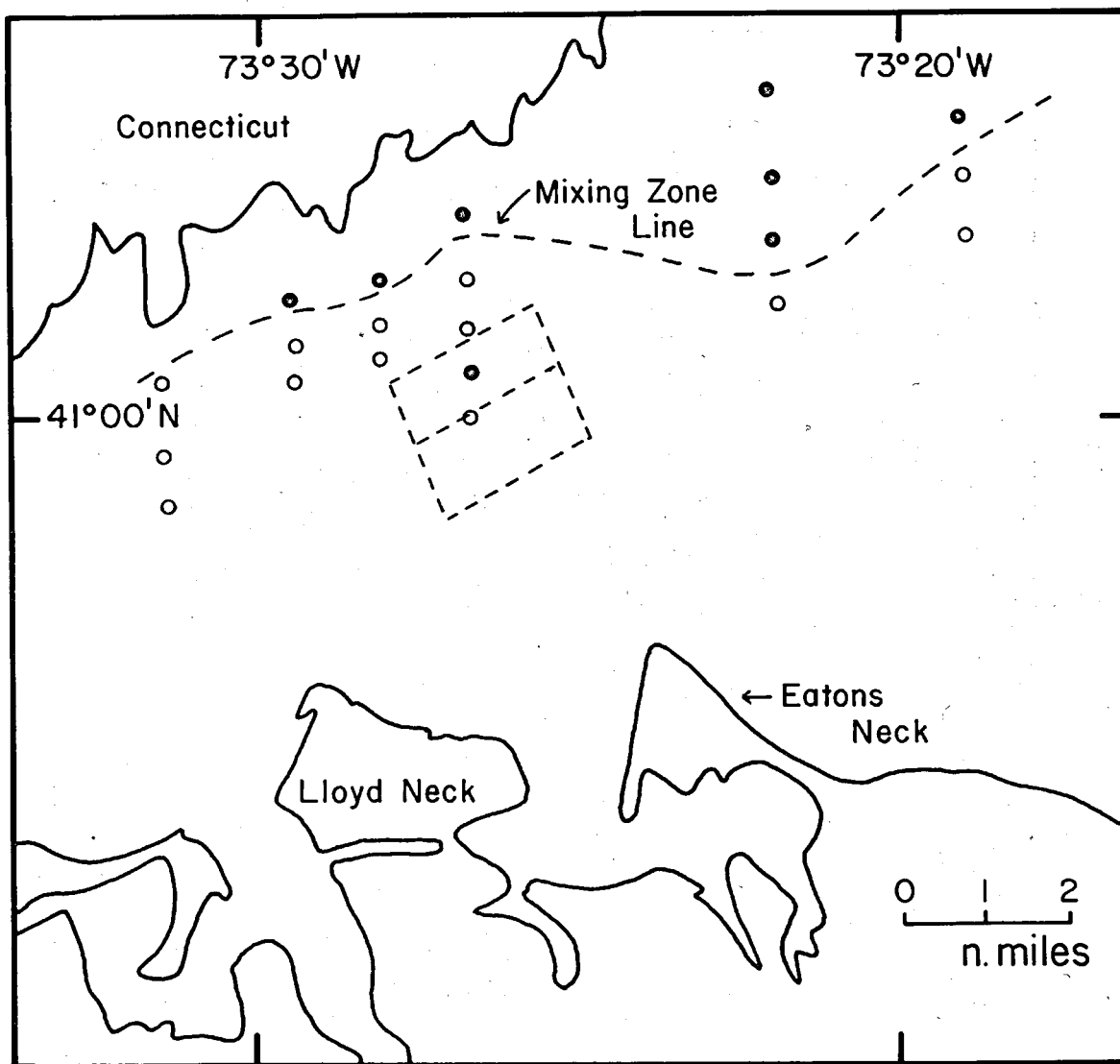


Figure 15. Mixing zone deduced from the salinity data. Closed circles are stations where salinity profiles indicated that the water column was well mixed; open circles indicate stations at which the water column was stratified

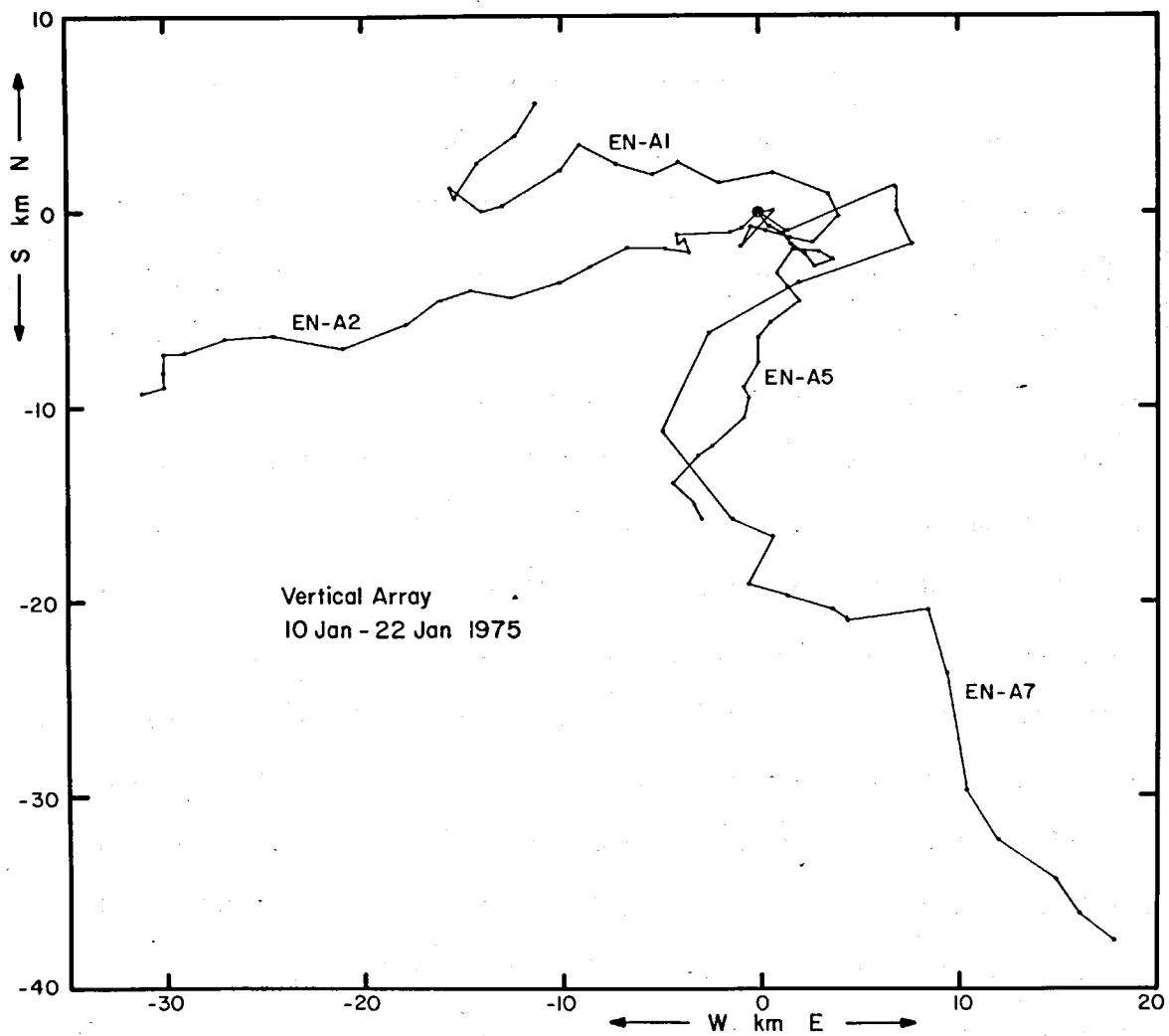


Figure 16. The resultant flow over successive tidal cycles recorded at EN-A between 10 January and 22 January 1975 at four depths. A1 is 2 m above the bottom; A2, 3 m above the bottom; A5, 11 m above the bottom; and A7, 21 m above the bottom. The water depth is 24 m

10 January 1975 to 22 January 1975. The flow becomes progressively more southerly as the surface is approached. The resultant flow vectors from the top meter, about 8 ft below the surface, are plotted alongside the appropriate wind vectors in Figure 17, and the close correspondence between the two diagrams indicates that the surface circulation is largely wind-driven at this depth.

56. Progressive vector diagrams calculated from data obtained at EN-A over a 5-month period are plotted in Plate 31 and show the near-bottom drift to be fairly uniform for long periods of time. In Figures 18 and 19, low-pass filtered velocity data from EN-A (31 October 1974 - 12 December 1974) are graphed. The filter was chosen to eliminate all components with periods less than 24 hr and is a more accurate method of removing tidal components than progressive vector summation. The resultant vectors and low-passed velocities show variations with periods on the order of days. These variations are probably large-scale current fluctuations. No relation of these variations to variations in wind or freshwater runoff was found. However, the frequency of occurrence of large variations is observed to increase in stormy weather. For example, the diagram in Plate 31 shows a large, confused loop in the resultant vector diagram from March, 1975. This loop coincides with two storms, one on March 8-9th with winds up to 25 knots, and the other on March 14-15th with winds up to 33 knots. Changes in the resultant flow vectors that reflect changes in the driving forces of the estuarine circulation probably occur on the order of weeks to months. It is likely that the circulation is buffered

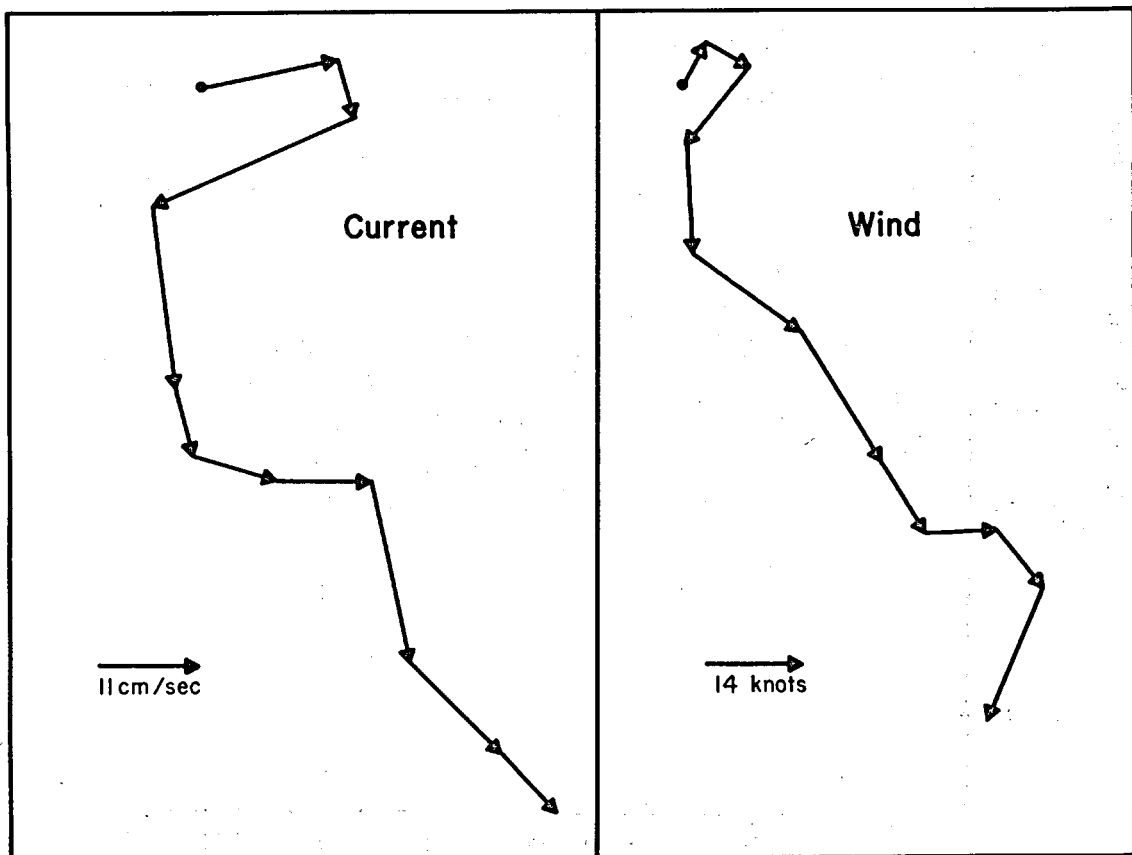


Figure 17. The 25-hr net current flow recorded in the surface water at station EN-A between 10 January and 22 January 1975 compared to the 25-hr average wind velocity recorded at Stratford Point, Connecticut, for this same time interval

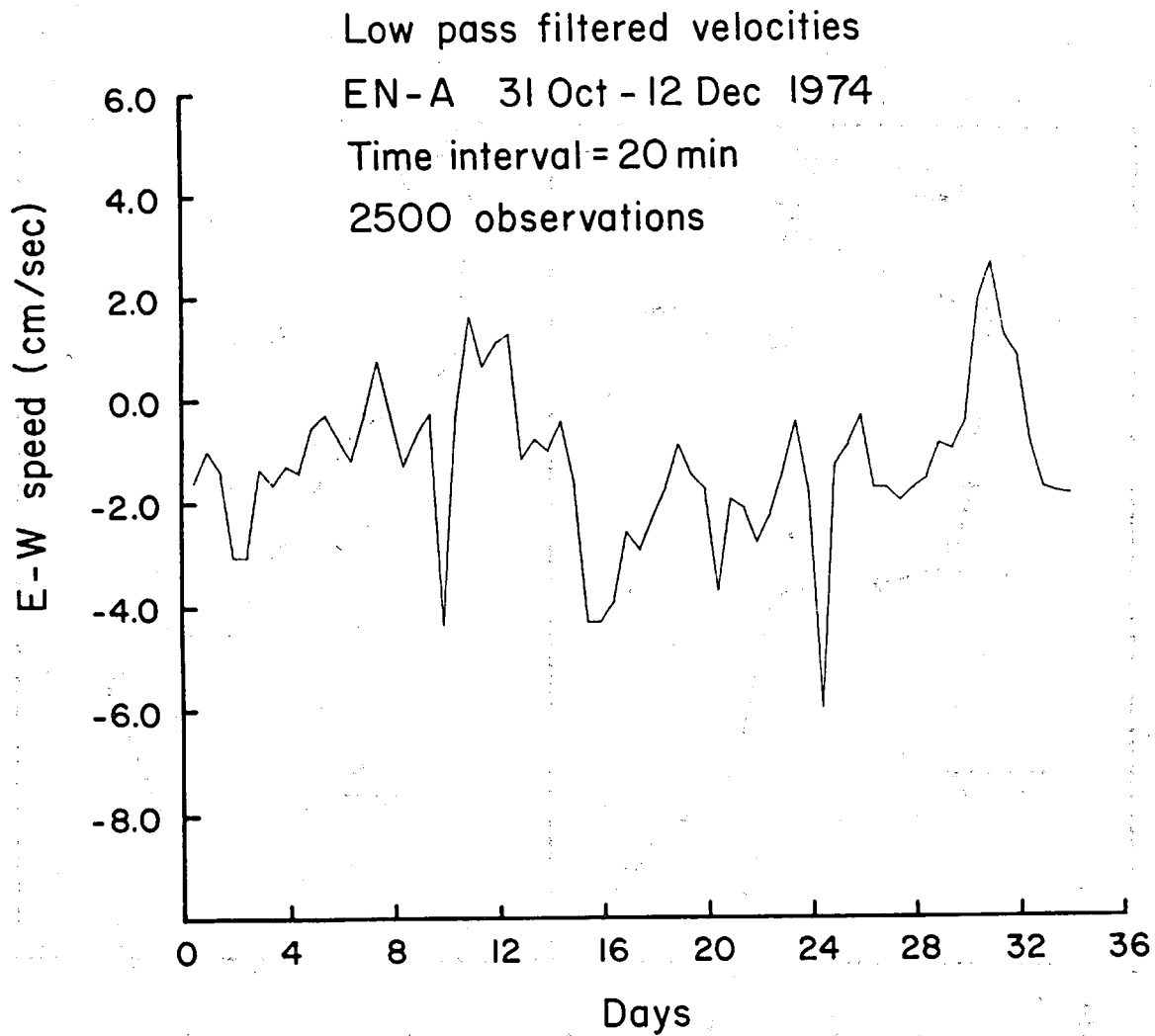


Figure 18. E-W current velocities 2 m above the bottom recorded at EN-A between 30 October and 12 December 1974 from which all periods less than 24 hr have been removed by a low-pass filter

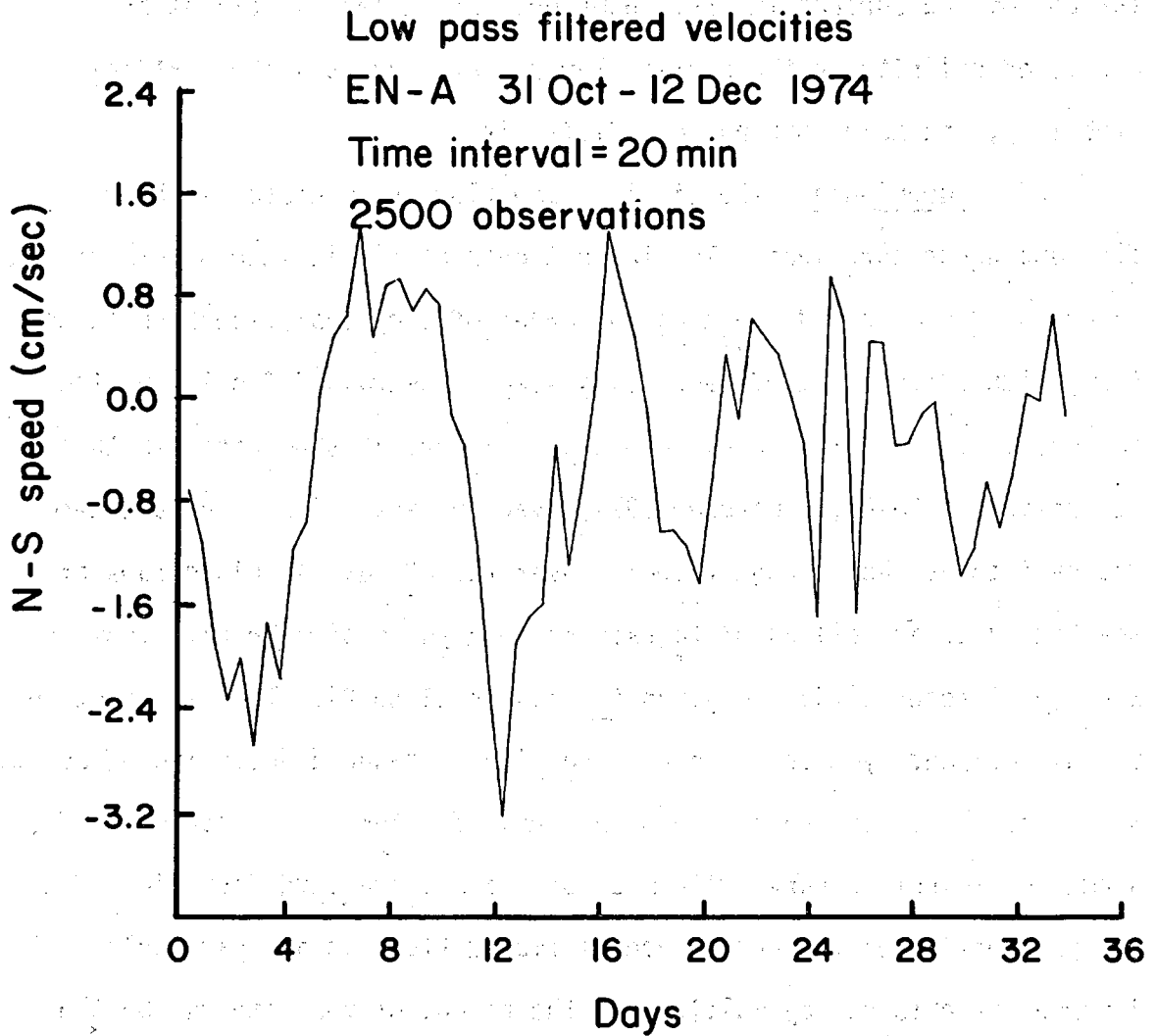


Figure 19. N-S current velocities 2 m above the bottom recorded at EN-A between 30 October and 12 December 1974 from which all periods less than 24 hr have been removed by a low-pass filter



against rapid changes in freshwater input and only responds to seasonal changes. For example, a sudden increase in freshwater runoff will increase flow in the surface layer and tends to increase mixing between the bottom and surface layers. However, this effect is offset by decreased salinity in the surface layer that increases the vertical stability, and makes mixing more difficult.

57. Turbulence. The tidal stream flow is an unstable shear flow and hence turbulent. The largest characteristic length for this turbulence is expected to be on the order of the tidal excursion (2 to 4 km) with a continuum of decreasing sizes constrained finally by the conversion of kinetic energy into heat. Figure 20 shows the fluctuating velocities at EN-A (31 October 1974) over 29 days. (The constant term was defined as the average velocity over the 29 days.) Histograms of the same data as well as histograms of 15 days of similar data from EN-C (31 October 1974) are given in Figures 21 to 24. The distribution is unimodal and symmetric around zero with a standard deviation of about 3 cm/sec. The histograms have been normalized for comparison with a normal distribution curve with mean of 0 and a standard deviation of 1. The probability of the occurrence of fluctuations in any particular interval is obtained by multiplying the height of the interval by the area of the interval ( $= 1/\text{standard deviation}$ ). The fluctuations studied are independent of position in the tidal cycle.

58. The magnitude of the velocity fluctuations was found to be sensitive to the wind speed in the Eatons Neck region. A similar relationship has been documented in the central Sound where

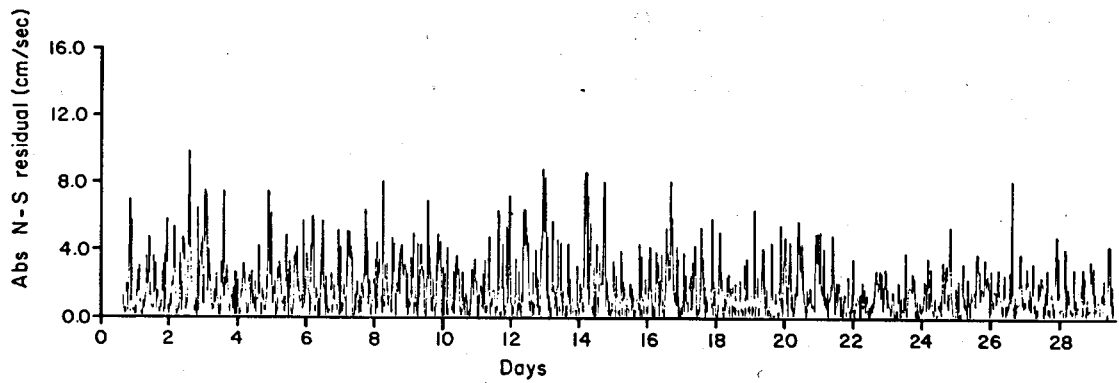
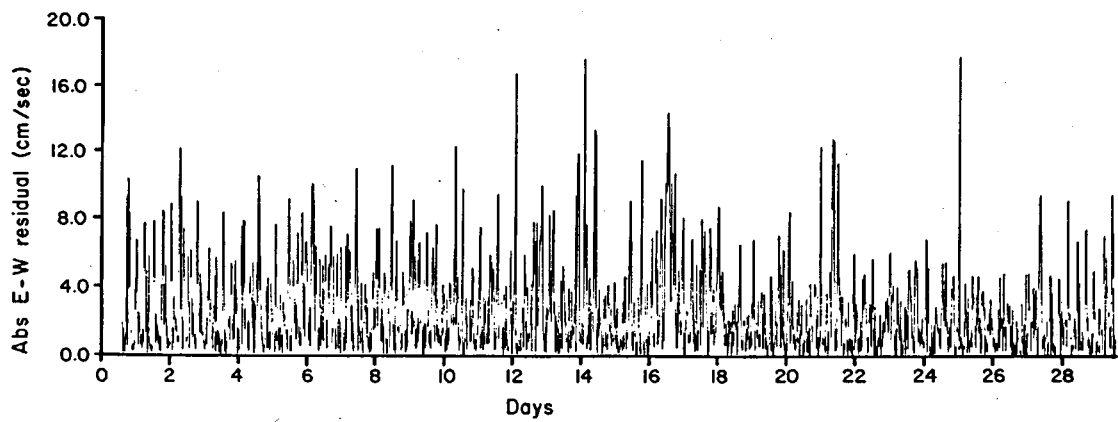


Figure 20. E-W and N-S fluctuating current speeds (see paragraph 22) recorded 2 m above the bottom at EN-A between 31 October and 12 December 1974

EN-A  
31 Oct 74  
E-W velocity component  
2089 observations  
 $\sigma = 3.5$

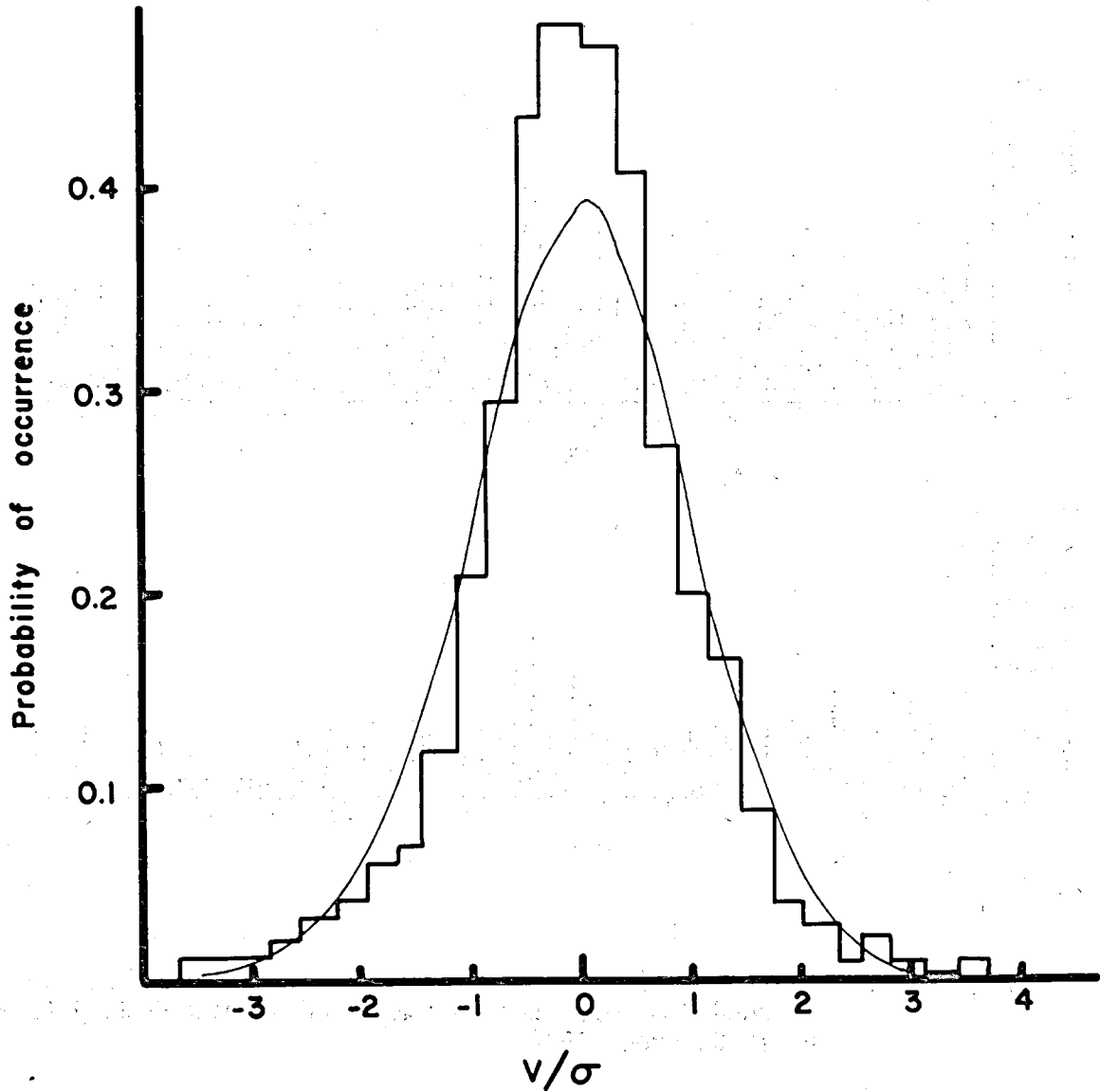


Figure 21. The distribution of E-W fluctuating current velocities recorded at EN-A between 31 October and 12 December 1974 compared to a Gaussian distribution (thin line) with the same mean and standard deviation ( $\sigma$ , in cm/sec)

EN-A  
31 Oct 74  
N-S velocity component  
2089 observations  
 $\sigma = 2.3$

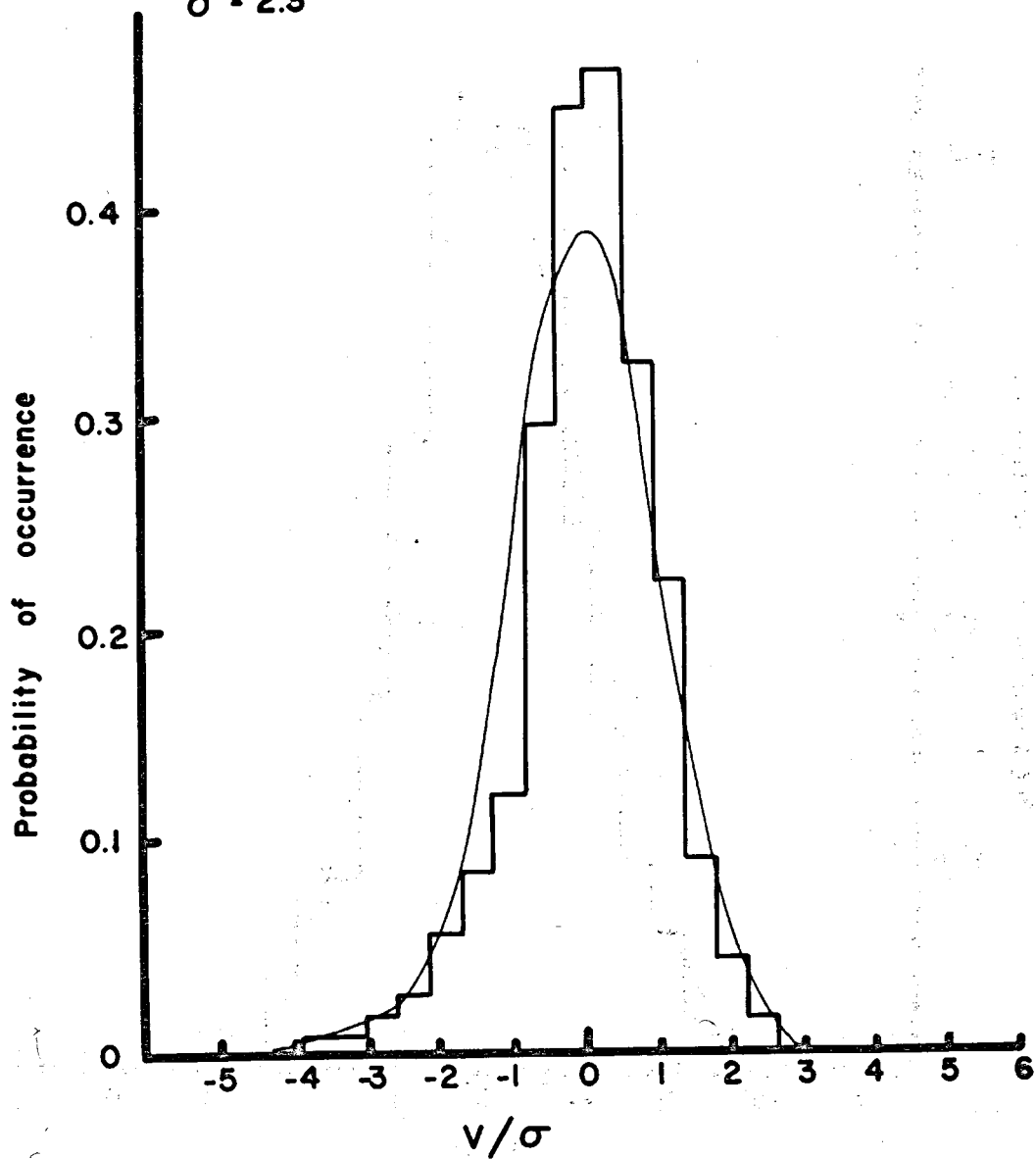


Figure 22. The distribution of N-S fluctuating current velocities recorded at EN-A between 31 October and 22 December 1974 compared to a Gaussian distribution (thin line) with the same mean and standard deviation ( $\sigma$ , in cm/sec)

EN-C  
31 Oct 74  
E-W velocity component  
1081 observations  
 $\sigma = 3.0$

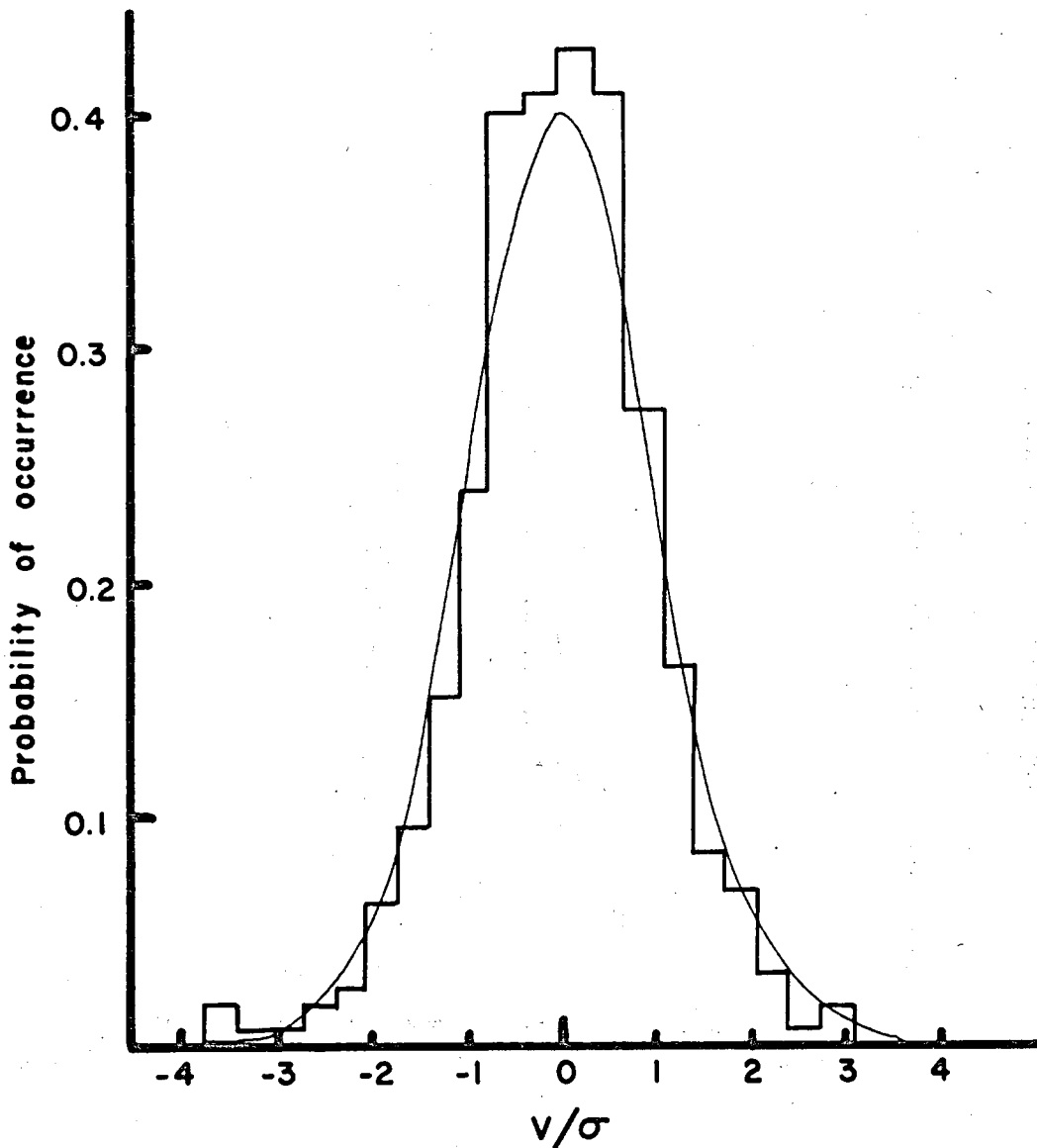


Figure 23. The distribution of E-W fluctuating current velocities recorded at EN-C between 10 October and 25 November 1974 compared to a Gaussian distribution (thin line) with the same mean and standard deviation ( $\sigma$ , in cm/sec)

EN-C  
31 Oct 74  
N-S velocity component  
1081 observations  
 $\sigma = 3.0$

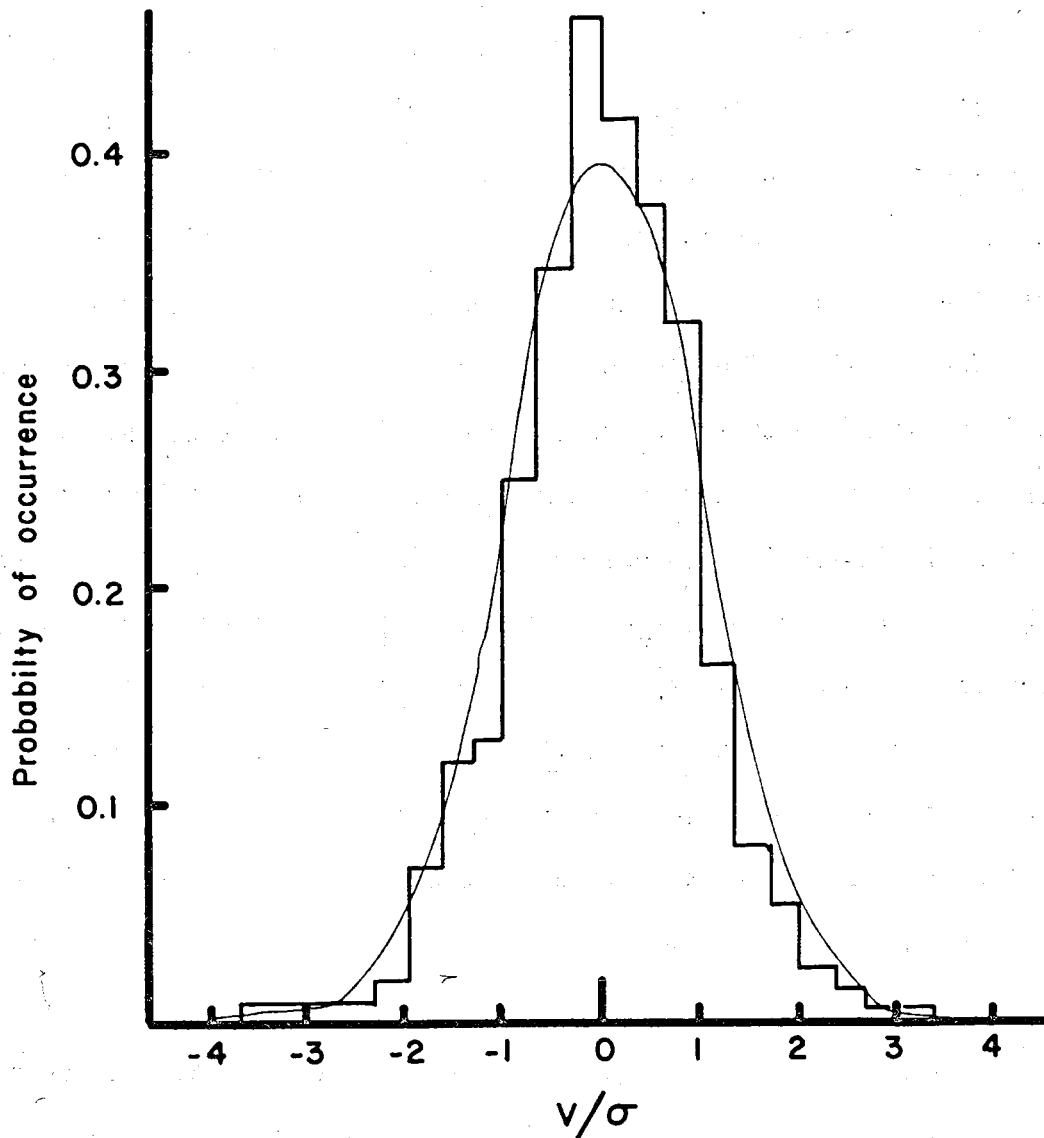


Figure 24. The distribution of N-S fluctuating current velocities recorded at EN-C between 10 October and 25 November 1974 compared to a Gaussian distribution (thin line) with the same mean and standard deviation ( $\sigma$ , in cm/sec)

the fluctuating speeds increase with increasing wind velocities<sup>33</sup>. In the central Sound in 20 m of water, the standard deviation of the fluctuating water velocities was found to increase by as much as a factor of two during stormy conditions.

#### Summary and discussion

59. Tidal flow at the Eatons Neck site is generally in accord with that expected on the basis of the model of Redfield<sup>14</sup>. However, the shallow-water constituents are much more strongly developed here than in the central and eastern Sound. They are responsible for the substantial departure of the current curves from simple sinusoidal form. The net flow of bottom water through the study area is westward. This is in accord with the general picture of estuarine circulation in the Sound, but the rate of the net drift is substantially greater than that indicated in original work of Riley<sup>17</sup> on this problem. None of the current meters detected a shoreward flow of water into longshore mixing zones, such as exist in the central Sound<sup>12</sup>. The regional description of the average net drift is indicative of the long-term motion of suspended material near the bottom. There should not be, therefore, any shoreward advective transport of disposed material from the Eatons Neck study area.

60. The shallow-water tidal constituents decrease the time during which the tidal stream flows faster than the critical erosion velocity of the sediment. No significant seasonal variation in the westward drift of the bottom water was detected. As in the central Sound<sup>12</sup>, the bottom water drift is not directly influenced by wind

stress. At site EN-A Cable and Anchor Reef apparently shields the bottom from the net bottom drift. This would, therefore, be a particularly favorable location for the retention of material placed on the bottom.

61. The water depth at EN-N and EN-S is sufficiently great that disturbance of the bottom by the orbital particle motion due to waves on the surface is not expected during ordinary winter storms, such as occurred in March 1975. The most important source of disturbance of the bottom during storms is the enhanced level of the fluctuating component of the tidal stream speed in central Long Island Sound<sup>33</sup>. A similar relationship is found at the Eatons Neck site, and the effect of this disturbance on the suspension of bottom material is discussed in a later section.

62. Both sedimentary and hydraulic conditions at the Eatons Neck study site are generally similar to those at the New Haven disposal site. Thus, many of the observations on the consequences of the disposal of dredged material at New Haven are expected to be applicable at Eatons Neck.

#### Sediment Resuspension

63. The variations in the suspended sediment load were measured over a 22-hr period at the EN-N site beginning at 1800 hr on 24 March 1975. The water depth was 20.5 m and the bottom sediment was sandy silt at this station. The concentration contour interval in Figure 25 is  $1 \times 10^{-5}$  g of sediment per gram of water; "H" and "L" denote times



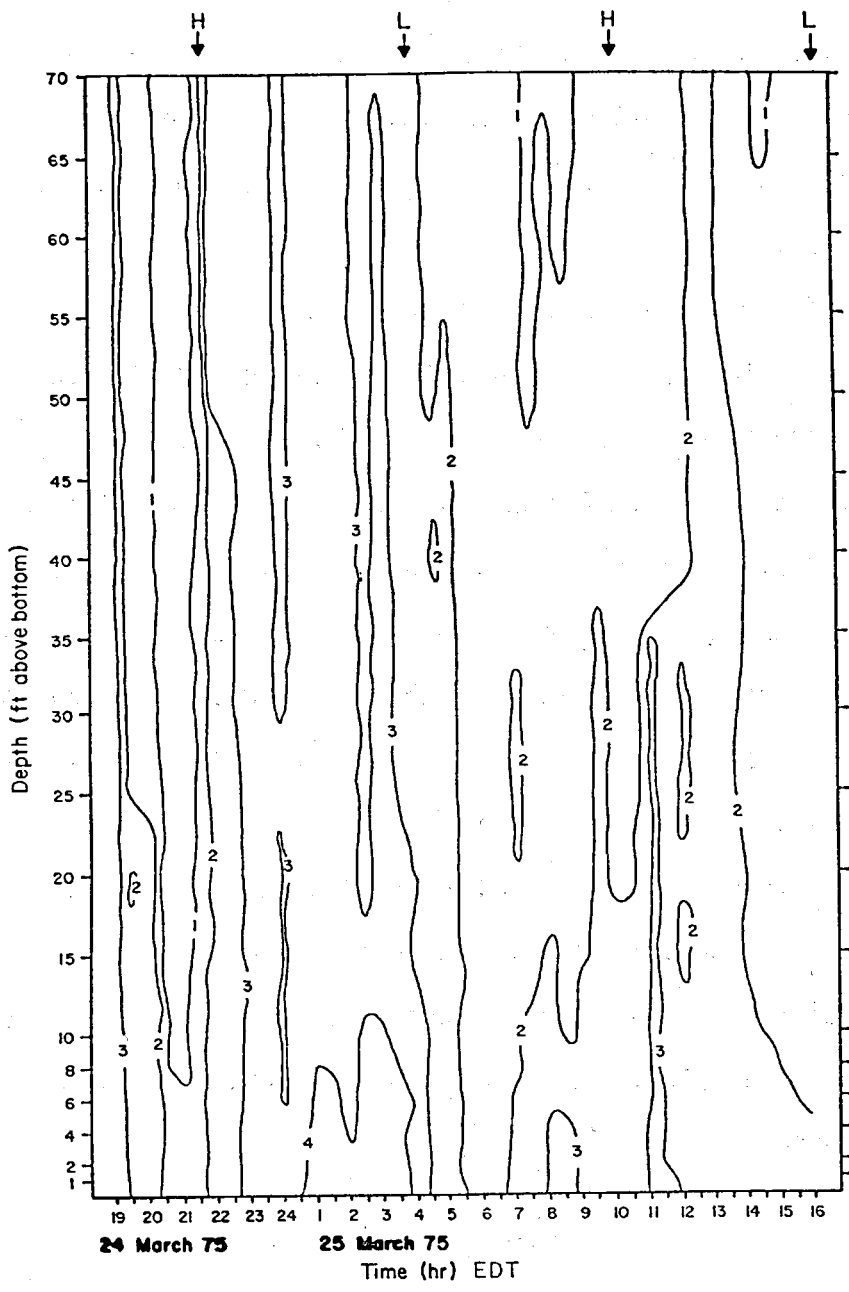


Figure 25. Contours of suspended sediment concentration as a function of water depth from transmissometer measurements made about every 30 min from 1900 hr 24 March until 1600 hr 25 March 1974, at EN-N. The concentration contour interval is  $1 \times 10^{-5}$  g of sediment/g of water. "H" and "L" denote times of high and low water. Wind velocity vectors recorded on shipboard are also plotted beneath the contour plot

of high and low water respectively. The wind velocity vectors are also shown below the contour plot.

64. A northeast wind blew for the first 5 hr of the experiment; however, the wave gauge in operation at Cable and Anchor Reef did not record any significant wave activity at the bottom. Calculated maximum orbital velocities would be less than 1 cm/sec at EN-N during the turbidity observations. While the bottom water flow was undisturbed by wind-generated waves, the wind stress at the surface increased the magnitude of the fluctuating water velocity near the bottom (see paragraph 57). This phenomenon has been documented in central Long Island Sound by Bokuniewicz, Gordon, and Pilbeam<sup>33</sup>.

65. The current speed at the EN-N during the turbidity experiment exhibited large variations until 2100 hr on 24 March 1975 (Figure 26a). Figure 26b is a graph of the magnitude of the fluctuating water-velocity component for the current meter record during this period and the wind speed squared recorded at the station. The period of high winds between 1900 and 2100 hr corresponds with about a twofold increase in the magnitude of the water-velocity fluctuations.

66. While the wind speeds and, consequently, the fluctuations in the water speeds, were high, there was little vertical suspended sediment concentration gradient in the water column (Figure 25). Even though the wind did not generate waves large enough to produce significant orbital velocities at the bottom, vertical mixing was enhanced by an increase in the magnitude of water-velocity fluctuations.

67. The total amount of suspended sediment in the water column

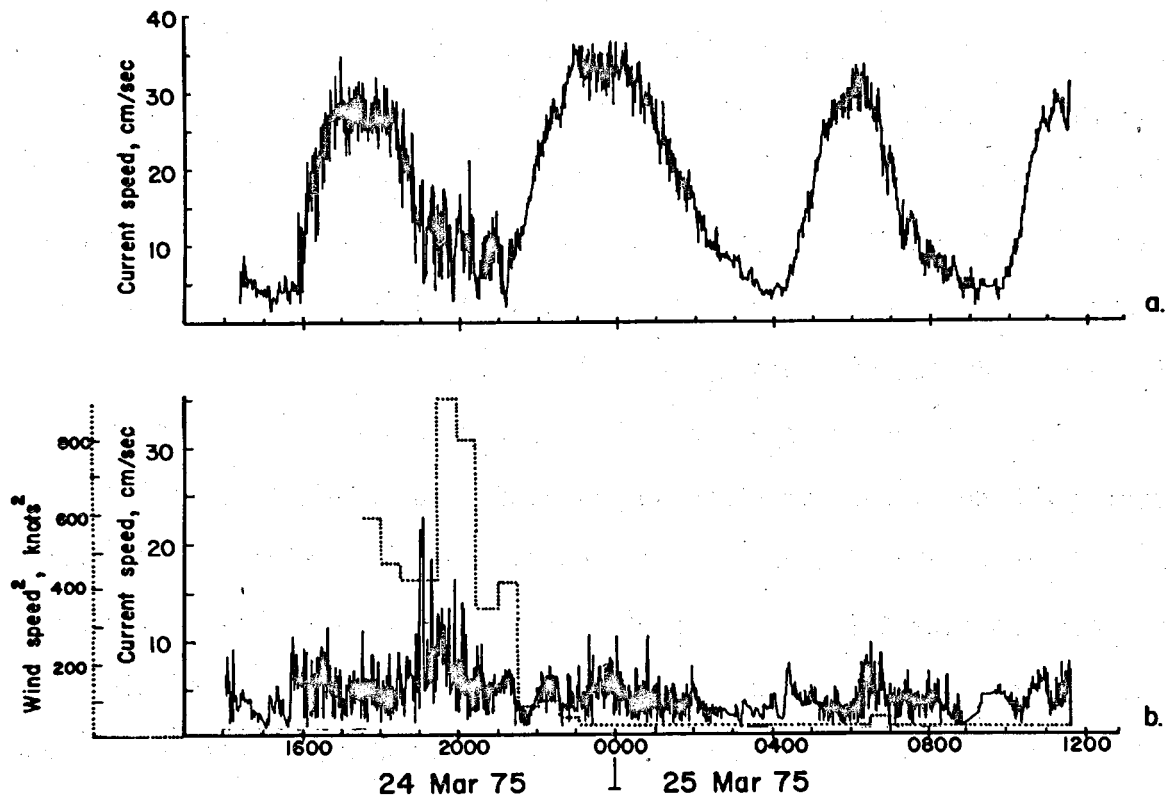


Figure 26. a. Current speed recorded 2 m above the bottom at EN-N during the transmissometer measurements, 24 March 1974  
b. Fluctuating current speed (solid line) from the record in a compared to the wind speed (dotted line) squared on shipboard

is shown in Figure 27. The greatest increase in the suspended sediment concentration occurs between 2000 and 2100 hr on 24 March 1975. During this period the mean tidal current speed was low (8 cm/sec, Figure 26), so little water was advected past the observation point. Thus, it is reasonable to assume that the change in turbidity is due to the addition of bottom sediment to the water column and not caused by the sampling of water masses of different turbidities being advected past the station. Although the mean flow velocity during this period was low, large fluctuations in the velocity about this mean occurred and occasionally raised the velocity to as much as 21 cm/sec. These events would sporadically resuspend bottom sediment. The observed increased concentration requires an addition of  $0.04 \text{ g/cm}^2$  of sediment to the water column. This change in the suspended load would require the resuspension of about 0.5 mm of the bottom sediment and is equivalent to a net flux of  $1.1 \times 10^{-5} \text{ g/cm}^2\text{-sec}$  into the water column between 2000 and 2100 hr. (The maximum observed turbidity level during the experiment could be accounted for by the resuspension of about 0.8 mm of bottom sediment.)

68. The high rate of resuspension observed between 2000 and 2100 hr is apparently due to the increase in water-velocity fluctuations at this time (Figure 26). The suspended load remains high throughout the ebb tide (2100 to 0300 hr, Figure 27). The observed suspended load was insensitive to the tidal currents since there is no measurable increase in the suspended sediment load during the subsequent flood tide (0430 to 0900 hr, Figure 27).

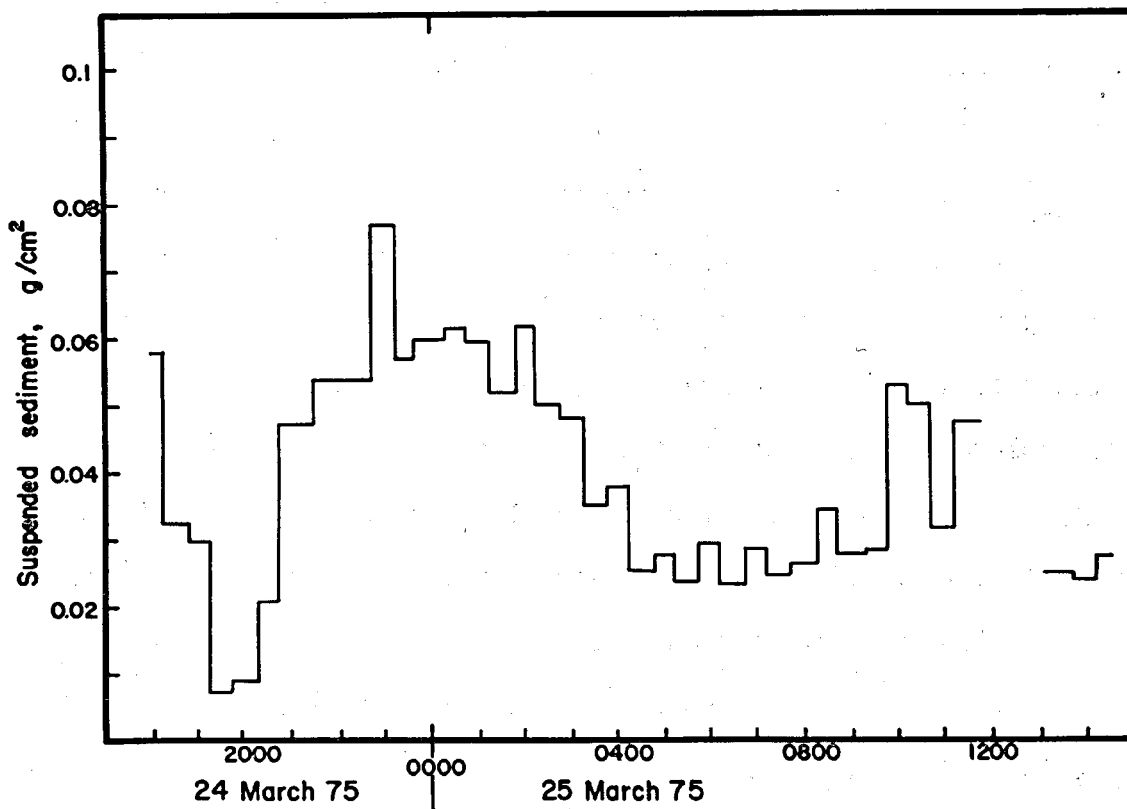


Figure 27. Total suspended sediment load in the water column measured with a transmissometer at EN-N, 24 March 1974

## Disturbance of the Bottom by Waves

69. Since the Eatons Neck disposal site is in relatively deep, protected water, frequent disturbance of the bottom by wind-generated waves on the water surface is not expected. The extent to which disturbance may occur is indicated by the record obtained from the wave recorder on Cable and Anchor Reef.

70. In Table 6 the smallest surface wave height that could be detected  $H_{\min}$  is listed as a function of wave period for this station. The tabulation shows that only waves with  $P > 3$  sec could be expected to be detected.

71. The maximum horizontal particle velocity on the bottom at the site of the wave recorder  $u_m$  is found from the relation

$$u_m = \frac{\pi H}{P \sinh 2\pi \frac{d}{\lambda}} \quad (15)$$

where  $H$  is the height,  $P$  the period, and  $\lambda$  the length of a wave on the surface and  $d$  is the water depth. Because the wave recorder was placed in relatively shallow water of the reef, particle velocities there would be higher than those expected to occur at the disposal site. Wave characteristics are not expected to change significantly between the disposal area and the measuring station on Cable and Anchor Reef. Hence,  $u_m$  at the disposal site can be calculated simply in terms of the increased depth and the wave period. Velocity ratios for 60- and 90-ft depths relative to the velocity at 45 ft are displayed in Table 7.

72. Shown in Plate 32 is  $u_m$  determined at the wave gauge site for the period when the recorder was in operation. Shown for comparison

are the square of the wind speed and the wind direction recorded at Eatons Neck Coast Guard Station. The figure shows that significant wave action on the bottom occurs only during easterly winds, as on 14 March 1975 and 19 May 1975; quite strong winds from other directions have very little effect, as on 26 March 1975. This is expected since it is only from the east that there is a long fetch at the Eatons Neck site, as is shown in Table 8 where the ratio of the fetch in each direction relative to the minimum fetch at this site is recorded. Values of  $u_m$  (Plate 32) were calculated from the average wave height in each 3-min recording period. Greater peak velocities may be expected to occur according to the same statistical distribution as do peak wave heights. For example, if  $\bar{u}_m$  is the mean peak speed,  $\bar{u}_m(1/10)$  the average of the highest ten percent, and  $\bar{u}_m(1/3)$  the "significant" value, then

$$\bar{u}_m / \bar{u}_m(1/3) = 0.625 \quad \bar{u}_m(1/10) / \bar{u}_m(1/3) = 1.27 \quad (16)$$

(Reference 34). The occasional occurrence of very high bottom velocities may be important in the excitation of sediment transport or in applying "stress" to benthic animals.

73. The development of waves during the storm of 14-15 March 1975 may be followed in the data presented in Table 9. Table 9 shows the average period  $\bar{P}$ , height  $\bar{H}$ , and wavelength  $\bar{\lambda}$ , as determined by each hourly record made by the recorder. The wind speeds and directions reported at Eatons Neck are also shown for comparison. During the period of easterly winds, waves are first detected with  $P = 4.4$  sec, the limit of sensitivity for this location. There is a progres-

sive increase in  $P$  and  $\lambda$  as the strength of the wind increases. However, the ratio of  $\bar{H}/\bar{\lambda}$  remains relatively small; only three observations exceed the 2.85% figure that marks the dividing point between swell and wind-driven waves. Thus, although waves of considerable height develop, the wave steepness remains quite small. The greatest  $\bar{u}_m$  (17 cm/sec) occurred at 1912 hr; at the disposal site the corresponding  $\bar{u}_m$  would be 11 cm/sec. Waves with the low  $\bar{H}/\bar{\lambda}$  observed are not fully developed and would, therefore, be expected to become larger if the easterly wind were to continue for a longer time. As soon as the wind diminishes or changes into the northwest, the sea state drops rapidly. Reliable estimates of the extent and frequency of bottom disturbance by waves could probably be made from weather records using the long-term wave climate data at the site. It is clear, however, that the principal effect of wind on the bottom at the disposal site is to increase the level of tidal stream turbulence and that effects due to wind-generated waves are less important.



#### PART IV: CONCLUSIONS

74. Summarized herein are the principal results that have an influence on the use of the Eatons Neck site as a repository for dredged material.

75. There is no physical evidence of significant dispersion of disposed material from the designated site; abundant evidence of the presence of disposed material is found within the site boundaries. In many places large mounds of deposited material are identified that must have been on the site for many years. Their continued presence is evidence that no large-scale dispersal is occurring. No physical evidence of the presence of dredged material is found outside of the site boundaries.

76. The physical evidence indicates that exchange of sediments with the surrounding sea floor occurs only for silt and clay-sized particles found in a layer approximately a centimeter thick at the sediment-water interface. This layer of sediment is being continually reworked by benthic animals and is subject to resuspension by the tidal stream. It is expected, therefore, that after disposal, the thin surficial layer of dredged material is intermixed with surficial sediments of the surrounding areas. Freshly deposited dredged material will soon be covered by this intermixed sediment, which then becomes a new habitat for benthic animals. Material below the intermixed layer is disturbed only to the depth penetrated by burrowing benthic animals. All material below this depth remains undisturbed.

77. There is no advective transport of water from the disposal

area toward either the Connecticut or the Long Island shore. The net drift of bottom water throughout the study area is observed to be westward; it is expected that most of it eventually flows out of the Sound through the East River into New York Harbor. The tidal displacement ellipse for water over the disposal site never reaches the shoreside mixing zone. Thus, the probability that any material entering the water column from the disposal site will ever reach either shore is very small.

78. The dominant source of energy to drive sediment transport processes in the study area is the tide. Although high wind stress increases the level of tidal stream turbulence, storms do not have an appreciable effect on the bottom at the disposal site. The sedimentary regime is in steady state and is not subject to large-scale perturbations.

79. On the basis of the evidence presented in this report, it is concluded that the Eatons Neck disposal site is well chosen to be a dredged material repository where sediment dispersion will be minimal.

## REFERENCES

1. Nittrouer, C. A., and Sternberg, R. W., "The Fate of a Fine Grained Dredge Spoils Deposit in a Tidal Channel of Puget Sound, Washington", Jour. Sed. Pet., Vol 45, 1975, pp 160-170.
2. Mauer, D., et al., "Effect of Soil Disposal on Benthic Communities Near the Mouth of Delaware Bay", submitted to Delaware River and Bay Authority, 1974, 235 pp.
3. Hydrographer of the Navy, Admiralty Manual of Hydrographic Surveying, Vol I, London, England, 1965.
4. Bokuniewicz, H. J., Gebert, J., and Gordon, R. B., "Sediment Mass Balance of a Large Estuary", Est. and Coast, Mar. Sci., in press, 1975.
5. Rhoads, D. C., and Cande, S., "Sediment Profile Camera for In Situ Study of Organism-Sediment Relations", Limnol. and Oceanogr., Vol 16, 1971, pp 110-114.
6. Gordon, R. B., "Hardness of the Sea-Floor in Near-Shore Waters", J. Geophys. Res., Vol 77, 1972, pp 3287-3293.
7. Bokuniewicz, H. J., Gordon, R. B., and Rhoads, D. C., "Mechanical Properties of the Sediment-Water Interface", Mar. Geol., Vol 18, 1975, pp 263-278.
8. Drunkers, J. J., Tidal Computations, North Holland Publ. Co., Amsterdam, 1964.
9. Doodson, A. T., and Warburg, H. O., Admiralty Manual of Tides, H.M.S.O., London, 1941.

10. Hydrographer of the Navy, Admiralty Tide Tables, Vol II, Taunton, England, 1975, 432 pp.
11. Williams, J., "Optical Properties of the Sea", U. S. Naval Institute, Annapolis, 1970.
12. Gordon, R. B., and Pilbeam, C. C., "Circulation in Central Long Island Sound", J. Geophys. Res., Vol 80, 1975, pp 414-422.
13. LeLacheur, E. A., and Sammons, J. C., "Tides and Currents in Long Island and Block Island Sounds", Spec. Publ. 174, U. S. Coast and Geod. Surv., Washington, D. C., 1932.
14. Redfield, A. C., "The Analysis of Tidal Phenomena in Narrow Embayments", Pap. Phys. Oceanogr. Meteorol., Vol 11, 1950, pp 1-35.
15. Ippen, A. T., and Harleman, D. R. F., "Tidal Dynamics of Estuaries", Estuary and Coastline Hydrodynamics, A. T. Ippen, ed., McGraw-Hill, New York, 1966.
16. Riley, G. A., "Hydrography of Long Island and Block Island Sounds", Bull. Bingham Oceanogr. Coll., Vol 13, 1952, pp 5-39.
17. Riley, G. A., "Oceanography of Long Island Sound, 1952-1954, Part 2", Bull. Bingham Oceanogr. Coll., Vol 15, 1956, pp 15-46.
18. Riley, G. A., "Transport and Mixing Processes in Long Island Sound", Bull. Bingham Oceanogr. Coll., Vol 19, 1967, pp 35-61.
19. Dana, J. D., "Geology of the New Haven Region, with Special Reference to the Origin of its Topographic Features", Trans. Connecticut Acad. of Arts and Sciences, Vol 2, 1870, pp 44-112.
20. Dana, J. D., "On Southern New England During the Melting of the Great Glacier; Absence of Marine Life from Long Island Sound

- Throughout the Glacial and Part of the Champlain Periods", Am. Jour. Sci., Third Series, Vol 10, 1875, pp 280-282.
21. Dana, J. D., "Long Island Sound in the Quaternary Era, with Observations on the Submarine Hudson River Channel", Amer. Jour. Sci., Third Series, Vol 40, 1890, pp 425-437.
  22. Smith, W. O., "Recent Underwater Surveys Using Low-Frequency Sound to Locate Bedrock", Geol. Soc. Am. Bull., Vol 69, 1958, pp 69-98.
  23. Grim, M. S., Drake, C. L., and Heirtzler, J. R., "Sub-Bottom Study of Long Island Sound", Geol. Soc. Am. Bull., Vol 81, 1970, pp 649-666.
  24. U.S.G.S. Misc. Geol. Inv., "Engineering Geology of the Northeast Corridor, Washington, D. C., to Boston, Massachusetts, Coastal Plain and Surficial Geology", Map 1-514-B, 1967.
  25. Flint, R. F., and Gebert, J., "The Latest Laurentide Ice Sheet: New Evidence from Southern New England", Geol. Soc. Am. Bull., in press, 1975.
  26. Bokuniewicz, H. J., Gordon, R. B., and Kastens, K., "Form and Migration of Sand Waves in a Large Estuary", Mar. Geol., submitted for publication, 1976.
  27. McCrone, A. W., Ellis, B. F., and Charmatz, R., "Preliminary Observation on Long Island Sound Sediments", New York Acad. Sci., Vol 24, 1961, pp 119-129.
  28. Buzas, M. A., "The Distribution and Abundance of Foraminifera in Long Island Sound", Smith Misc. Coll., Vol 149, No. 1, 1965.
  29. U. S. Army Engineer Waterways Experiment Station, CE, "Unified

- Soil Classification System", Technical Memorandum 3-357, 1953, Vicksburg, Mississippi.
30. Benninger, L., "The Uranium-Series Radionuclides as Tracers of Geochemical Processes in Long Island Sound", Ph.D. Thesis, submitted to Yale University, New Haven, Connecticut, 1976.
  31. McCall, P. L., "The Influence of Disturbance on Community Patterns and Adaptive Strategies of the Infaunal Benthos of Central Long Island Sound", Ph. D. Thesis, submitted to Yale University, New Haven, Connecticut, 1974.
  32. Bokuniewicz, H. J., et al., "Environmental Consequences of Dredge Spoil Disposal in Long Island Sound, Phase II", Geophysical Studies, November 1973 - November 1974, Report to New England Division, U.S.C.E.C.
  33. Bokuniewicz, H. J., Gordon, R. B., and Pilbeam, C. C., "Stress on the Bottom of an Estuary", Nature, Vol 257, 1975, pp 575-576.
  34. Defant, A., Physical Oceanography Vol 2, Macmillan, New York, 1961.
  35. Isaacs, J. D., et al., "Deep-Sea Moorings, Design and Use with Unmanned Instrument Stations", Bull. Scripps Inst. of Oceanography, Vol 8, 1963, pp 271-312.

Table 1

Eatons Neck Disposal Ground - Acoustic-Reflection Profiles

<u>Track #</u>	<u>Start</u>		<u>End</u>	
	<u>Latitude</u>	<u>Longitude</u>	<u>Latitude</u>	<u>Longitude</u>
1	40°55'55"	73°31'43"	41°00'12"	73°31'28"
2	41°01'30"	73°29'30"	40°57'41"	73°29'16"
3	40°57'23"	73°28'01"	41°01'37"	73°28'21"
4	40°57'14"	73°27'13"	41°02'18"	73°26'51"
5	41°01'49"	73°26'45"	40°58'10"	73°26'38"
6	41°01'38"	73°26'36"	40°58'07"	73°26'19"
7	41°02'19"	73°25'55"	40°57'21"	73°26'03"
8	41°02'25"	73°25'30"	40°55'51"	73°25'24"
9	41°02'35"	73°25'08"	40°57'20"	73°26'08"
10	40°57'21"	73°25'35"	41°02'02"	73°25'22"
11	41°02'27"	73°24'46"	40°57'06"	73°25'28"
12	40°58'11"	73°24'08"	41°02'28"	73°24'28"
13	40°58'16"	73°23'48"	41°03'15"	73°23'10"
14	41°03'41"	73°21'56"	40°58'11"	73°22'03"
15	41°04'35"	73°20'50"	40°57'31"	73°20'41"
16	40°57'15"	73°20'36"	41°04'32"	73°19'47"
17	41°01'22"	73°29'15"	40°58'56"	73°29'32"
18	40°58'54"	73°28'48"	41°01'08"	73°29'12"
19	41°01'35"	73°28'26"	40°58'36"	73°29'19"

Table 2

Bottom Photographs

<u>Station #</u>	<u>Depth, ft</u>	<u>Photograph #</u>	<u>Latitude</u>	<u>Longitude</u>
1	120	E3, E4	40 <sup>0</sup> 59'52.8"	73 <sup>0</sup> 25'38.4"
2	45	E1, E2, E5-E12	41 <sup>0</sup> 00'33.0"	73 <sup>0</sup> 25'13.2"



Table 3

Current Meter Stations

<u>Station</u>	<u>Location</u>	<u>Dates of Operation</u>	<u>Height of Meter(s) Above Bottom, ft</u>	<u>Mean Low Water Depth, ft</u>	<u>State of Data</u>
EN-A	41°00!2N 73°26!4W	31 Oct 74- 12 Dec 74	6	72	Processed
EN-A	41°00!2N 73°26!4W	18 Dec 74- 10 Jan 75	6	72	Processed
EN-A1	41°00!2N 73°26!4W	10 Jan 75- 22 Jan 75	6	72	Processed
EN-A2	41°00!2N 73°26!4W	10 Jan 75- 22 Jan 75	9	72	Processed
EN-A3	41°00!2N 73°26!4W	10 Jan 75- 22 Jan 75	15	72	No data
EN-A4	41°00!2N 73°26!4W	10 Jan 75- 22 Jan 75	25	72	Lost at General Oceanics
EN-A5	41°00!2N 73°26!4W	10 Jan 75- 22 Jan 75	35	72	Processed
EN-A6	41°00!2N 73°26!4W	10 Jan 75- 22 Jan 75	47	72	No data
EN-A7	41°00!2N 73°26!4W	10 Jan 75- 22 Jan 75	64	72	Processed

Table 3 (Continued)

<u>Station</u>	<u>Location</u>	<u>Dates of Operation</u>	<u>Height of Meter(s) Above Bottom, ft</u>	<u>Mean Low Water Depth, ft</u>	<u>State of Data</u>
EN-A	41 <sup>0</sup> 00:2N 73 <sup>0</sup> 26:4W	24 Jan 75-	6	72	Meter lost
EN-A	41 <sup>0</sup> 00:2N 73 <sup>0</sup> 26:4W	03 Mar 75- 01 Apr 75	6	72	Processed
EN-C	40 <sup>0</sup> 59:7N 73 <sup>0</sup> 27:6W	31 Oct 74- 25 Nov 74	6	86	Processed
EN-N 24a	41 <sup>0</sup> 00:55N 73 <sup>0</sup> 27:80W	24 Mar 75- 25 Mar 75	6	67	Processed
EN-N 24b	41 <sup>0</sup> 00:55N 73 <sup>0</sup> 27:80W	24 Mar 75- 25 Mar 75	6	67	Processed
EN-N 24c	41 <sup>0</sup> 00:55N 73 <sup>0</sup> 27:80W	24 Mar 75- 25 Mar 75	6	67	No data
EN-N 24d	41 <sup>0</sup> 00:55N 73 <sup>0</sup> 27:80W	24 Mar 75- 25 Mar 75	6	67	No data
EN-N 24e	41 <sup>0</sup> 00:55N 73 <sup>0</sup> 27:80W	24 Mar 75- 25 Mar 75	6	67	No data
EN-N	41 <sup>0</sup> 00:55N 73 <sup>0</sup> 27:80W	15 Apr 75- 07 May 75	6	67	Processed
EN-N	41 <sup>0</sup> 00:55N 73 <sup>0</sup> 27:80W	09 May 75- 29 May 75	6	67	Processed

Table 3 (Continued)

<u>Station</u>	<u>Location</u>	<u>Dates of Operation</u>	<u>Height of Meter(s) Above Bottom, ft</u>	<u>Mean Low Water Depth, ft</u>	<u>State of Data</u>
EN-Na	41°00'55N 73°27'80W	19 May 75- 10 Jun 75	6	67	No data
EN-Nb	41°00'55N 73°27'80W	19 May 75- 10 Jun 75	11	67	No data
EN-Nc	41°00'55N 73°27'80W	19 May 75- 10 Jun 75	21	67	Processed
EN-Nd	41°00'55N 73°27'80W	19 May 75- 10 Jun 75	36	67	Processed
EN-Ne	41°00'55N 73°27'80W	19 May 75- 10 Jun 75	45	67	No data
EN-1	41°01'09N 73°24'13W	10 Sep 74- 20 Sep 74	6	67	Processed
EN-2	41°00'3N 73°23'9W	09 Sep 74-	6	190	Meter lost
EN-3	41°00'32N 73°24'65W	09 Sep 74- 20 Sep 74	6	85	Processed
EN-4	41°00'7N 73°25'0W	09 Sep 74-	6	41	Meter lost
EN-5	40°59'82N 73°26'33W	09 Sep 74- 20 Sep 74	6	105	Processed

Table 3 (Continued)

<u>Station</u>	<u>Location</u>	<u>Dates of Operation</u>	<u>Height of Meter(s) Above Bottom, ft</u>	<u>Mean Low Water Depth, ft</u>	<u>State of Data</u>
EN-6a	40°58!2N 73°29!4W	10 Apr 75- 22 Apr 75	6	62	Processed
EN-6b	40°59!0N 73°29!3W	10 Apr 75- 22 Apr 75	6	71	Processed
EN-6c	40°59!8N 73°29!4W	10 Apr 75- 22 Apr 75	6	108	Processed
EN-6d	41°00!4N 73°29!4W	10 Apr 75- 22 Apr 75	6	76	Processed
EN-6e	41°00!9N 73°29!3W	10 Apr 75- 22 Apr 75	6	65	No data
EN-6f	41°01!3N 73°29!2W	10 Apr 75- 22 Apr 75	6	56	Processed
EN-7a	40°58!8N 73°20!5W	30 Apr 75- 09 May 75	6	65	Processed
EN-7b	40°59!8N 73°20!9W	30 Apr 75- 09 May 75	6	81	No data
EN-7c	41°00!2N 73°20!5W	30 Apr 75- 09 May 75	6	96	Processed
EN-7d	41°01!2N 73°20!2W	30 Apr 75- 09 May 75	6	92	Processed

Table 3 (Concluded)

<u>Station</u>	<u>Location</u>	<u>Dates of Operation</u>	<u>Height of Meter(s) Above Bottom, ft</u>	<u>Mean Low Water Depth, ft</u>	<u>State of Data</u>
EN-7e	41°02'1N 73°20'1W	30 Apr 75- 09 May 75	6	42	Processed
EN-7f	41°03'4N 73°19'7W	30 Apr 75- 09 May 75	6	32	Processed

Table 4  
Parameters for Wave Calculations

<u>P sec</u>	<u><math>\lambda</math> ft</u>	<u><math>d/\lambda</math></u>	<u><math>2\pi d/\lambda</math></u>	<u><math>\cosh 2\pi d/\lambda</math></u>	<u><math>\tanh 2\pi d/\lambda</math></u>
1	5.1	8.78	55.1		
2	20.4	2.21	13.9	>200,000	1.0
3	46.0	0.978	6.14	233	1.0
4	81.8	0.550	3.45	15.7	0.998
5	126	0.354	2.22	4.65	0.977
6	171	0.263	1.65	2.70	0.929
7	217	0.207	1.30	1.97	0.862
8	261	0.172	1.08	1.64	0.793

Table 5

Harmonic Constants

<u>Tidal Component</u>	<u>Speed deg/hr</u>	<u>Tidal Constants</u>	
		<u>g deg</u>	<u>H cm/sec</u>
<u>EN-A 15 Nov 74: 29-day Regression Analysis</u>			
K <sub>1</sub>	15.0411	342.36	0.63
O <sub>1</sub>	13.9430	93.27	0.04
Q <sub>1</sub>	13.3987	331.80	0.27
L <sub>2</sub>	29.5285	316.65	1.89
M <sub>2</sub>	28.9841	56.39	14.99
MU <sub>2</sub>	27.9682	215.44	0.54
N <sub>2</sub>	28.4397	23.65	4.56
S <sub>2</sub>	30.0000	74.15	3.38
MK <sub>3</sub>	44.2517	237.09	0.21
MO <sub>3</sub>	42.9271	304.26	0.19
M <sub>4</sub>	57.9682	305.45	0.91
MN <sub>4</sub>	57.4238	316.56	0.38
MS <sub>4</sub>	58.9841	359.86	0.43
M <sub>6</sub>	86.9523	142.94	3.40
2MN <sub>6</sub>	86.4079	131.44	2.33
2MS <sub>6</sub>	87.9682	166.94	1.92
MSN <sub>6</sub>	87.4238	144.34	0.77
2SM <sub>6</sub>	88.9841	151.14	0.29

(Continued)

Table 5 (Concluded)

Tidal Component	Speed deg/hr	Tidal Constants	
		g deg	H cm/sec
<u>EN-C 7 Nov 74: 15-day Regression Analysis</u>			
K <sub>1</sub>	15.0411	25.39	1.62
O <sub>1</sub>	13.9430	110.21	0.75
Q <sub>1</sub>	13.3987	337.80	0.64
L <sub>2</sub>	29.5285	146.66	7.55
M <sub>2</sub>	28.9841	87.55	24.11
MU <sub>2</sub>	27.9682	308.25	2.10
N <sub>2</sub>	28.4397	19.41	4.91
S <sub>2</sub>	30.0000	20.97	4.48
MK <sub>3</sub>	44.2517	236.73	0.47
MO <sub>3</sub>	42.9271	223.16	0.30
M <sub>4</sub>	57.9682	295.23	1.40
MN <sub>4</sub>	57.4238	330.12	0.85
MS <sub>4</sub>	58.9841	266.06	0.52
M <sub>6</sub>	86.9523	251.75	1.28
2MN <sub>6</sub>	86.4079	167.75	3.42
2MS <sub>6</sub>	87.9682	135.12	2.29
MSN <sub>6</sub>	87.4238	297.87	2.29
2SM <sub>6</sub>	88.9841	154.05	0.57



Table 6

Minimum Detectable Wave Height

<u>P</u> <u>sec</u>	<u>H</u> <sub>min</sub> <u>ft</u>
1	
2	>800
3	28
4	0.63
5	0.18
6	0.11
7	0.08
8	0.06

Table 7

Velocity Ratios Relative to Velocity at 45-ft Depth

<u>P, sec</u>	<u>d = 60 ft</u>	<u>d = 90 ft</u>
4	0.320	0.019
5	0.468	0.106
6	0.655	0.235
7	0.790	0.358

Table 8

Fetch Factors for Eatons Neck - Cable and Anchor Reef

<u>Fetch/minimum fetch</u>	
10 <sup>0</sup>	1.23
20 <sup>0</sup>	1.67
30 <sup>0</sup>	2.50
40 <sup>0</sup>	3.20
50 <sup>0</sup>	4.85
60 <sup>0</sup>	9.50
70 <sup>0</sup>	10.0
80 <sup>0</sup>	10.0
90 <sup>0</sup>	10.0
100 <sup>0</sup>	4.47
110 <sup>0</sup>	4.43
120 <sup>0</sup>	3.76
130 <sup>0</sup>	2.53
140 <sup>0</sup>	2.04
150 <sup>0</sup>	1.97
160 <sup>0</sup>	1.13
170 <sup>0</sup>	1.30
180 <sup>0</sup>	1.70
190 <sup>0</sup>	1.50
200 <sup>0</sup>	1.53
210 <sup>0</sup>	1.57
220 <sup>0</sup>	1.57
230 <sup>0</sup>	2.84
240 <sup>0</sup>	6.10
250 <sup>0</sup>	2.47
260 <sup>0</sup>	3.74
270 <sup>0</sup>	3.10
280 <sup>0</sup>	1.57
290 <sup>0</sup>	1.63
300 <sup>0</sup>	1.47
310 <sup>0</sup>	1.13
320 <sup>0</sup>	1.20
330 <sup>0</sup>	1.13
340 <sup>0</sup>	1.17
350 <sup>0</sup>	1.00
360 <sup>0</sup>	1.27

Table 9  
Storm Wave Properties

Date	Hour (R)	$\bar{P}^*$ , sec	$\bar{H}^{**}$ , ft	$\bar{\lambda}^{***}$ , ft	$\bar{H}/\bar{\lambda}$ Percent	Wind	
						Speed, kt	Direction
14 Mar 75	0712	4.4	1.2	103	1.1	20	070
14 Mar 75	0812	4.4	1.2	99	1.1		
14 Mar 75	0912	4.3	1.4	98	1.4		
14 Mar 75	1012	4.0	3.9	83	4.7	23	135
14 Mar 75	1212	5.1	1.7	134	1.3		
14 Mar 75	1312	5.2	1.8	135	1.3	24	135
14 Mar 75	1412	5.6	2.0	152	1.3		
14 Mar 75	1512	6.3	2.0	183	1.1		
14 Mar 75	1612	6.7	3.6	203	1.8	33	135
14 Mar 75	1712	6.3	4.7	181	2.6		
14 Mar 75	1812	6.2	5.0	178	2.8		

(Continued)

\* $\bar{P}$  = average period of wave  
 \*\* $\bar{H}$  = average height of wave  
 \*\*\* $\bar{\lambda}$  = average wavelength of wave

Table 9 (Concluded)

Date	Hour (R)	$\bar{P}$ , sec	$\bar{H}$ , ft	$\bar{\lambda}$ , ft	$\frac{\bar{H}}{\bar{\lambda}}$ Percent	Wind	
						Speed, kt	Direction
14 Mar 75	1912	5.9	6.2	166	3.7	30	135
14 Mar 75	2012	6.6	3.3	195	1.7		
14 Mar 75	2112	6.3	3.4	185	1.8		
14 Mar 75	2212	5.4	3.5	143	2.4	20	090
14 Mar 75	2312	6.1	2.3	175	1.3		
15 Mar 75	0012	5.7	1.9	157	1.2		
15 Mar 75	0112	5.8	1.6	161	1.0	20	045
15 Mar 75	0212	6.0	1.2	172	0.7		
15 Mar 75	0312	5.3	1.0	140	0.7		
15 Mar 75	0412	4.8	1.3	120	0.9	20	020
15 Mar 75	0512	5.1	0.6	129	0.4		
15 Mar 75	0712					15	360

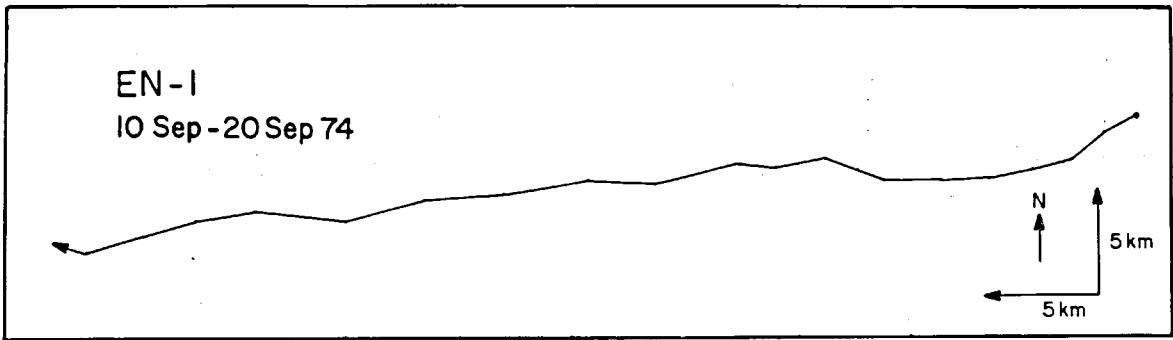


Plate 1

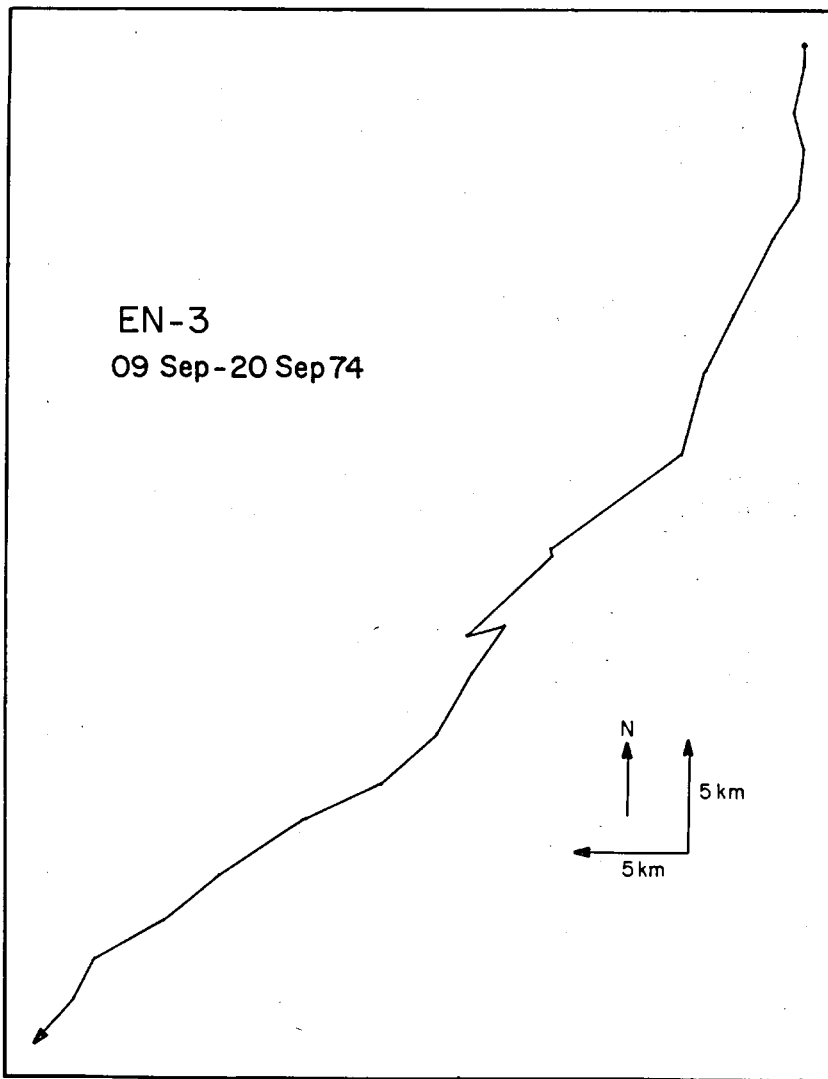


Plate 2

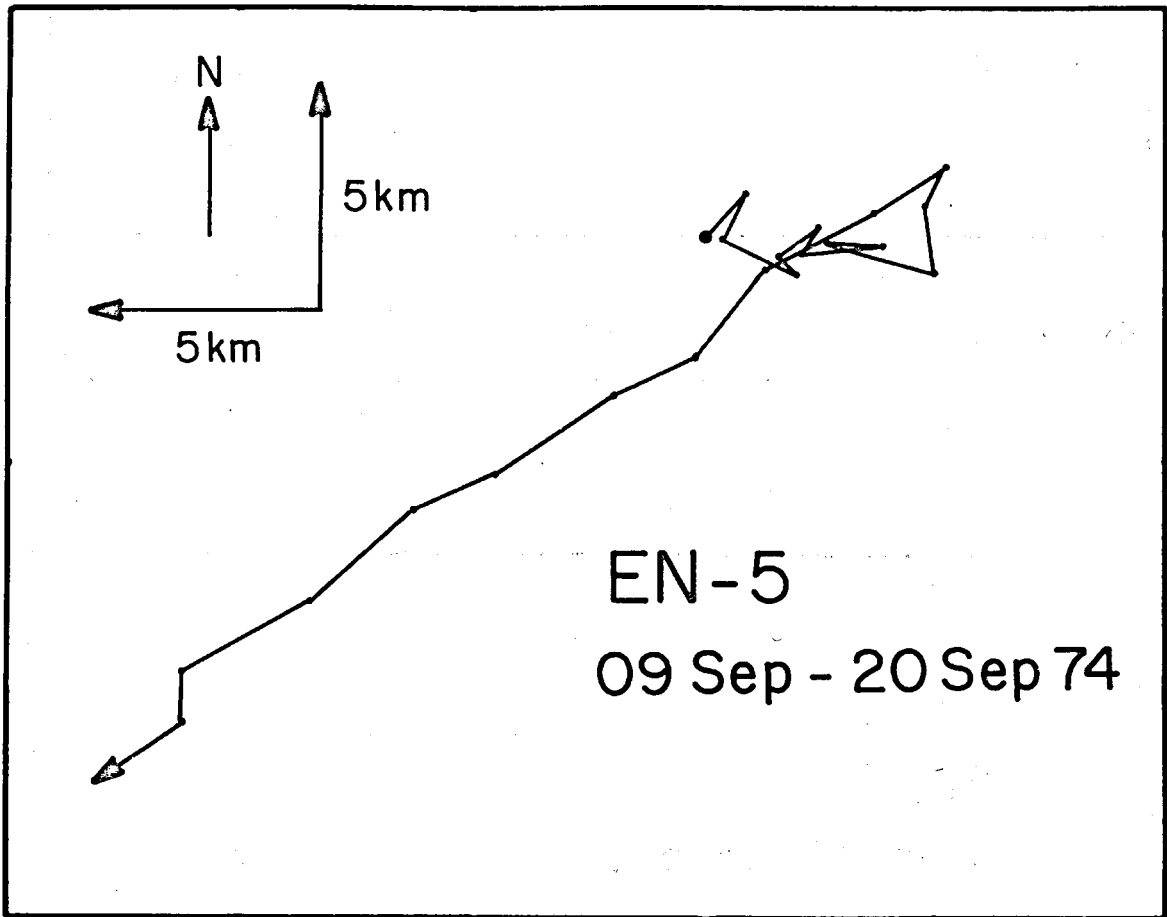


Plate 3

**EN-6b**

10 Apr - 22 Apr 75

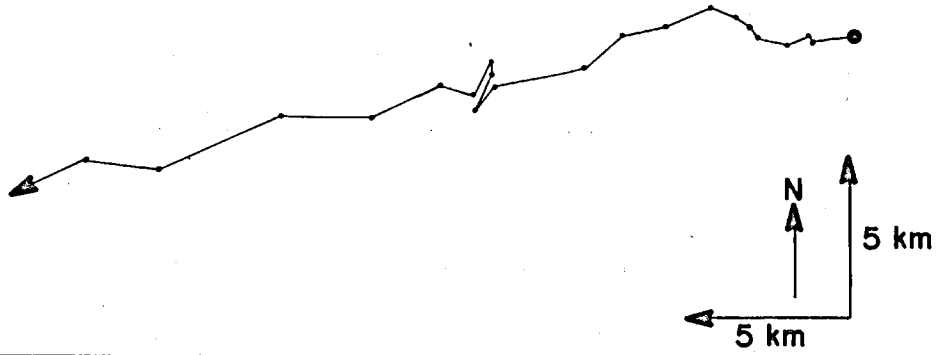


Plate 4

**EN-6c**

10 Apr - 23 Apr 75

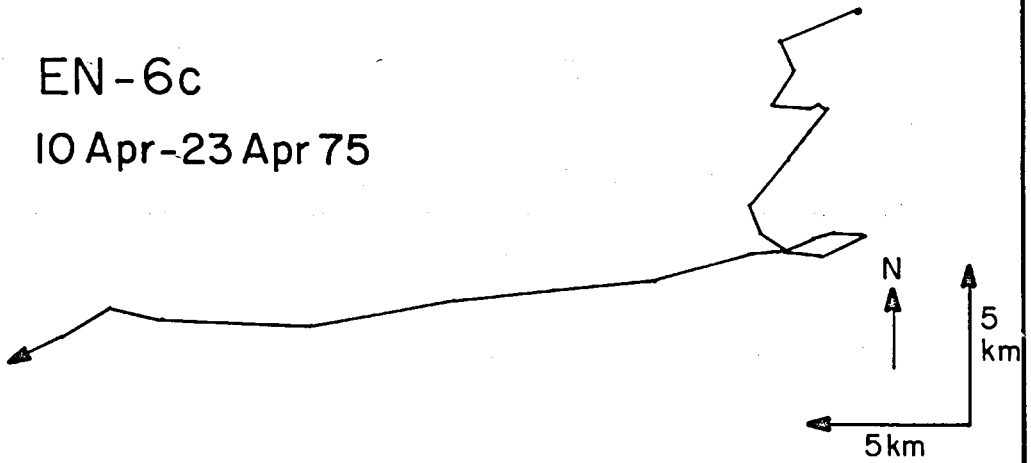


Plate 5

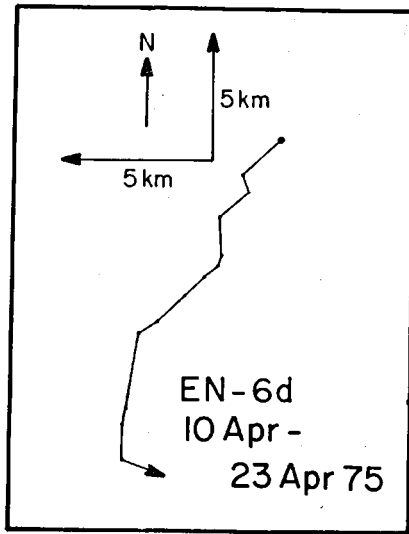


Plate 6

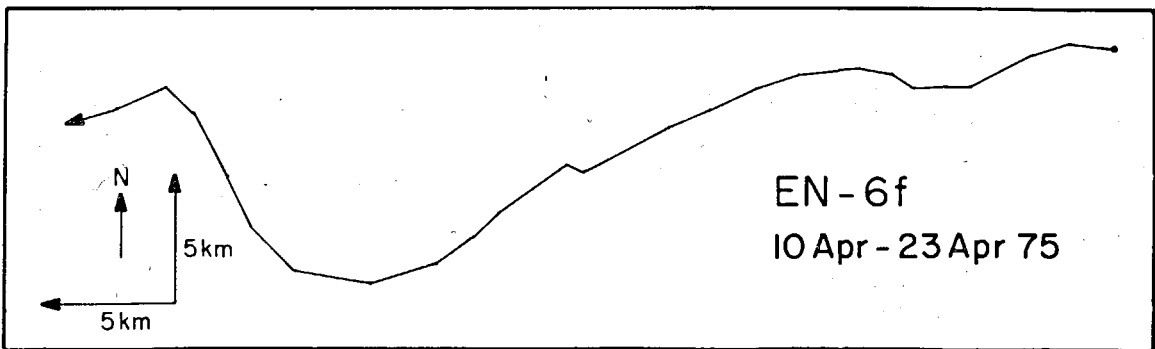


Plate 7



**EN-7c**

30 Apr - 09 May 75

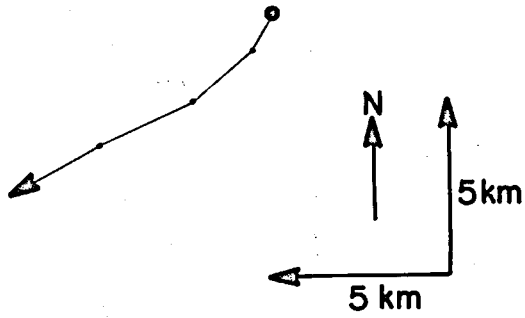


Plate 8

**EN-7d**

30 Apr - 09 May 75

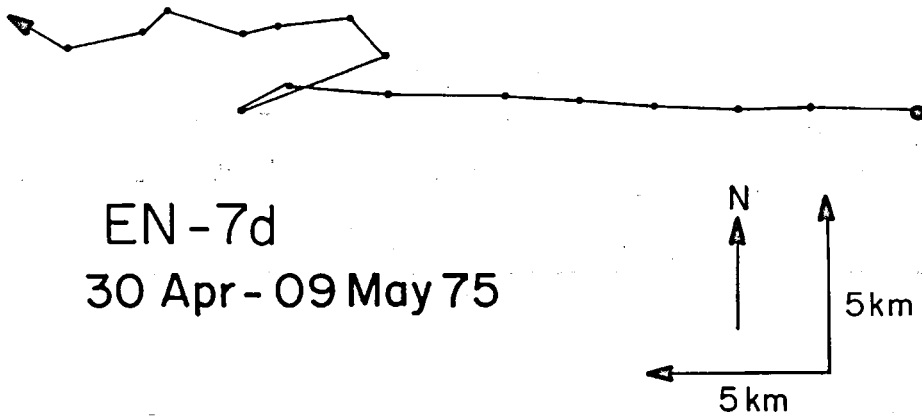


Plate 9

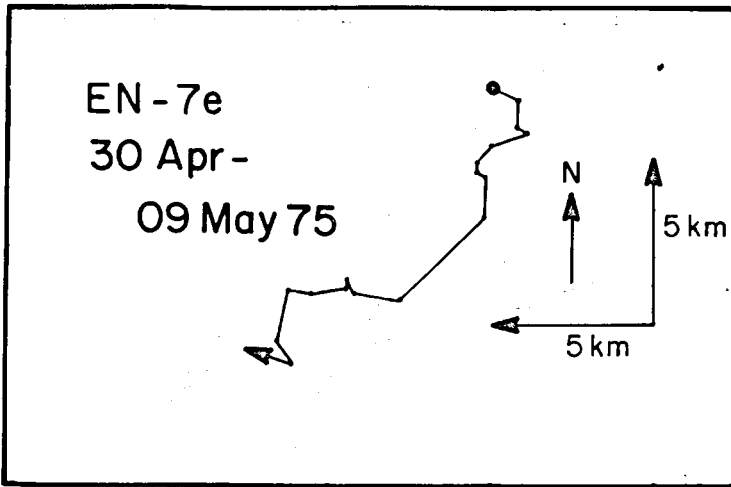


Plate 10

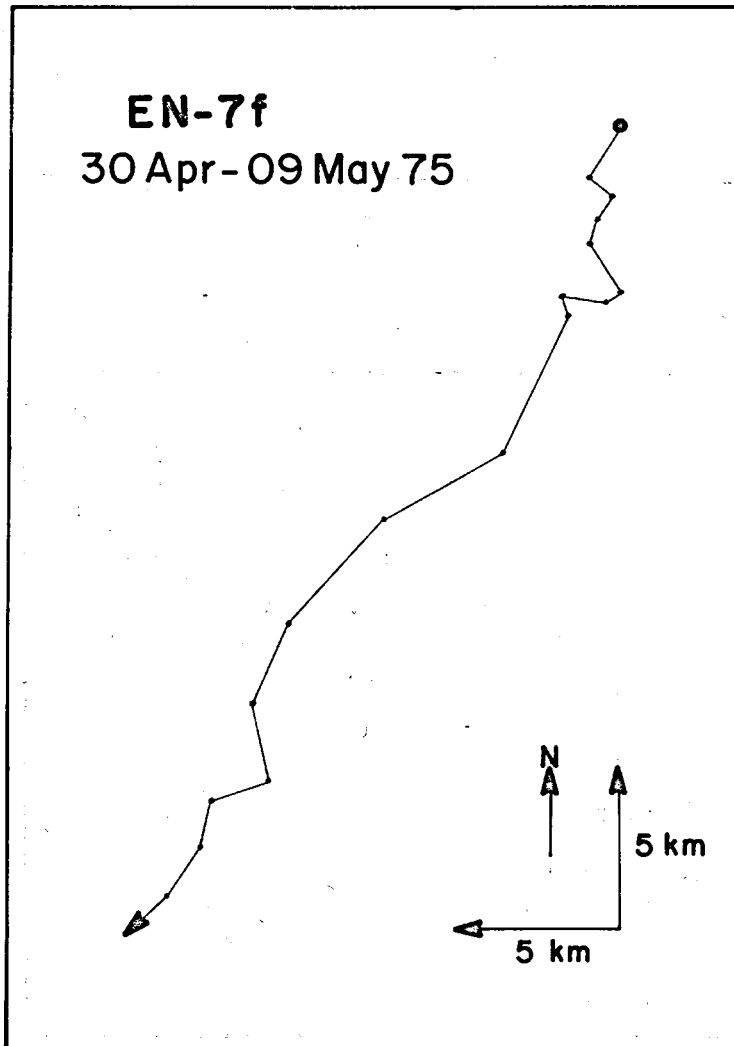


Plate 11

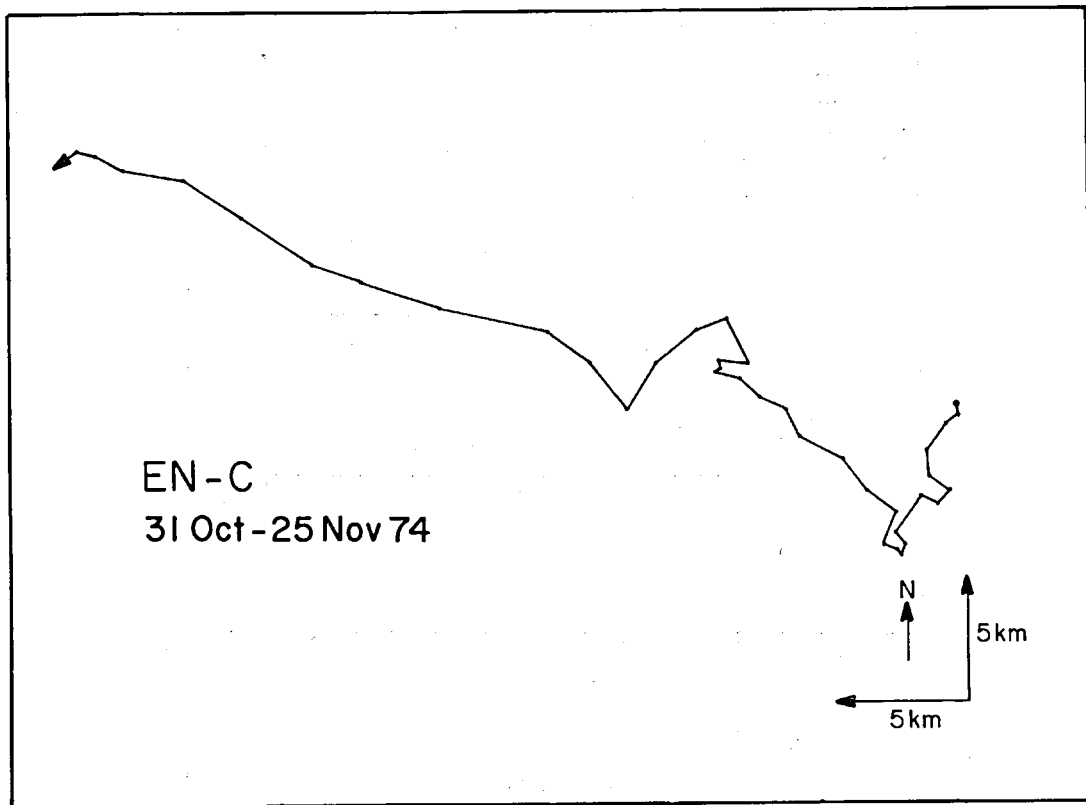


Plate 12

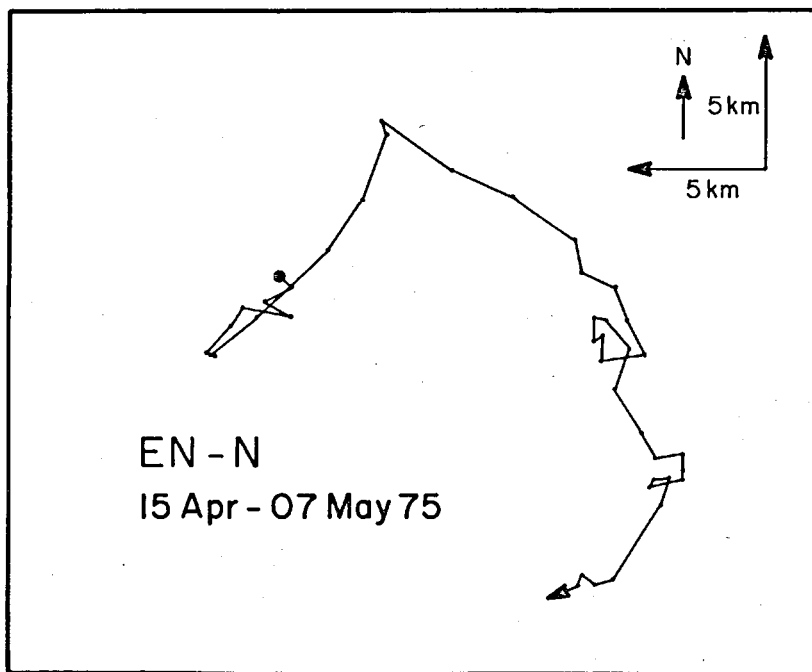
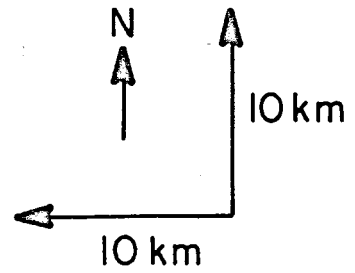
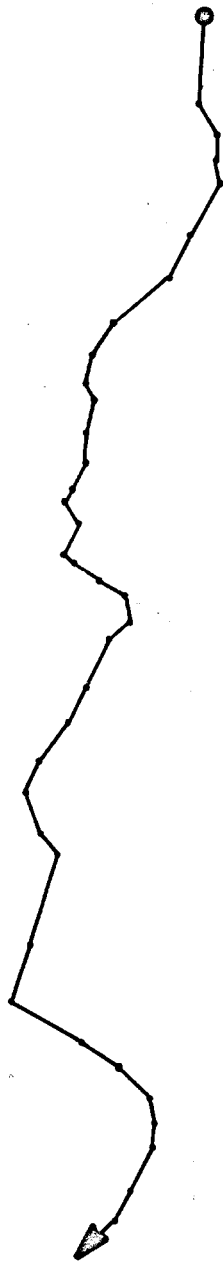


Plate 13

EN - N  
09 May -  
29 May 75



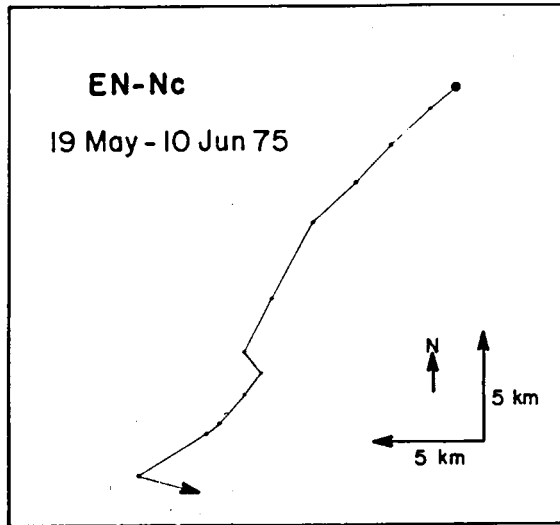


Plate 15

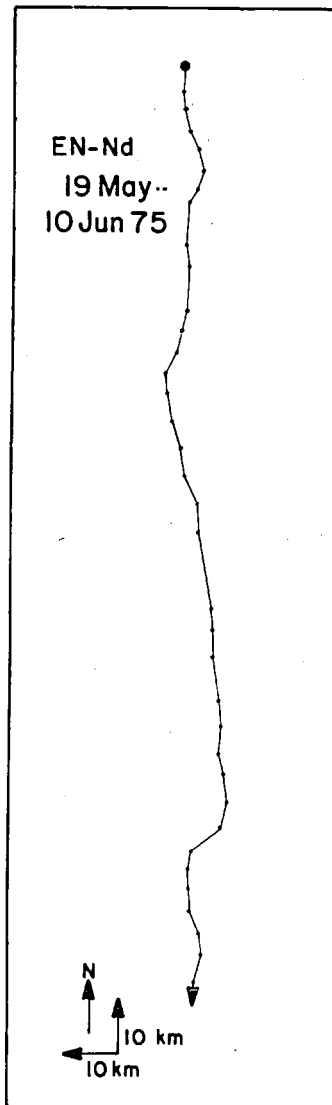


Plate 16

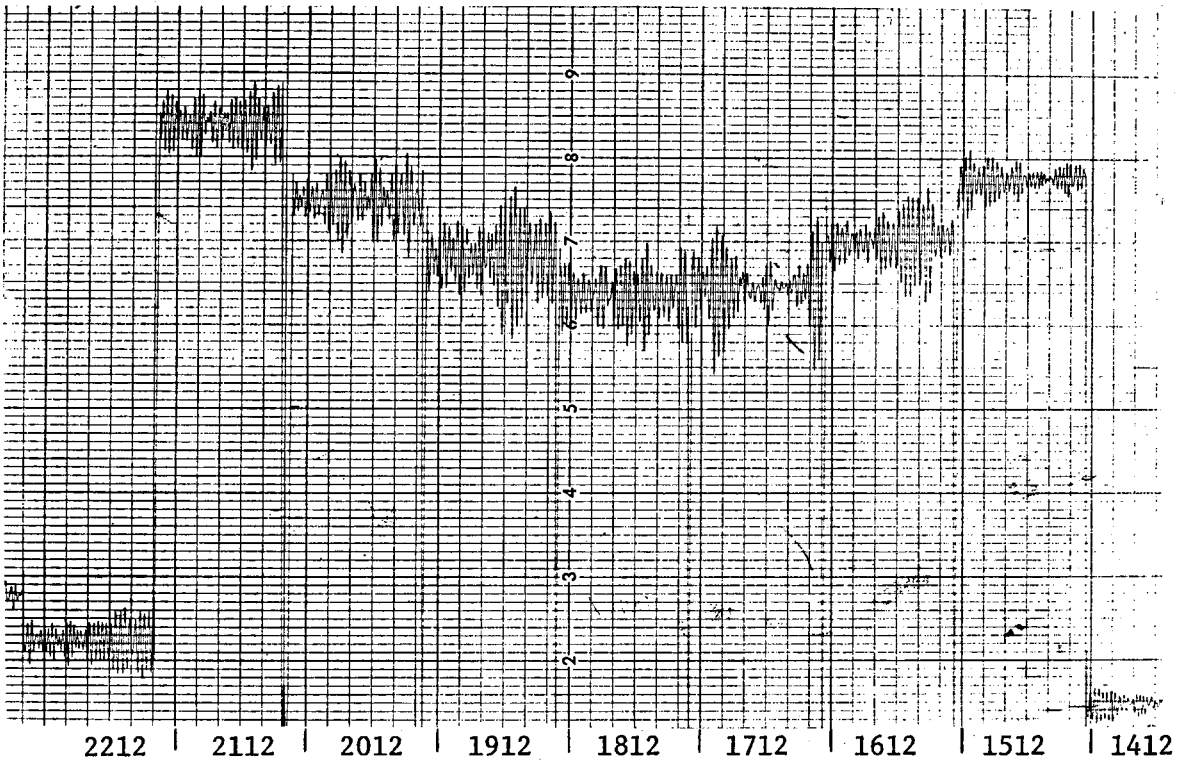
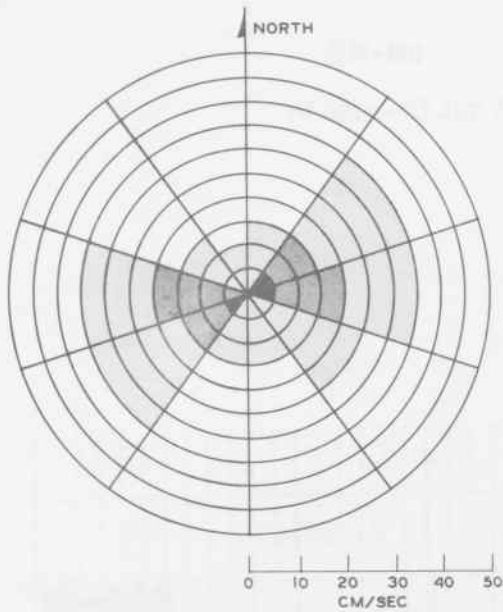
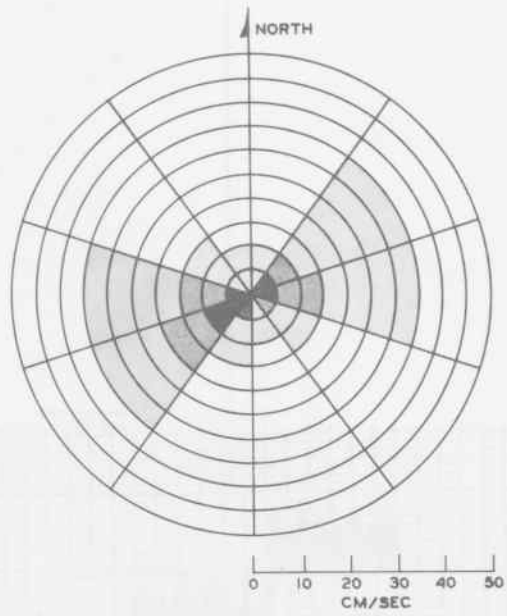


Plate 17

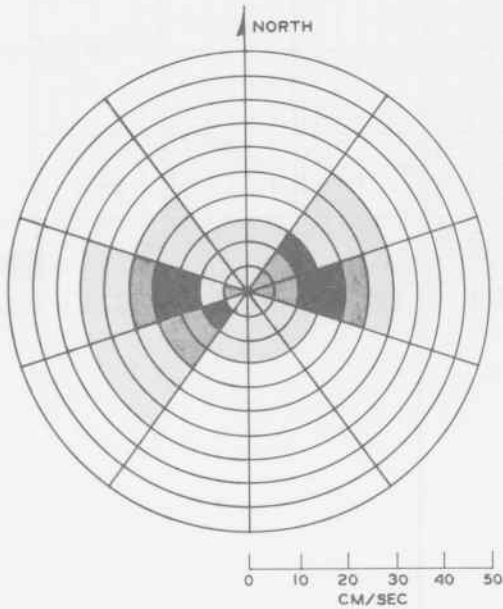


EN-A 31 OCT-12 DEC 74  
2534 obs

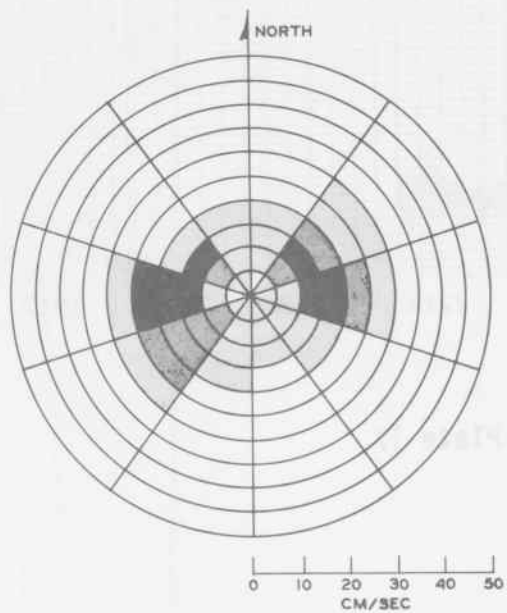


EN-A 18 DEC 74-10 JAN 75  
1648 obs

Plate 18

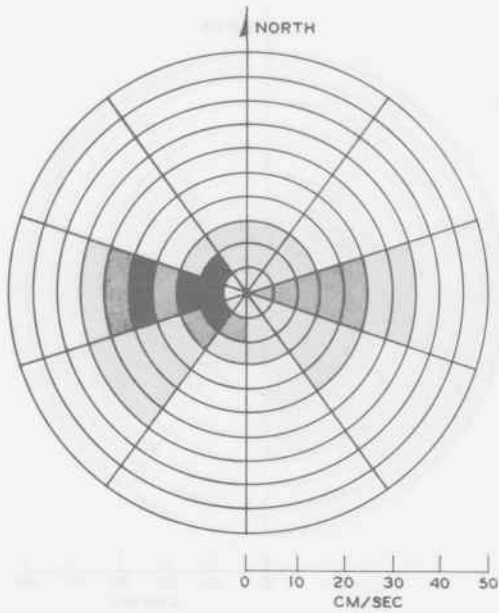


EN-A 03 MAR-01 APR 75  
2218 obs

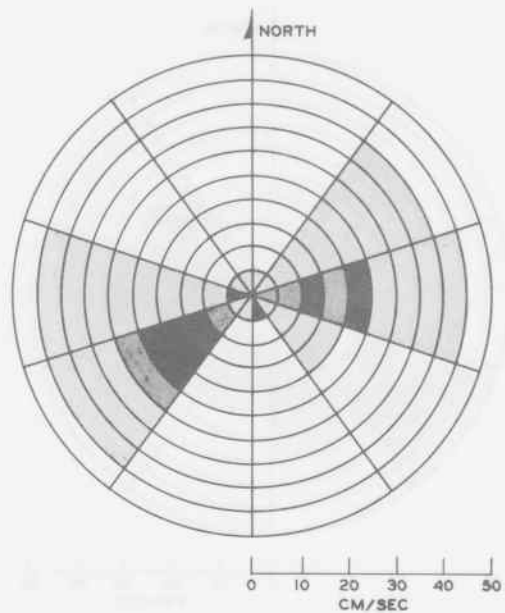


EN-A1 10 JAN-22 JAN 75  
852 obs

Plate 19

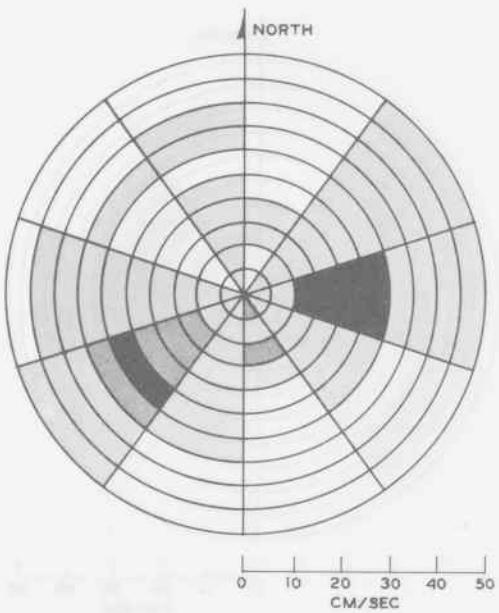


EN-A2 10 JAN-22 JAN 75  
1158 obs

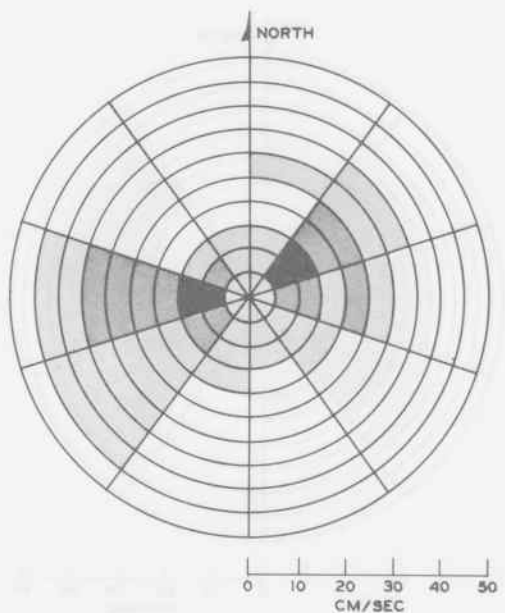


EN-A5 10 JAN-22 JAN 75  
1140 obs

Plate 20



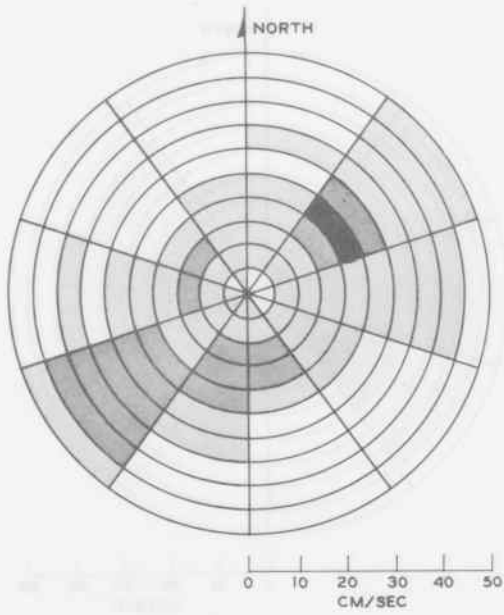
EN-A7 10 JAN-22 JAN 75  
997 obs



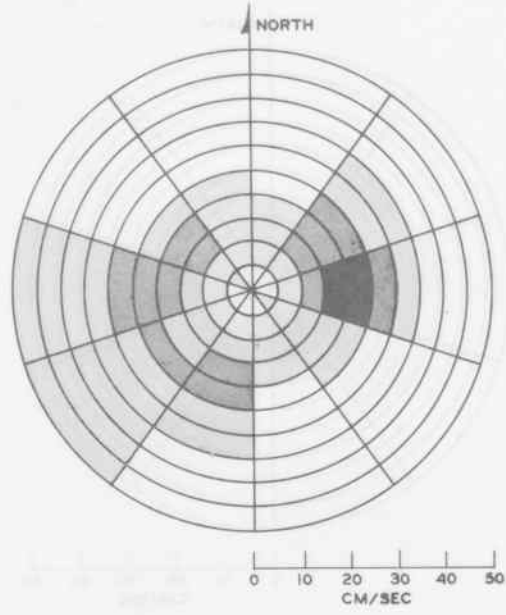
EN-C 31 OCT-25 NOV 74  
1794 obs

Plate 21



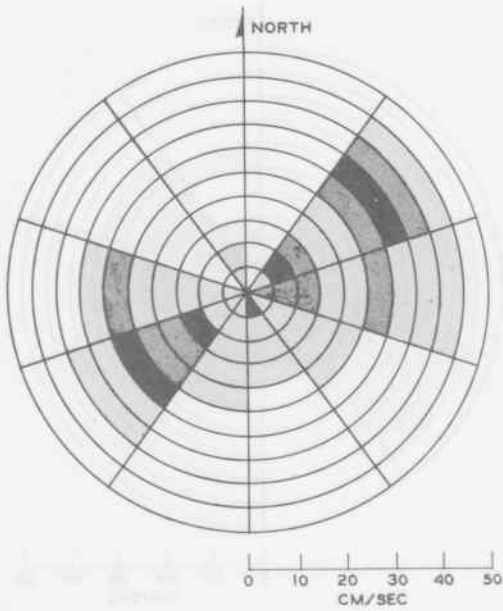


EN-3 09 SEP-20 SEP 74  
792 obs

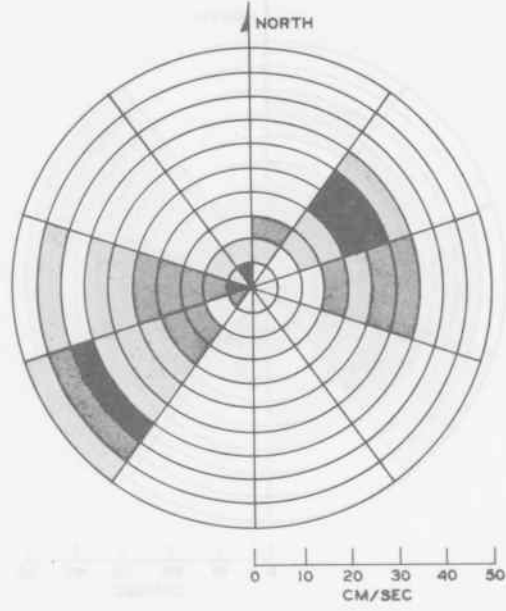


EN-5 09 SEP-20 SEP 74  
795 obs

Plate 22

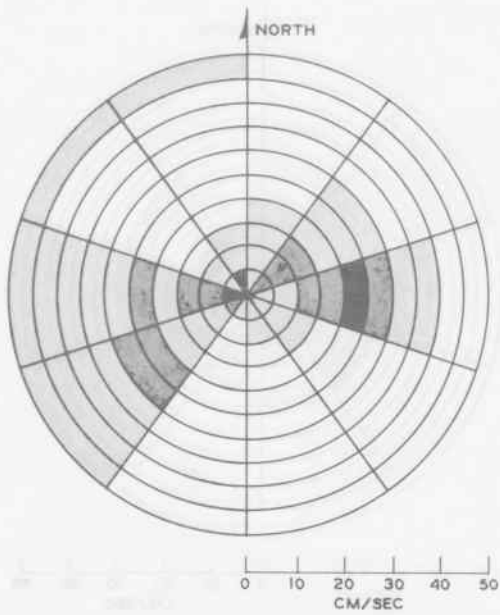


EN-N24a 24 MAR-25 MAR 75  
2868 obs

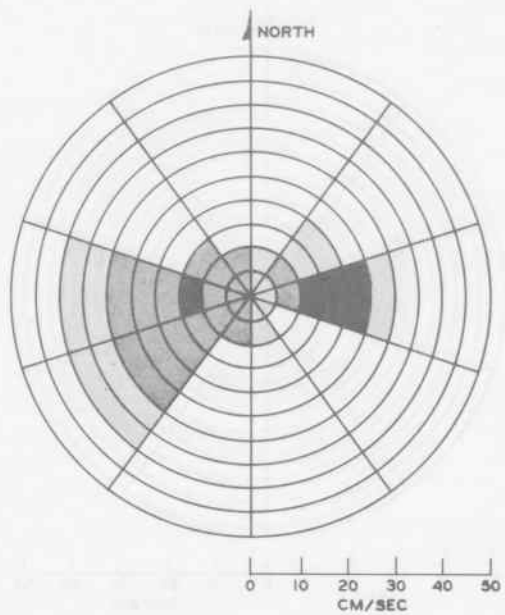


EN-6a 10 APR-23 APR 75  
107 obs

Plate 23

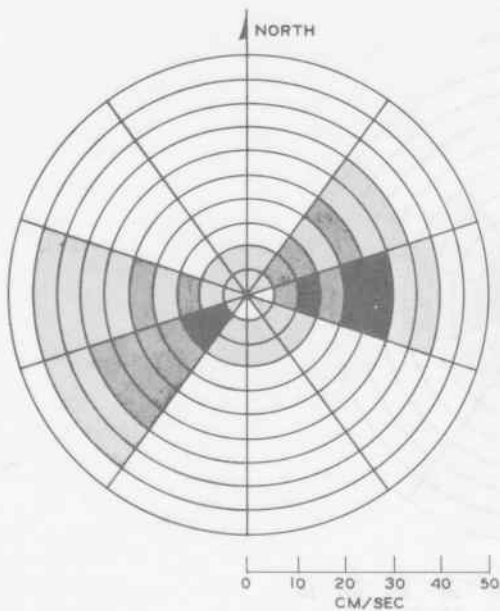


EN-6b 10 APR-22 APR 75  
2285 obs

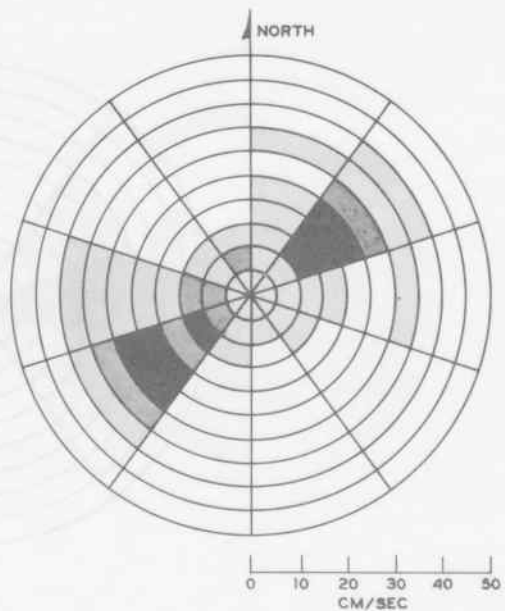


EN-6c 10 APR-23 APR 75  
944 obs

Plate 24

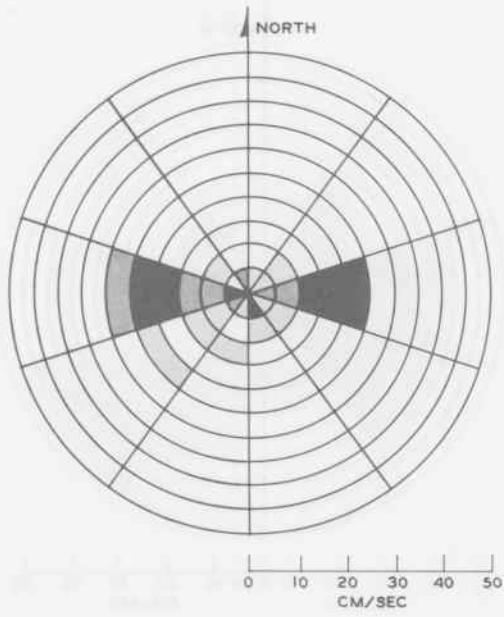


EN-6d 10 APR-22 APR 75  
1375 obs

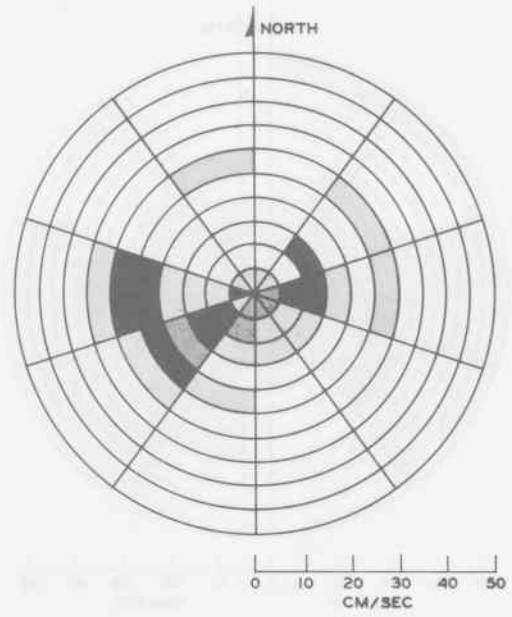


EN-6f 10 APR-23 APR 75  
1253 obs

Plate 25

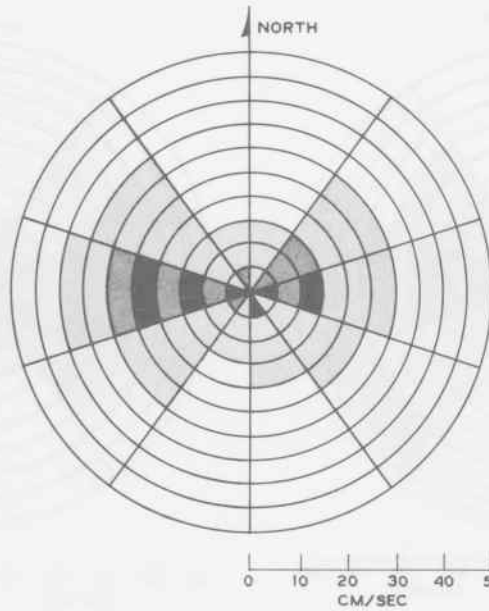


EN-7a 30 APR-09 MAY 75  
290 obs



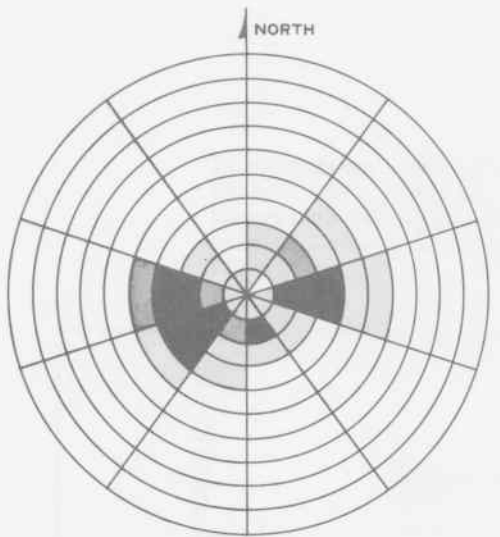
EN-7c 30 APR-09 MAY 75  
397 obs

Plate 26

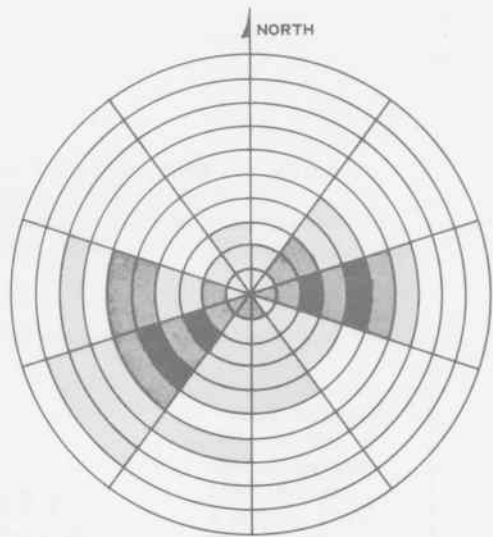


EN-7d 30 APR-09 MAY 75  
1739 obs

Plate 27

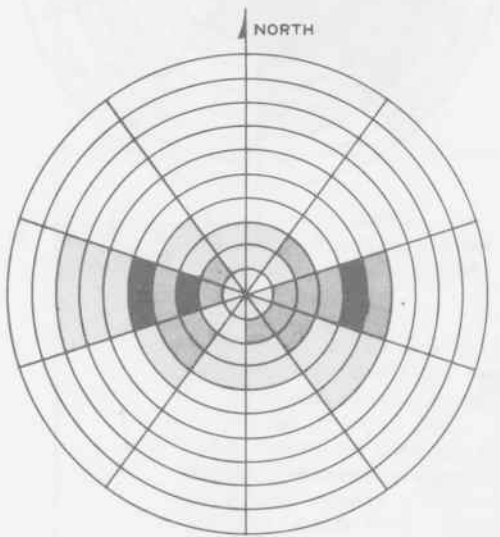


EN-7e 30 APR-09 MAY 75  
656 obs



EN-7f 30 APR-09 MAY 75  
819 obs

Plate 28

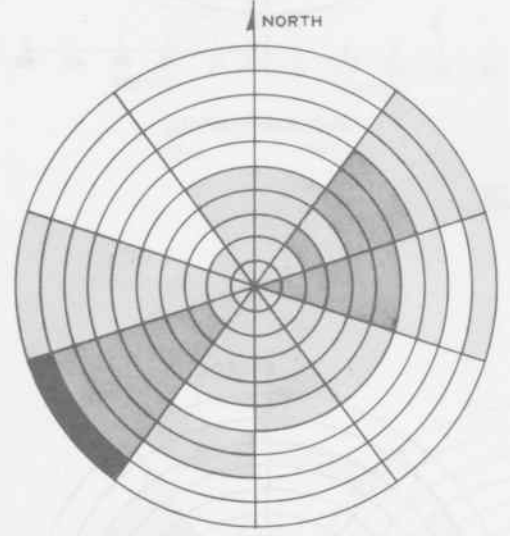


EN-N 15 APR-07 MAY 75  
1504 obs



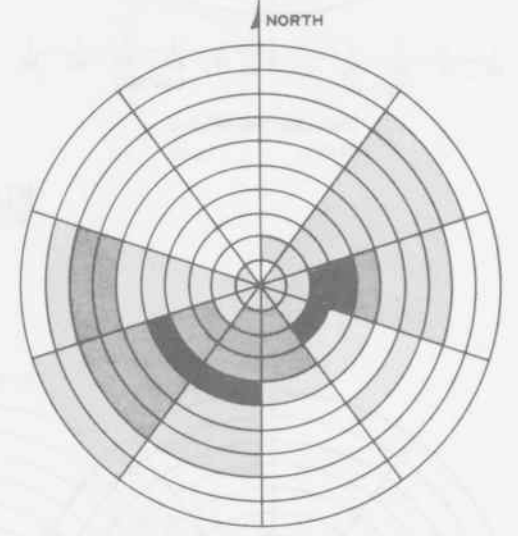
EN-N 09 MAY-29 MAY 75  
1446 obs

Plate 29



0 10 20 30 40 50  
CM/SEC

EN-Nc 19 MAY-03 JUN 75  
1093 obs

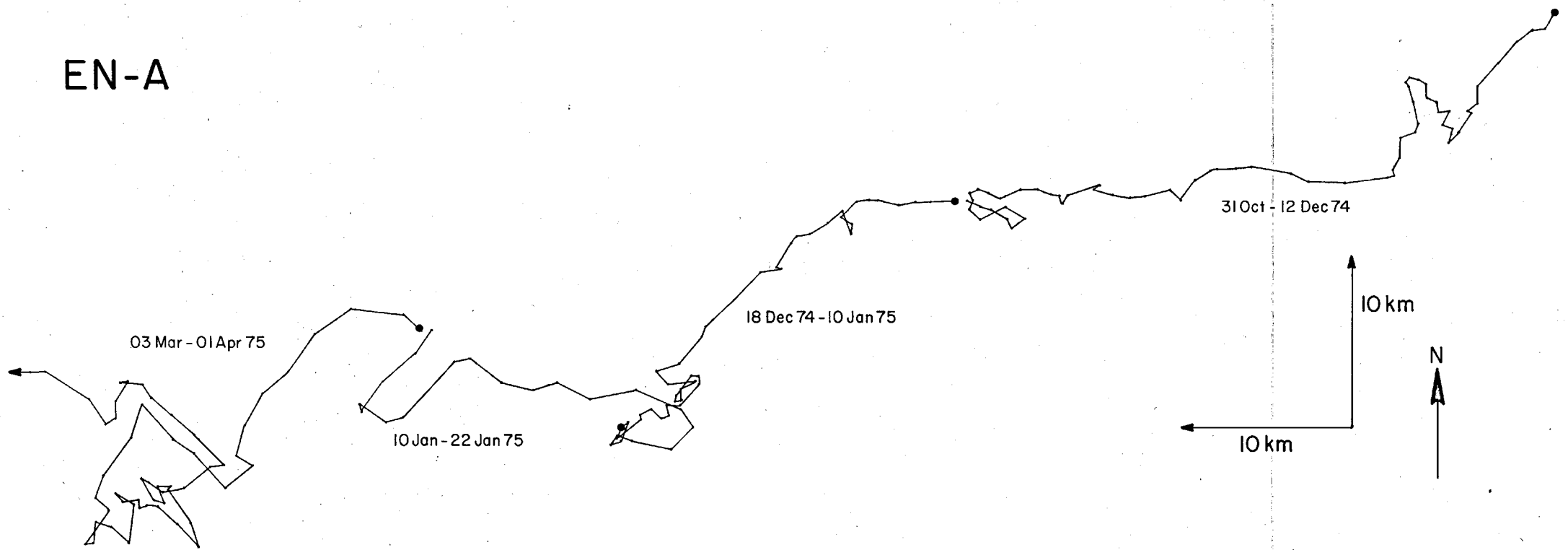


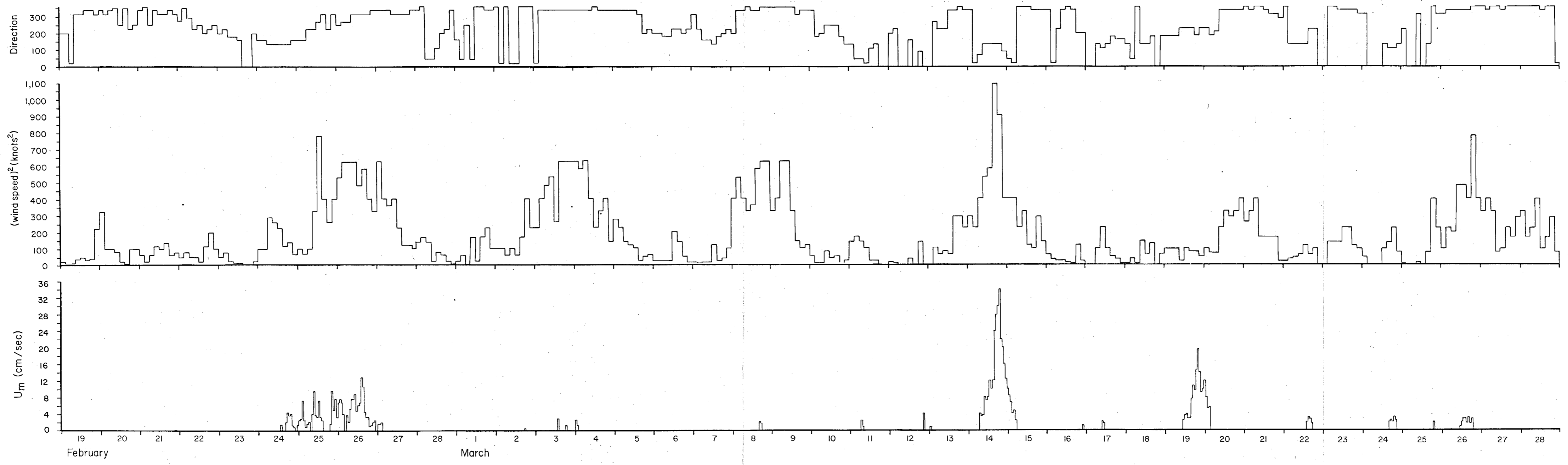
0 10 20 30 40 50  
CM/SEC

EN-Nd 19 MAY-03 JUN 75  
2042 obs

Plate 30

EN-A





In accordance with letter from DAEN-RDC, DAEN-ASI dated 22 July 1977, Subject: Facsimile Catalog Cards for Laboratory Technical Publications, a facsimile catalog card in Library of Congress MARC format is reproduced below.

Bokuniewicz, Henry

Aquatic disposal field investigations, Eatons Neck disposal site, Long Island Sound; Appendix A: Investigation of the hydraulic regime and the physical characteristics of bottom sediment / by Henry Bokuniewicz ... et al., Yale University, Department of Geology and Geophysics, New Haven, Connecticut. Vicksburg, Miss. : U. S. Waterways Experiment Station, 1977.

108 p., [19] leaves of plates : ill. ; 27 cm. (Technical report - U. S. Army Engineer Waterways Experiment Station ; D-77-6, Appendix A)

Prepared for Office, Chief of Engineers, U. S. Army, Washington, D. C., under Contract No. DACW51-75-C-0008 (DMRP Work Unit 1A06A)

Appendixes A-E on microfiche in pocket.

References: p.74-77.

1. Benthic fauna. 2. Disposal areas. 3. Dredged material

(Continued on next card)

Bokuniewicz, Henry

Aquatic disposal field investigations, Eatons Neck disposal site, Long Island Sound; Appendix A: Investigation of the ... 1977. (Card 2)

disposal. 4. Eatons Neck disposal area. 5. Field investigations. 6. Sediment sampling. 7. Sediment transport. 8. Sedimentation. 9. Waste water disposal. 10. Water quality. I. United States. Army. Corps of Engineers. II. Yale University. Dept. of Geology and Geophysics. III. Series: United States. Waterways Experiment Station, Vicksburg, Miss. Technical report ; D-77-6, Appendix A. TA7.W34 no.D-77-6 Appendix A





1081

Technical Report D-77-6, Appendixes A-E.

Aquatic Disposal Field Investigations, Eatons Neck Disposal Site,  
Long Island Sound;

Dated: September 1977

Authors: Henry Bokuniewicz, Michael Dowling, Jeffrey Gebert,  
Robert Gordon, Peter Kaminsky, Carol Pilbeam,  
Catherine Tuttle

APPENDIX A: NAVIGATION PROCEDURES AND PERMANENT BUOY CONSTRUCTION

## Navigation Plotting Sheet Calculations

1. When horizontal sextant angles are measured the observer is measuring an angle between two points in a plane tangent to the earth at the point of contact of the observer. The points between which the angle is measured are defined by the intersection of the plane of observation with a line which passes through the center of the earth and the latitude and longitude of the reference object, assuming the object is built perpendicular to the earth's surface. For example, an observer at O (Figure A1) measures  $180^{\circ}$  in the plane P between the intersection of the stack with the plane (point A) and the tower with the plane (point B).

2. A sextant angle plotting chart was calculated and drawn for both EN-N and EN-S. Each chart is constructed on a gnomonic projection plane tangent to the earth at the disposal site (either EN-N or EN-S). In this projection plane the x and y Cartesian coordinates for the disposal site (point of tangency) are (0, 0); for all other points they are given by

$$x = \frac{R\{\cos \phi_0 \sin \phi - \sin \phi_0 \cos \phi \cos (\lambda - \lambda_0)\}}{\sin \phi_0 \sin \phi + \cos \phi_0 \cos \phi \cos (\lambda - \lambda_0)} \quad (17)$$

$$y = \frac{R \cos \phi \sin (\lambda - \lambda_0)}{\sin \phi_0 \sin \phi + \cos \phi_0 \cos \phi \cos (\lambda - \lambda_0)} \quad (18)$$

where R is the radius of the earth,

$\phi_0$  = the latitude of the disposal site,

$\lambda_0$  = the longitude of the disposal site,

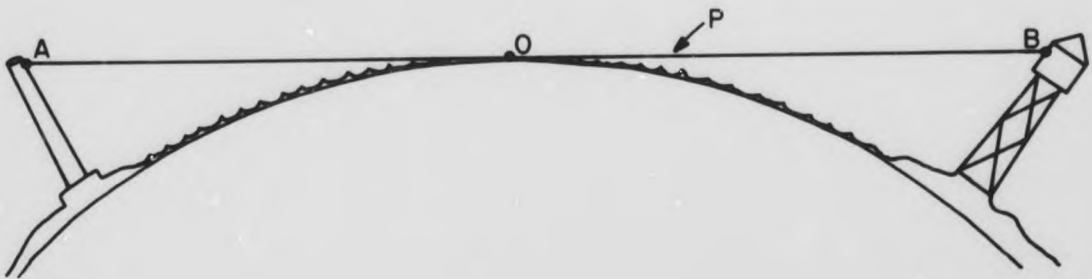


Figure A1. Geometry of sextant observations

$\phi$  = the latitude of the point on the earth, and

$\lambda$  = the longitude of the point on the earth.

For this calculation,  $R$  is given by the radius of the earth at the disposal site,

$$R = \sqrt{MN} \quad (19)$$

where  $M$  = the radius of curvature of the earth in the meridian and

$N$  = the radius of curvature of the earth in the prime vertical.

$M$  and  $N$  are calculated from the I.U.G.G. terrestrial ellipsoidal dimensions,

$a$  = equatorial radius = 6378206.4 m and

$b$  = polar radius = 6356583.3 m

by the relations,

$$M = a(1 - e^2)/(1 - e^2 \sin^2 \phi_0)^{3/2} \quad (20)$$

$$N = a/(1 - e^2 \sin^2 \phi_0)^{1/2} \quad (21)$$

$$e^2 = (a^2 - b^2)/a^2 \quad (22)$$

Thus,

$$R = a^2 b / (b^2 \sin^2 \phi_0 + a^2 \cos^2 \phi_0) \quad (23)$$

By assuming a sphere of radius  $R$  instead of an ellipsoid, a negligible error of 0.001 m in 103.7 km is introduced.

3. Two charts were generated for both EN-N and EN-S. One chart at each site used the following reference positions:

Long Neck Spire  
Greens Ledge Light  
Sheffield Island Tower

the other chart was based on:

Long Neck Spire  
Greens Ledge Light  
Manresa Island Stack

These reference positions were assigned Cartesian coordinates in the gnomonic projection from their latitude and longitude. If an observer measures an angle  $\alpha$  between two reference points in a plane, then his position lies on a circle passing through the reference points. Conversely, from any point on that unique circle, an observer will measure the angle  $\alpha$  between the two reference points. Given two reference positions and the angle  $\alpha$ , the points on the circle were calculated and plotted. The angle  $\alpha$  was then changed by  $1^\circ$  and the procedure repeated. The charted region covered a  $250,000 \text{ m}^2$  square area centered at the disposal site at a scale of 1 in. = 40 m. Reference latitude and longitude marks were placed every 5 sec of arc. All calculations were done maintaining 16 significant digits.

#### Design of Permanent Experimental Site Buoys

4. It was decided at the contractors' workshop of March 1975 that permanent, minimum-scope marker-buoys should be deployed to indicate the intended positions of "point-disposals" for experimental observations at Eatons Neck. Minimum excursion of these buoys in the tidal stream is required if point disposal is to be achieved. The basic design of these marker buoys included, from bottom to surface, an anchor, a length of mooring chain, a subsurface float, and finally tethering line to the surface marker.



5. The purpose of the subsurface float is to provide a buoyant force of such magnitude as to reduce as far as possible the excursion of the surface marker due to current-induced drag on the chain and float. A depth of about 30 ft below mean low water for the subsurface float is required to stay safely below the depth which the largest vessels using the area would draw ( $\approx 23$  ft). The line from the float to the surface marker is to be light enough such that the surface marker is expendable relative to the permanent float-chain-anchor assembly. It is also intended that an acoustic marker beacon be attached to the float such that it can be relocated should the surface marker be lost.

6. Given this overall design for the marker buoy, it was then necessary to calculate the drag on the assembly at several current velocities in order to determine the expectable excursion of the surface marker about a fixed point on the bottom as a function of the buoyancy of the float. Since the excursion (error of position) varies inversely with the buoyant force (money), the most useful compromise of cost with accuracy of position could be found.

#### Drag Calculations

7. The following assumptions have been made in determining drag.
  - a. The drag on a chain is assumed to be twice the drag on a cylinder for which the diameter equals the diameter of a chain link.
  - b.  $v$  = current velocity, assumed to be independent of depth  
 $D$  = diameter of chain link

$Re = Dv/0.01 = \text{Reynolds number}$

$C_D = \text{drag coefficient}$

c. Drag (cylinder) =  $C_D (DL) \rho v^2/2$

Drag (chain) =  $C_D (DL) \rho v^2$

1 dyne =  $2.25 \times 10^{-6}$  pounds force

d. Drag on a 70 ft long chain

$D = 0.6 \text{ cm}$        $L = 2.1 \times 10^3 \text{ cm}$

v cm/sec	Re	$C_D$	Drag (lb)
50	2500	1	7.1
100	6000	1	28.3

e. Drag on subsurface float

$D = 35 \text{ cm}$        $L = 150 \text{ cm}$

v cm/sec	Re	$C_D$	Drag (lb)
50	175,000	1.1	16.2
100	350,000	0.4	23.6

f. Schematic of marker buoy in tidal stream and terms used in calculations (Figure A2).

The expression

$$L (B \cos \alpha) = L/2 D_C \sin \alpha + D_B \sin \alpha \quad (24)$$

balances the torque around the anchor and gives

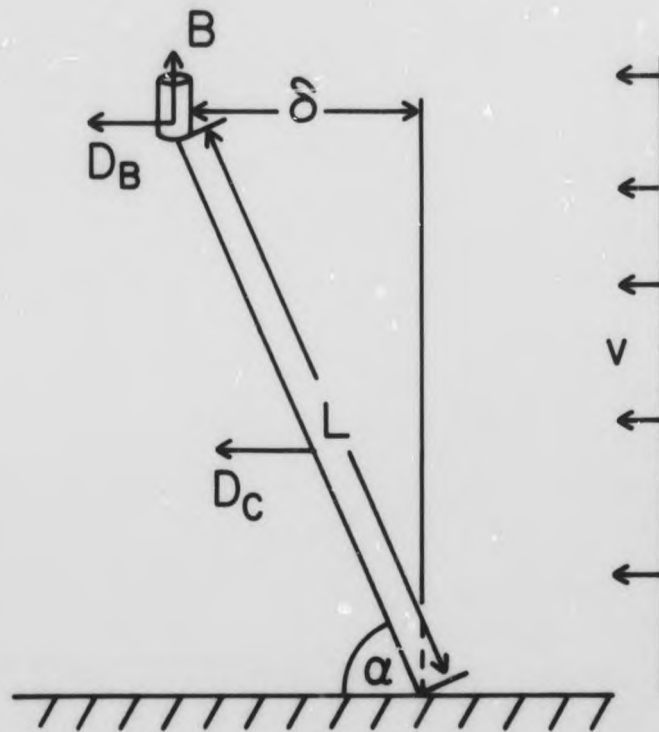


Figure A2. Schematic of marker buoy in tidal stream and terms used in calculations

- B = buoyancy
- $D_B$  = drag on float
- $D_C$  = drag on chain
- L = length of chain
- $\delta$  = excursion
- $\alpha$  = angle of chain
- v = velocity of tidal stream

$$B = \left( \frac{D_C}{2} + D_B \right) L / \delta \quad (25)$$

and when  $v = 50$  cm/sec,  $\delta = 1$  ft,  $L = 70$  ft, then

$$B = 1382 \text{ lb}$$

and when  $v = 100$  cm/sec,  $\delta = 1$  ft,  $L = 70$  ft, then

$$B = 2642 \text{ lb}$$

g. Graph of buoyancy  $B$  versus the inverse of excursion  $1/\delta$ , Figure A3. The two lines on the graph were constructed for 50 and 100 cm/sec by plotting  $B$  for  $\delta = 1$ , then extending the line through the origin. From the graph one can determine the expected excursion of the surface marker at 50 or 100 cm/sec for a given net buoyancy.

h. An independent check on these calculations was taken from Reference 35\*

$$L = 70 \text{ ft}$$

$$B (\text{float}) = 200 \text{ lb}$$

$$B (\text{net}) = 130 \text{ lb} \quad 200 \text{ lb flotation} - 70 \text{ lb chain}$$

when  $v = 50$  cm/sec,  $D_{\text{float}} = 16.2$ ,  $D_{\text{total}} = 23.3$ , and

$$\delta = 8.7 \text{ ft}$$

when  $v = 100$  cm/sec,  $D_{\text{float}} = 23.6$ ,  $D_{\text{total}} = 51.9$ , and

$$\delta = 17.4 \text{ ft}$$

These values are plotted in Figure 26 and show good agreement with the original calculation.

---

\* Raised numbers refer to similarly numbered items in the References at the end of the main text.

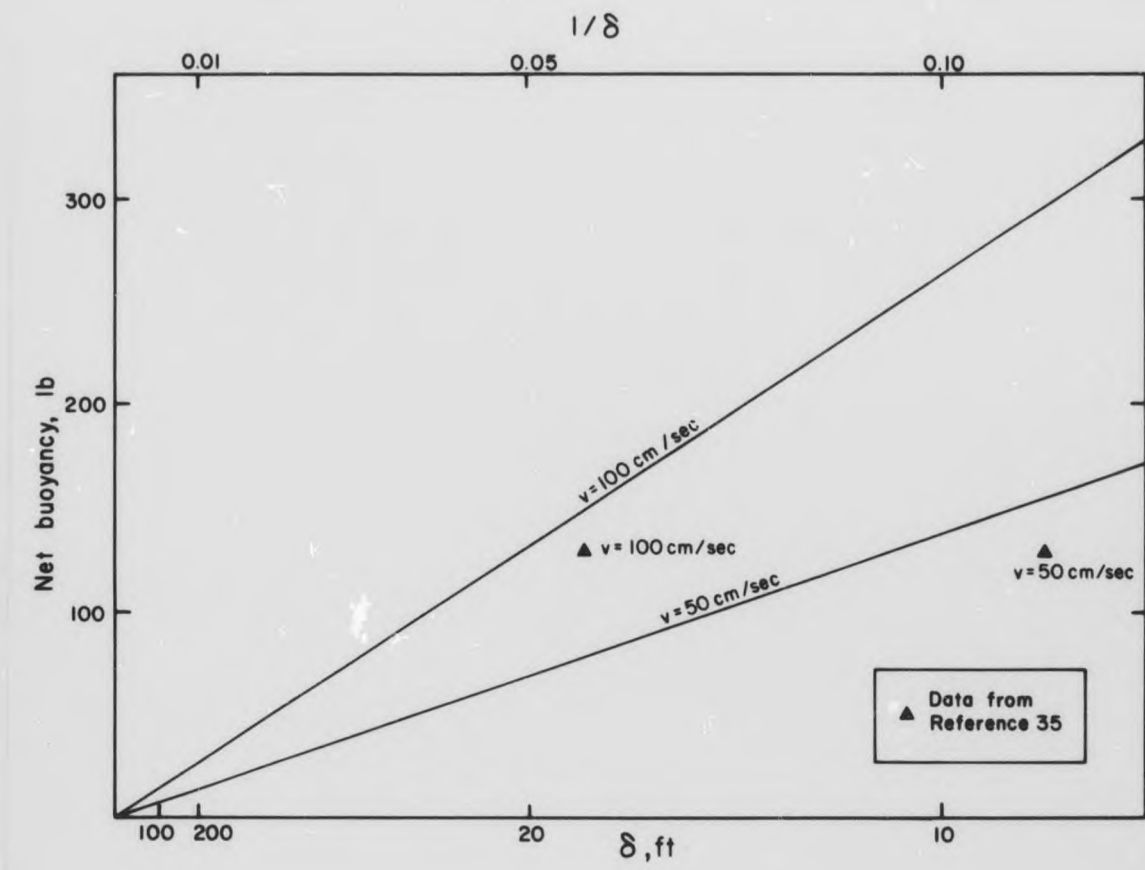
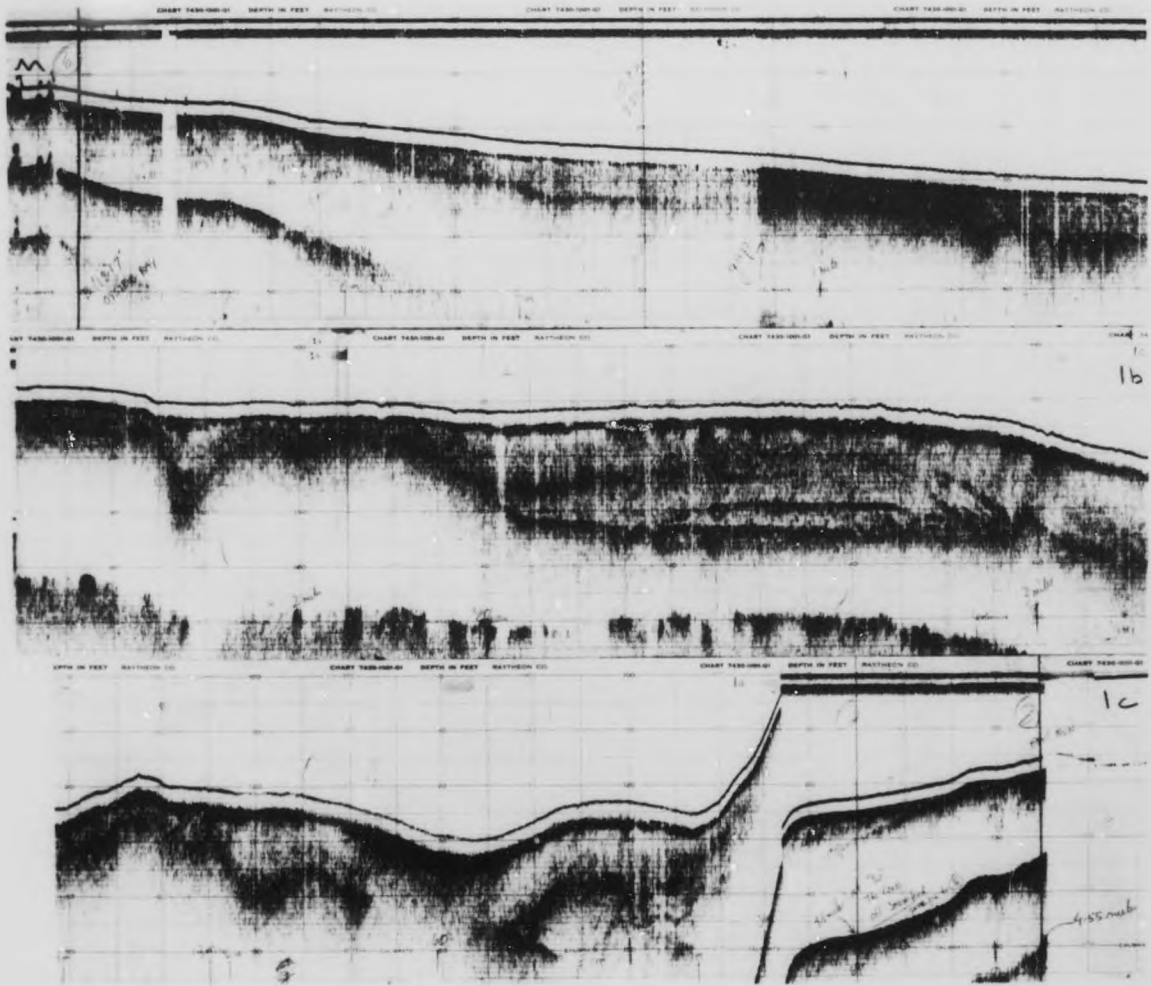


Figure A3. Graph of buoyancy B versus the inverse of excursion  $1/\delta$

From these calculations, it appears that a reasonable design for a permanent, minimum-scope marker buoy for the experimental disposal site(s) would include:

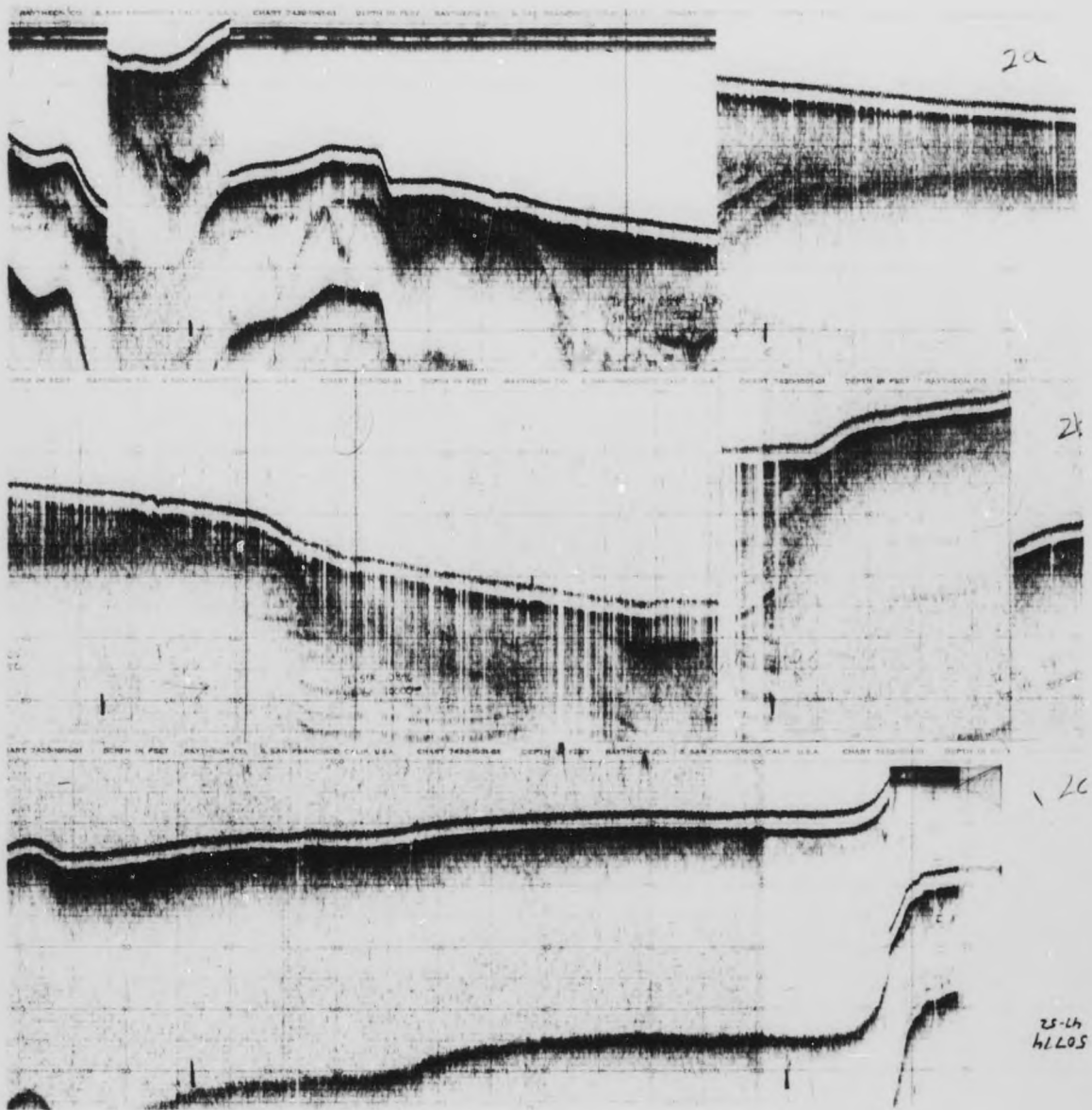
- ~300 lb steel I beam
- 100 lb mushroom anchor
- ~50 ft 3/8 in. galvanized chain
- ~300 lb flotation device
- acoustic marker beacon
- ~40 ft of 5/16 in-line
- surface marker

APPENDIX B: REFLECTION-PROFILE PHOTOS

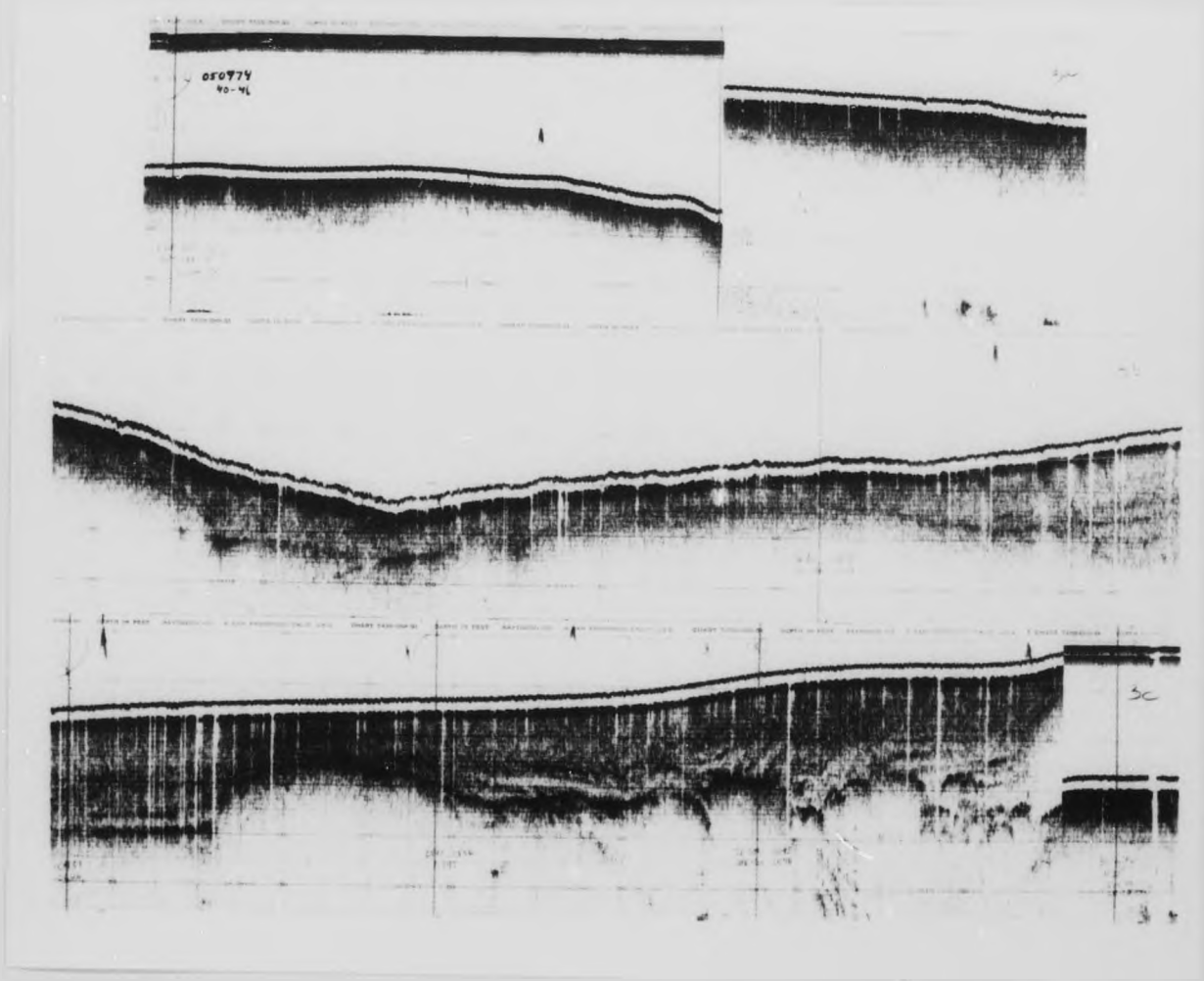


Reflection profile of track 1

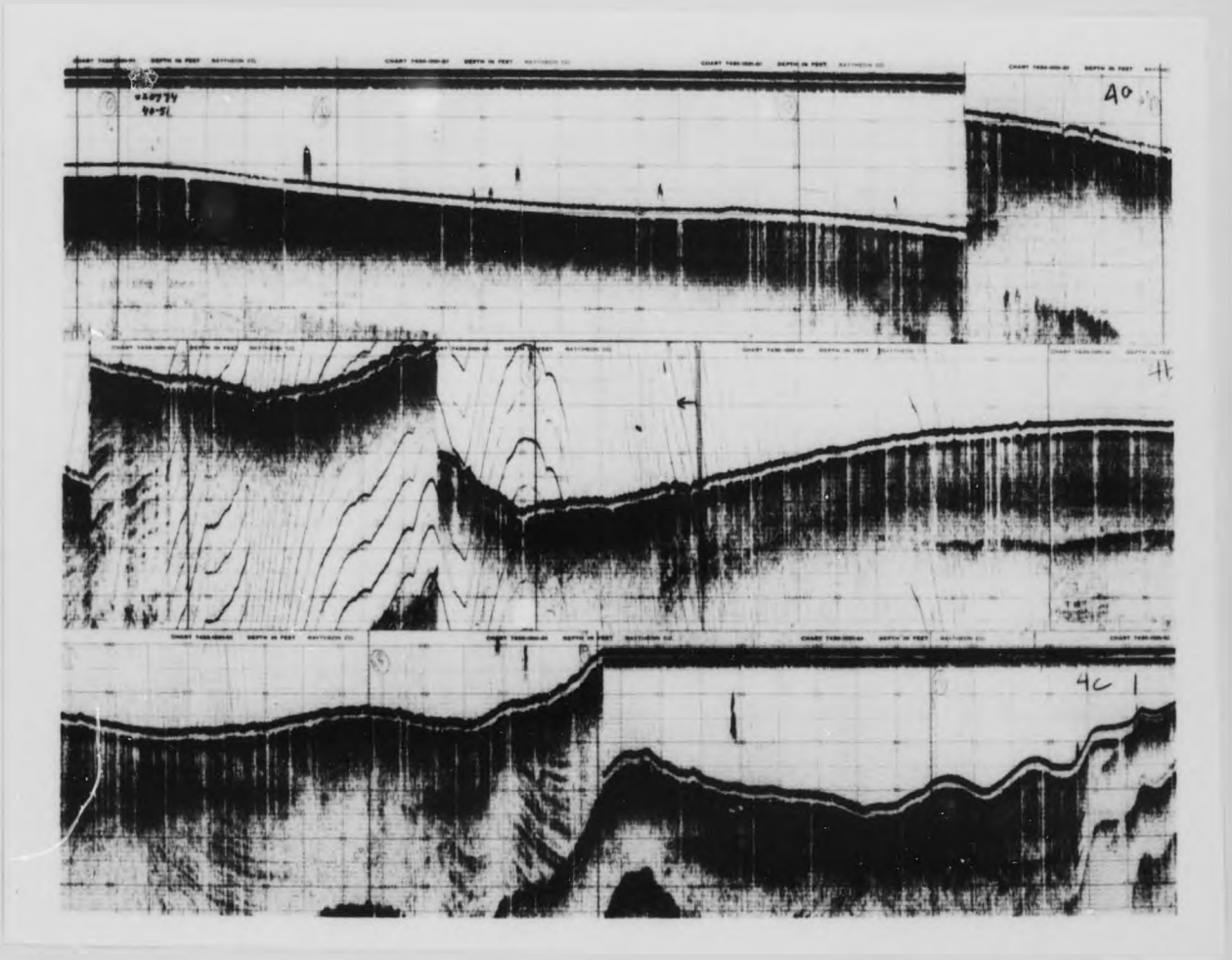




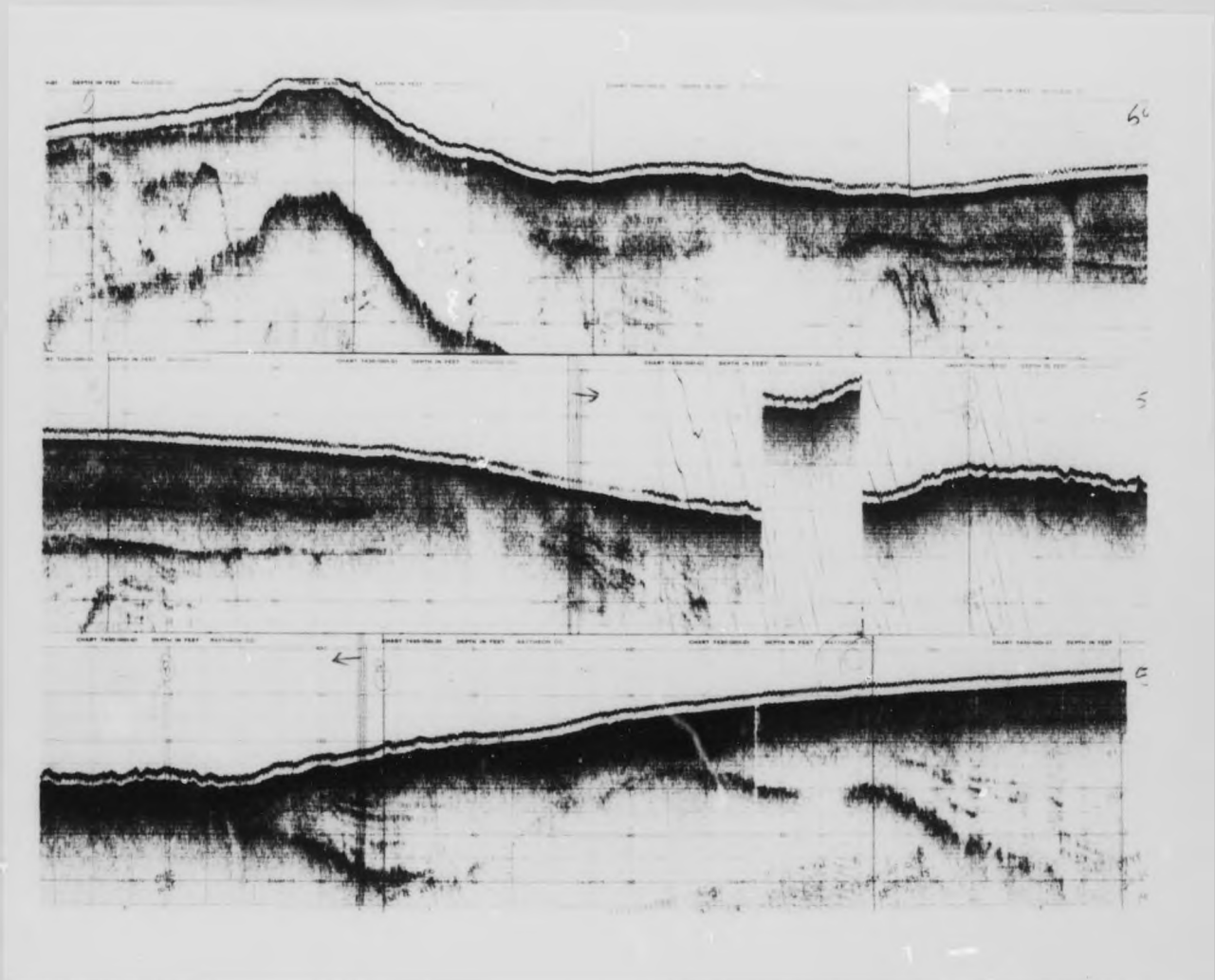
Reflection profile of track 2



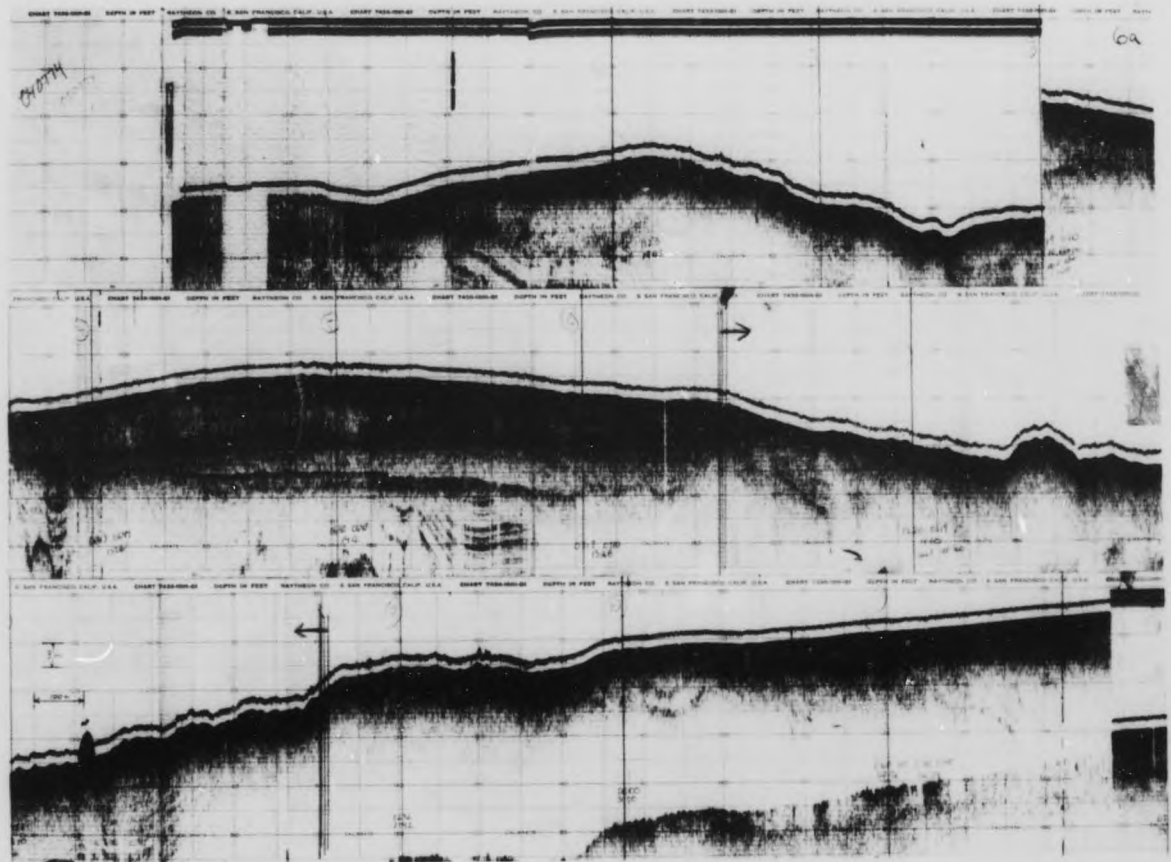
Reflection profile of track 3



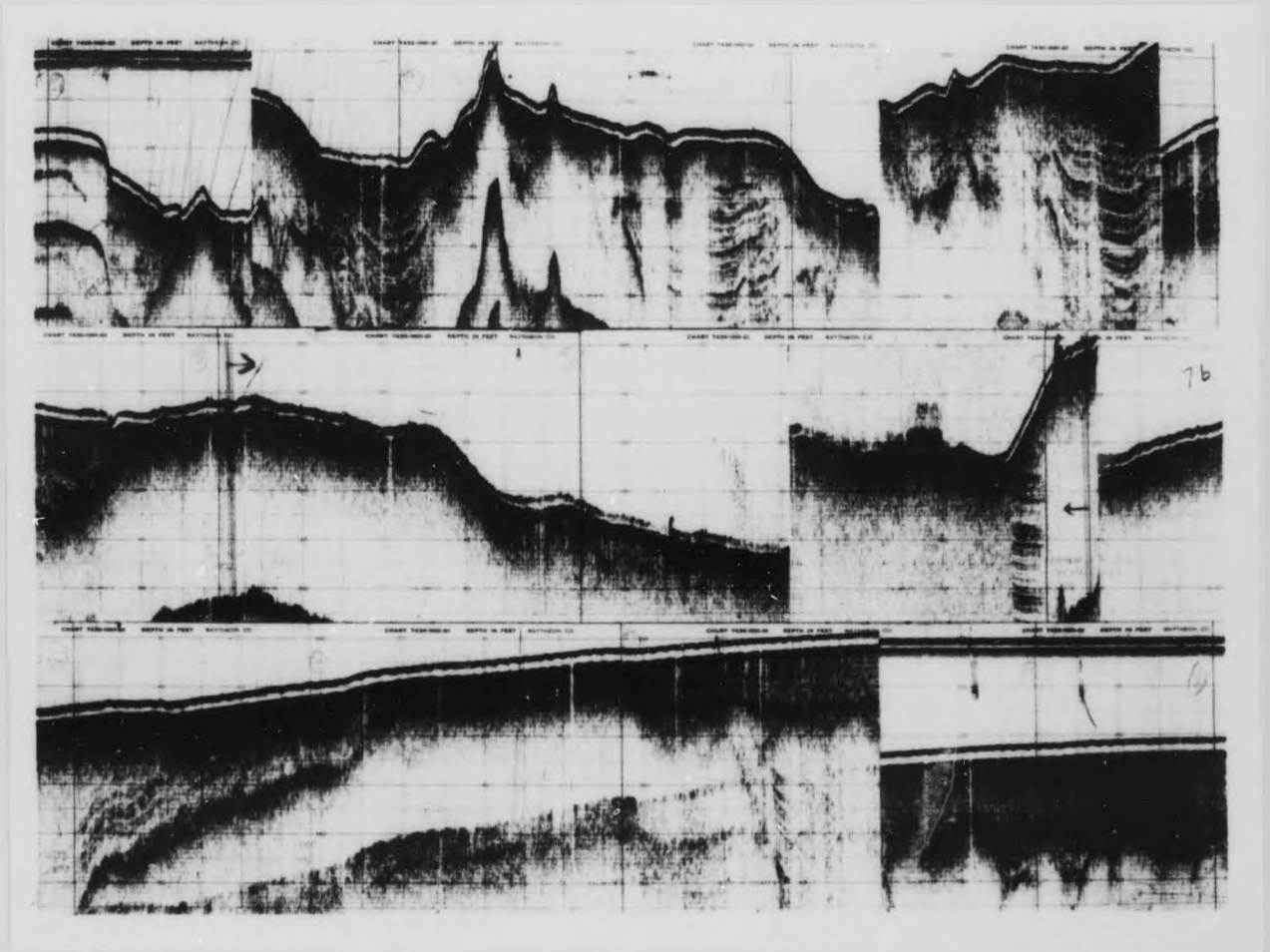
Reflection profile of track 4



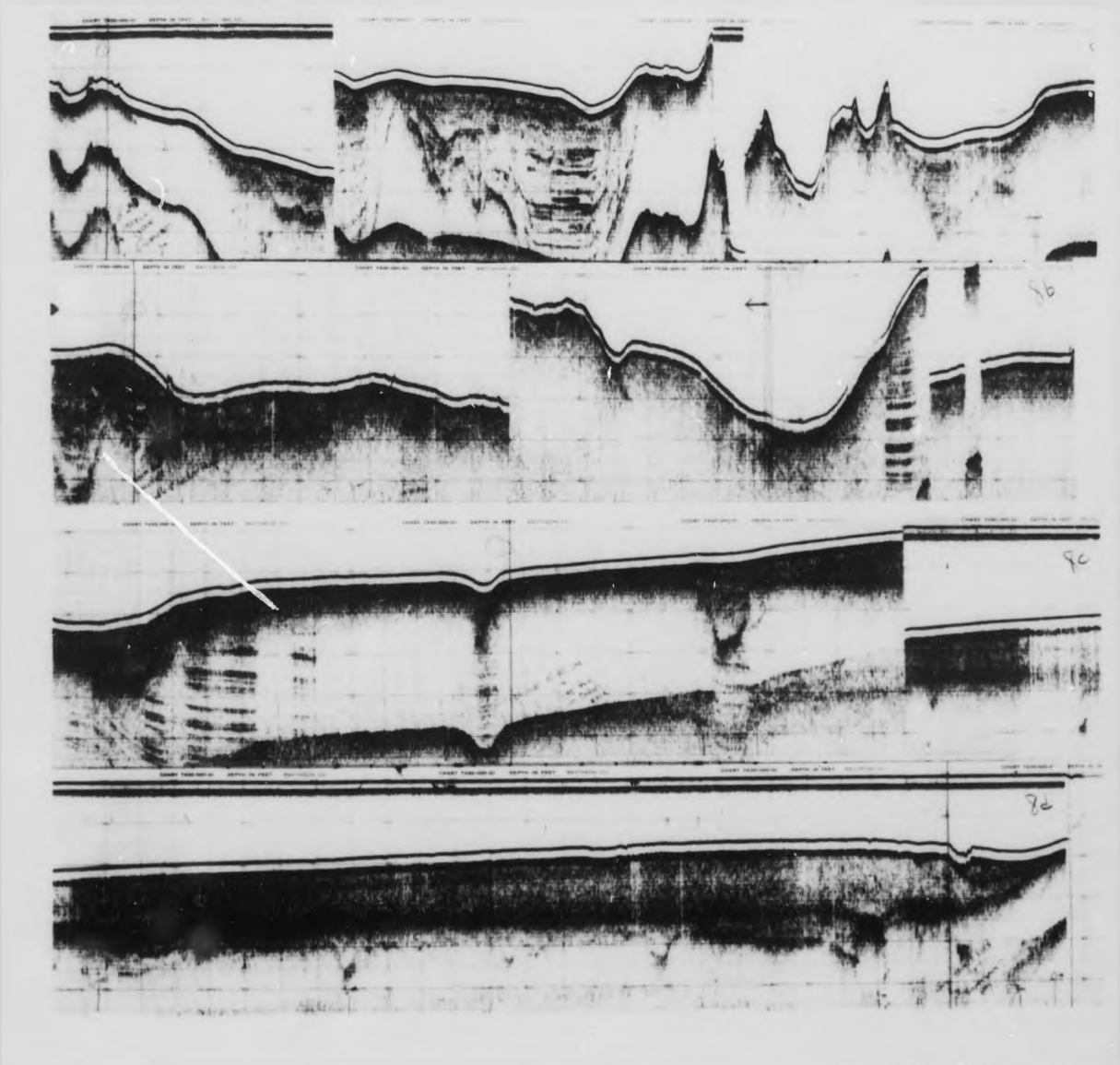
Reflection profile of track 5



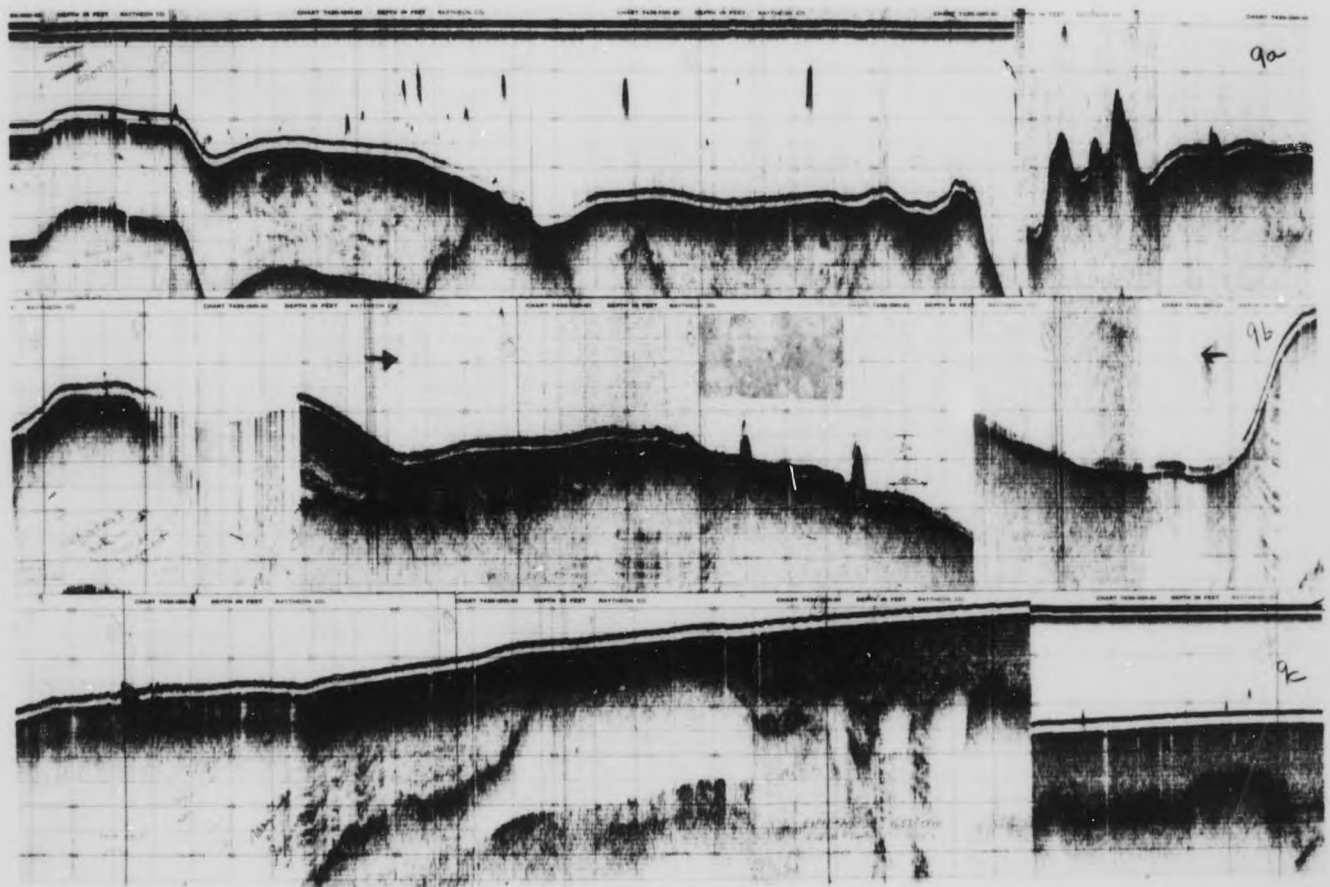
Reflection profile of track 6



Reflection profile of track 7

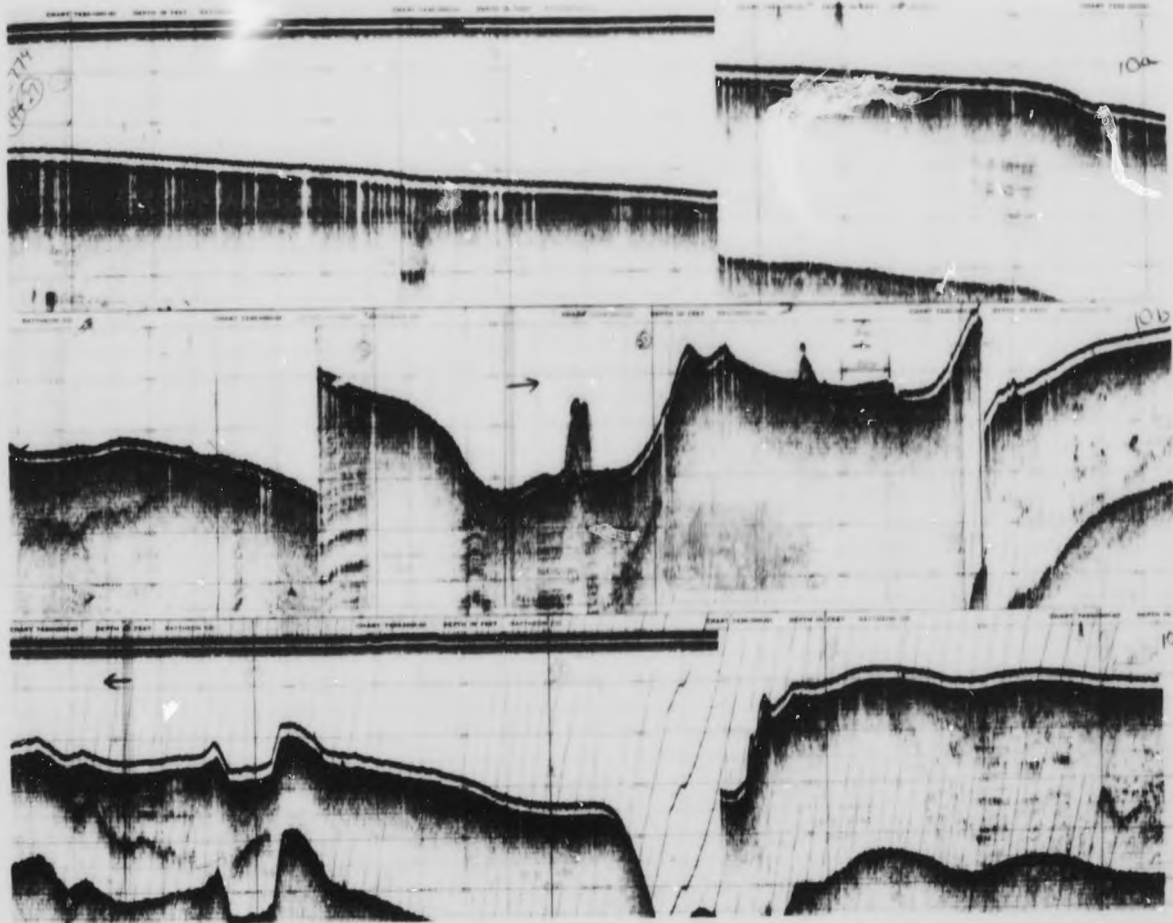


Reflection profile of track 8

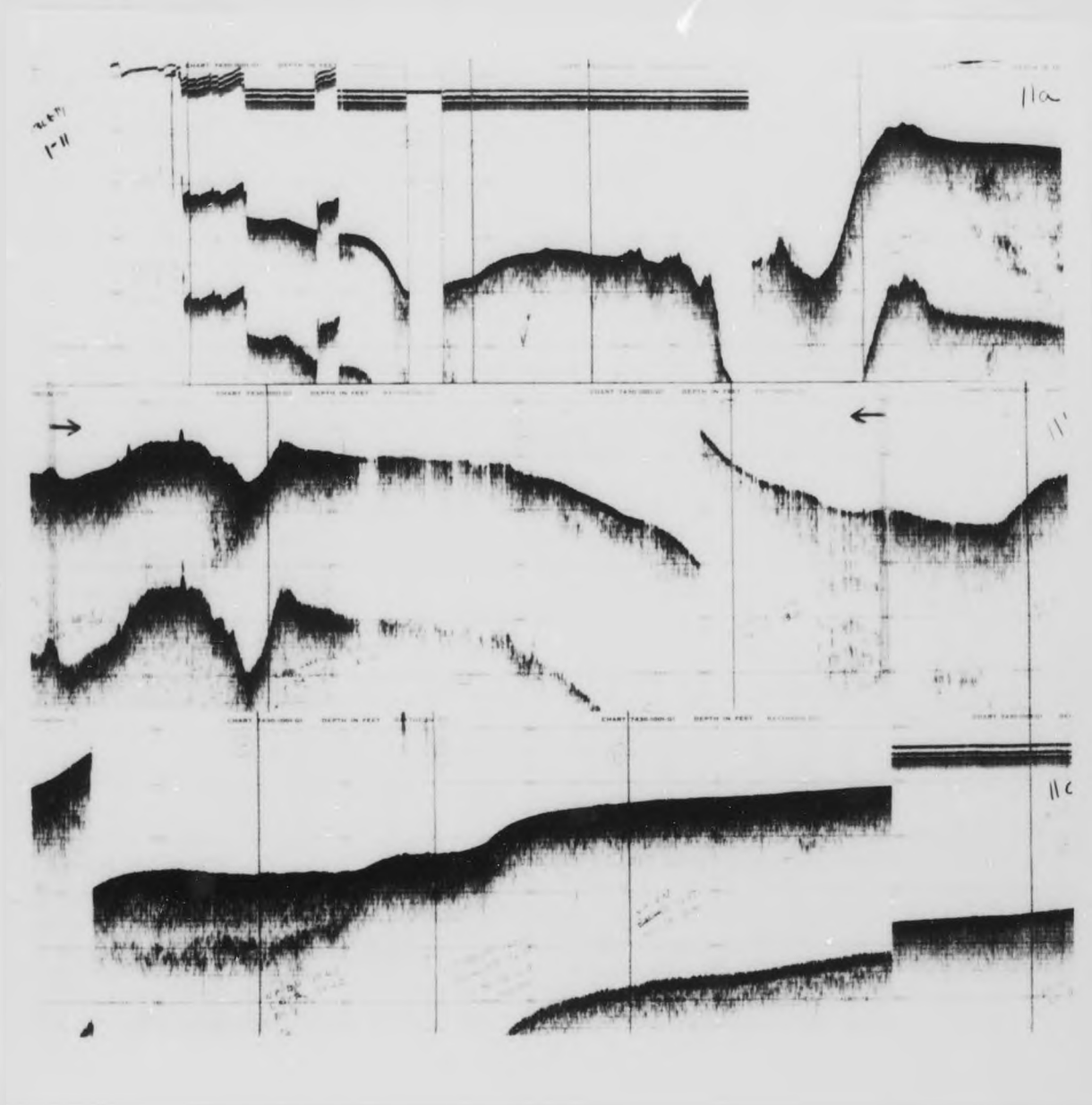


Reflection profile of track 9

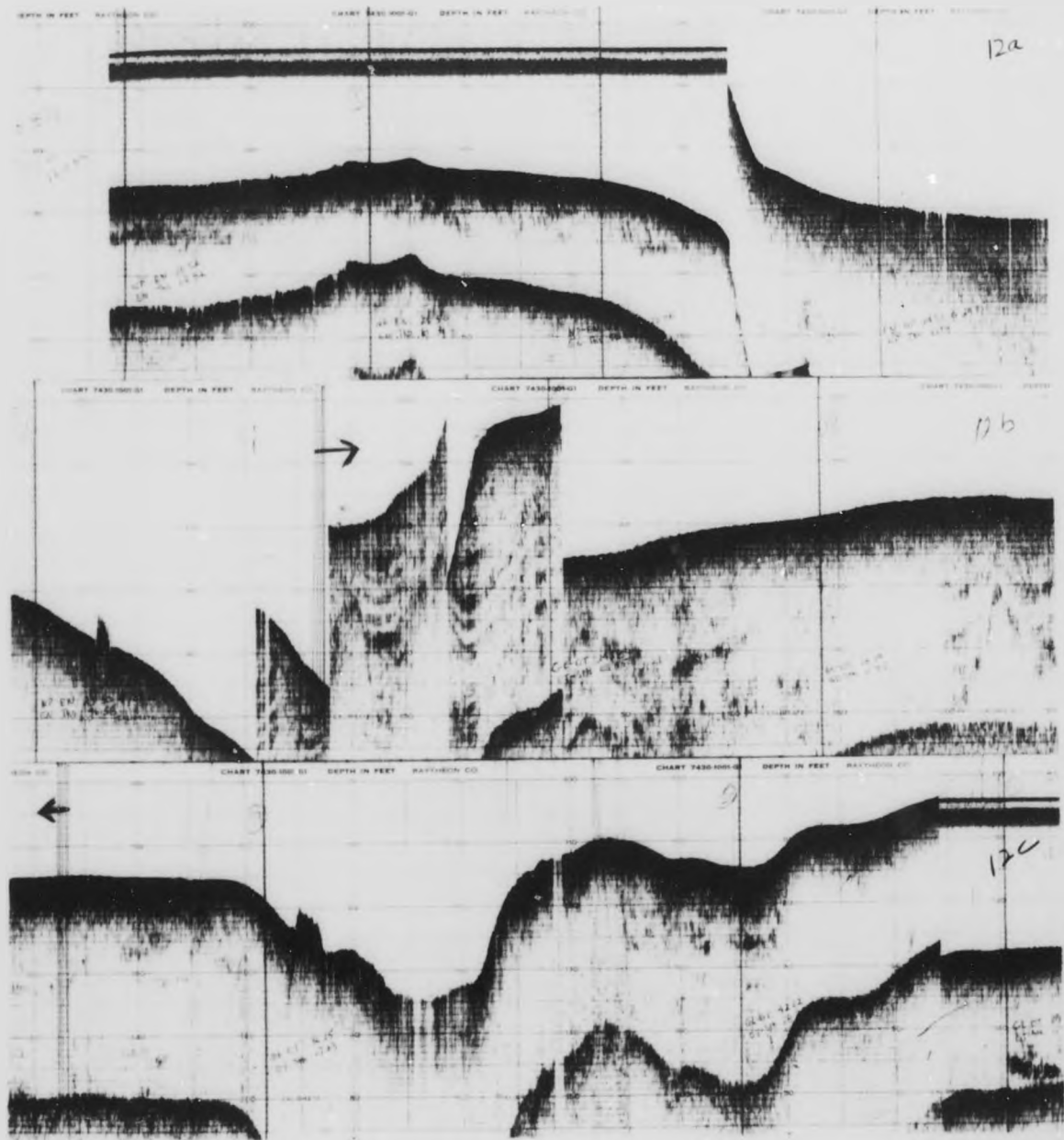




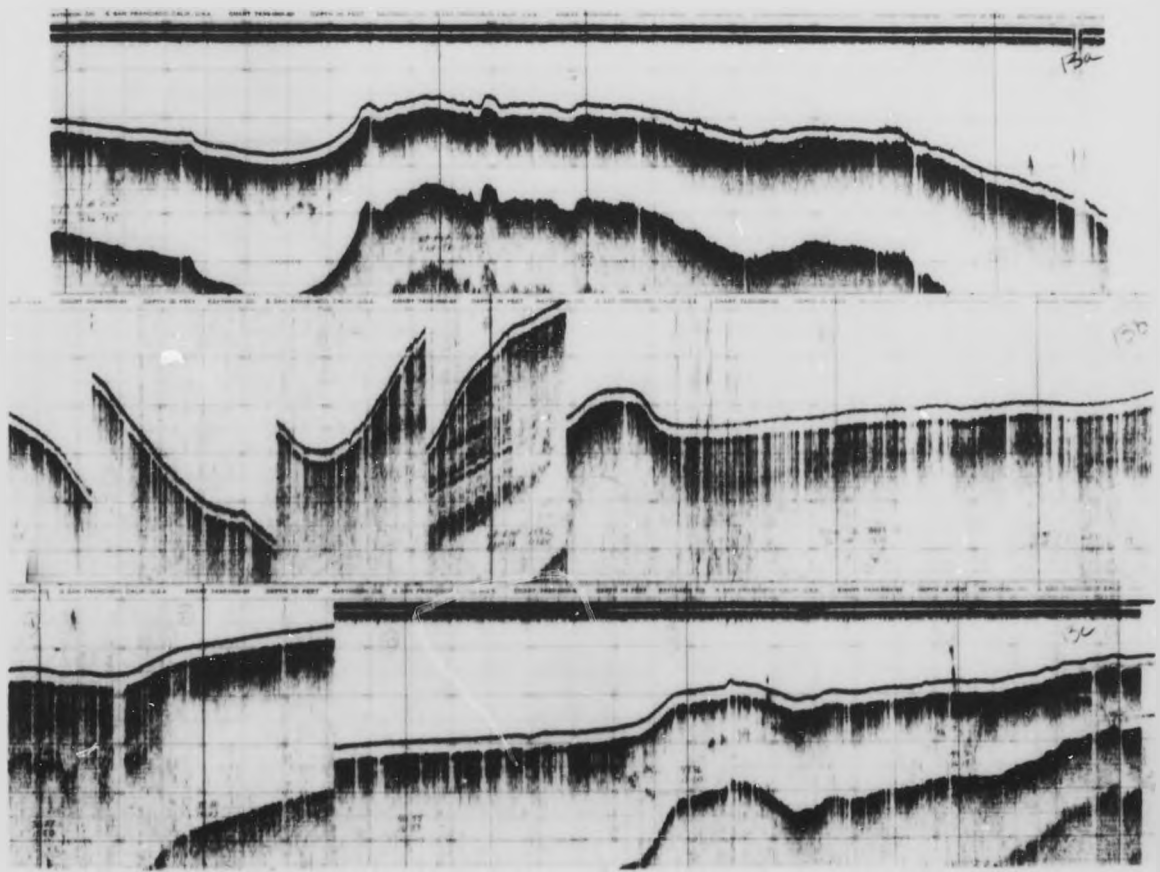
Reflection profile of track 10



Reflection profile of track 11



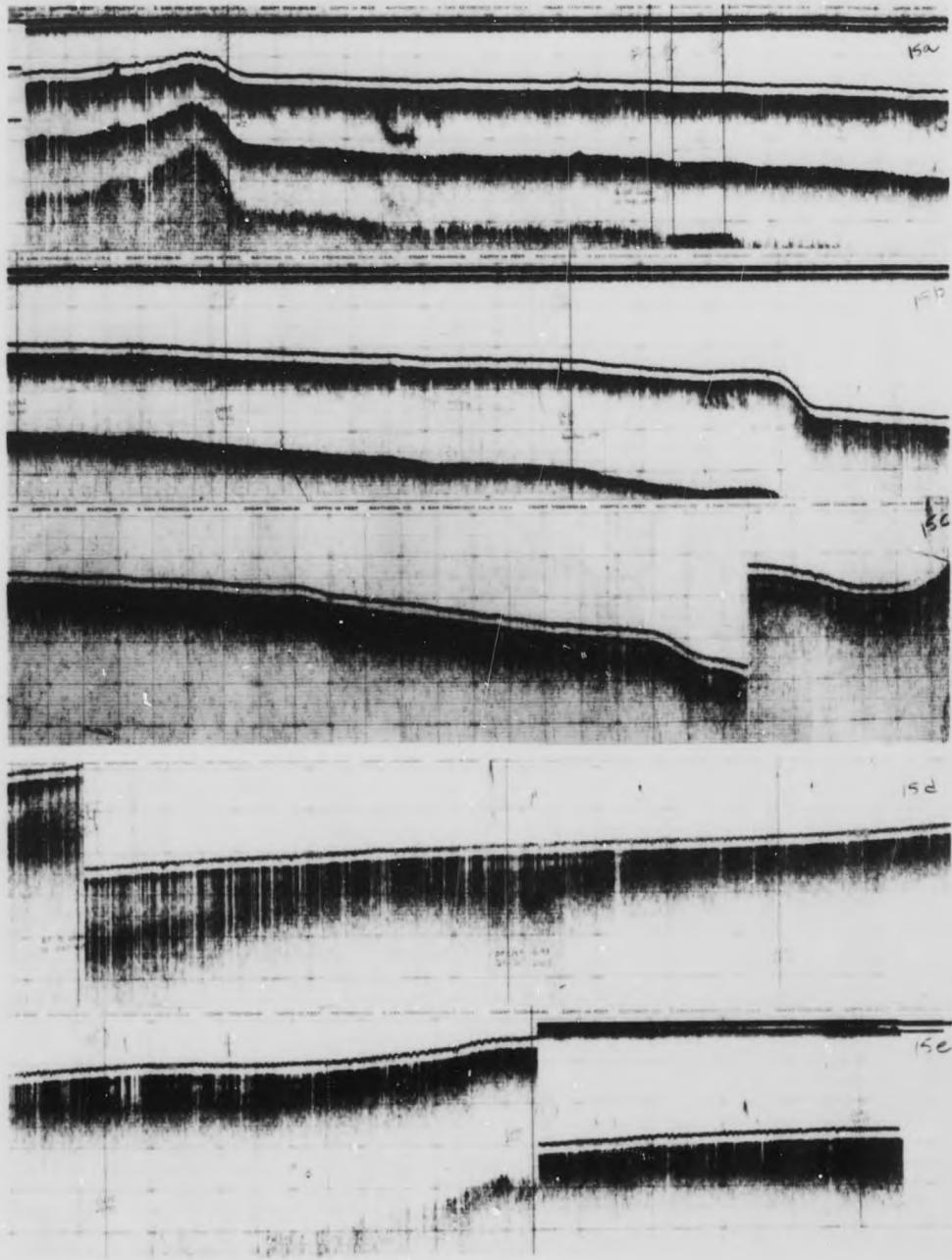
Reflection profile of track 12



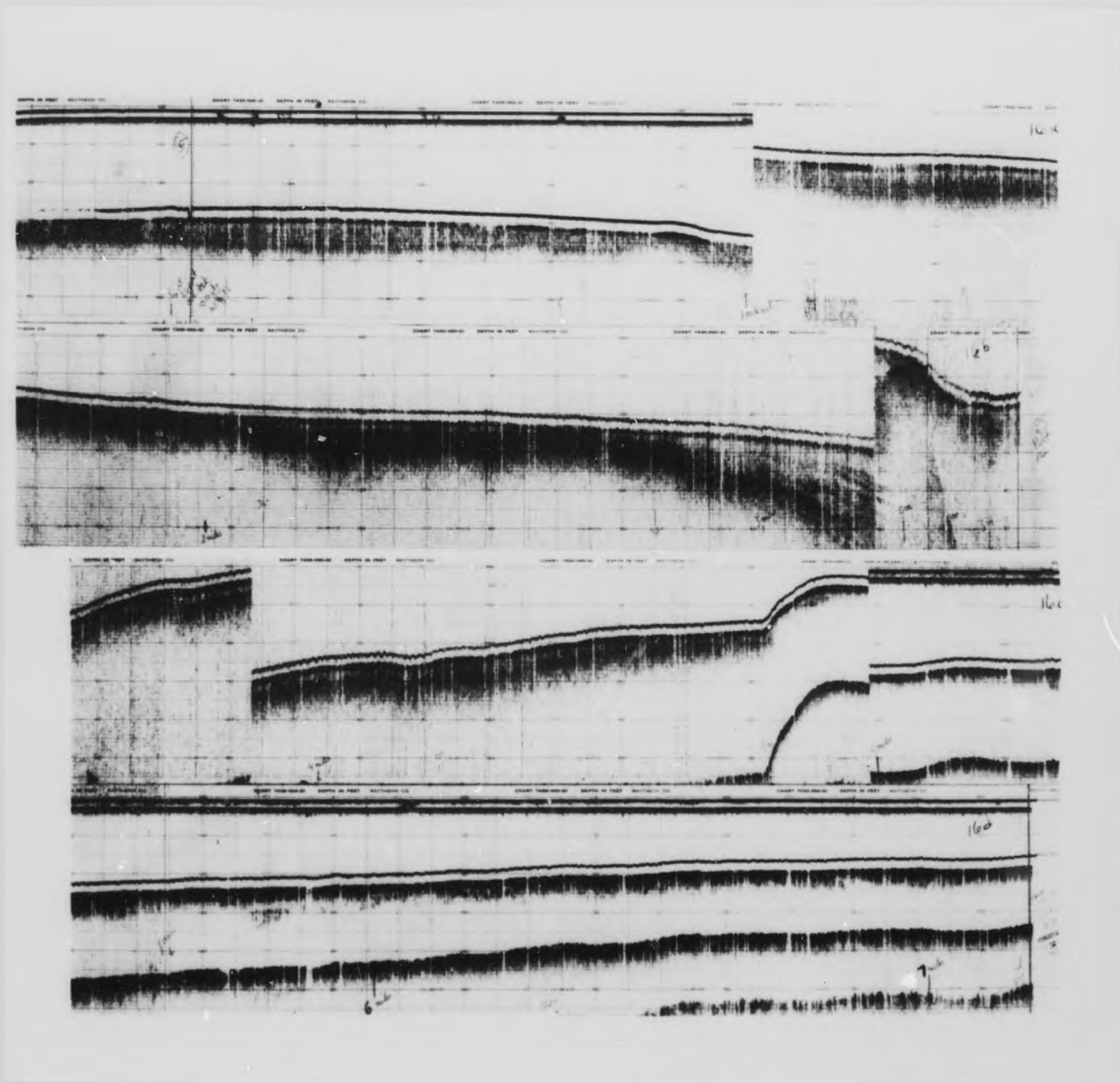
Reflection profile of track 13



Reflection profile of track 14



Reflection profile of track 15



Reflection profile of track 16

APPENDIX C: CORE AND GRAB SAMPLE DATA



Eatons Neck - Locations for Core and Grab Samples

---

<u>Sample Number</u>	<u>Date</u>	<u>Latitude</u>	<u>Longitude</u>
1	11 Jul 74	41°02.75'	73°24.96'
2	11 Jul 74	41°02.48'	73°24.92'
3	11 Jul 74	41°02.27'	73°24.90'
4	11 Jul 74	41°02.30'	73°25.61'
5	11 Jul 74	41°02.03'	73°25.46'
6	11 Jul 74	41°01.85'	73°25.49'
7	11 Jul 74	41°01.40'	73°25.61'
8	22 Jul 74	41°00.92'	73°25.74'
9	22 Jul 74	41°00.62'	73°25.61'
10	22 Jul 74	41°01.14'	73°25.57'
11	22 Jul 74	41°00.82'	73°25.49'
12	22 Jul 74	41°02.64'	73°25.00'
13	23 Jul 74	41°00.61'	73°25.15'
14	23 Jul 74	41°00.44'	73°25.67'
15	23 Jul 74	40°59.32'	73°25.91'
16	23 Jul 74	40°58.51'	73°26.14'
17	23 Jul 74	40°57.85'	73°26.55'
18	23 Jul 74	40°57.40'	73°25.85'
19	23 Jul 74	40°58.12'	73°24.03'
20	23 Jul 74	40°58.08'	73°23.96'
21	23 Jul 74	40°58.83'	73°23.62'
22	23 Jul 74	40°59.75'	73°23.75'
23	23 Jul 74	40°00.50'	73°23.62'
24	23 Jul 74	41°00.87'	73°23.55'
25	29 Jul 74	41°01.22'	73°23.52'
26	29 Jul 74	41°02.07'	73°23.56'

---

(Continued)

<u>Sample Number</u>	<u>Date</u>	<u>Latitude</u>	<u>Longitude</u>
27	29 Jul 74	41°02.61'	73°23.42'
28	29 Jul 74	41°02.71'	73°23.36'
29	29 Jul 74	41°02.73'	73°23.26'
30	29 Jul 74	41°03.38'	73°23.23'
31	29 Jul 74	41°04.29'	73°20.85'
32	29 Jul 74	41°03.16'	73°20.89'
33	29 Jul 74	41°02.35'	73°21.00'
34	29 Jul 74	41°01.79'	73°20.84'
35	29 Jul 74	41°00.67'	73°20.98'
36	29 Jul 74	40°59.54'	73°20.97'
37	31 Jul 74	40°58.48'	73°21.05'
38	31 Jul 74	40°57.67'	73°20.74'
39	31 Jul 74	40°56.91'	73°27.40'
40	31 Jul 74	40°56.98'	73°27.74'
41	31 Jul 74	40°57.50'	73°27.81'
42	31 Jul 74	40°58.35'	73°27.66'
43	31 Jul 74	40°59.24'	73°27.61'
44	31 Jul 74	40°00.39'	73°27.62'
45	31 Jul 74	41°01.30'	73°27.73'
46	31 Jul 74	41°02.04'	73°27.60'
47	31 Jul 74	41°02.14'	73°27.67'
48		No Sample	
49	01 Aug 74	41°01.43'	73°29.53'
50	01 Aug 74	41°01.06'	73°29.48'
51	01 Aug 74	41°00.57'	73°29.56'
52	01 Aug 74	40°59.73'	73°29.57'
53	01 Aug 74	40°59.06'	73°29.44'
54	01 Aug 74	40°58.26'	73°29.52'

(Continued)

<u>Sample Number</u>	<u>Date</u>	<u>Latitude</u>	<u>Longitude</u>
55	01 Aug 74	40°57.64'	73°29.30'
56	01 Aug 74	40°55.93'	73°31.65'
57	01 Aug 74	40°56.84'	73°31.75'
58	01 Aug 74	40°58.75'	73°31.86'
59	01 Aug 74	40°59.68'	73°31.92'
60	01 Aug 74	41°00.16'	73°31.93'
61	11 Sep 74	41°00.87'	73°25.11'
62	11 Sep 74	41°00.91'	73°25.13'
63	12 Sep 74	41°00.68'	73°23.98'
64	12 Sep 74	41°00.30'	73°24.67'
65	11 Sep 74	41°00.83'	73°25.13'
66	12 Sep 74	41°00.14'	73°24.67'
67	11 Sep 74	41°01.71'	73°26.05'
68	12 Sep 74	41°00.45'	73°23.41'
69	12 Sep 74	41°00.46'	73°25.22'
70	12 Sep 74	41°00.31'	73°23.95'
71	12 Sep 74	41°00.71'	73°24.27'
72	12 Sep 74	41°01.11'	73°24.16'
73 } 80		No Samples	
81	13 Sep 74	41°00.47'	73°25.36'
82	13 Sep 74	41°00.25'	73°25.35'
83	13 Sep 74	40°59.40'	73°25.88'
84	13 Sep 74	40°59.89'	73°26.29'
85	13 Sep 74	41°00.07'	73°26.26'
86	13 Sep 74	40°59.67'	73°27.26'
87	13 Sep 74	40°59.26'	73°27.09'
88	13 Sep 74	40°59.01'	73°26.81'

(Continued)

(Concluded)

---

<u>Sample Number</u>	<u>Date</u>	<u>Latitude</u>	<u>Longitude</u>
89	13 Sep 74	41 <sup>0</sup> 00.30'	73 <sup>0</sup> 25.96'
90	25 Nov 74	41 <sup>0</sup> 00.39'	73 <sup>0</sup> 25.88'
91	25 Nov 74	41 <sup>0</sup> 00.21'	73 <sup>0</sup> 26.40'
92	25 Nov 74	41 <sup>0</sup> 00.05'	73 <sup>0</sup> 27.02'
93	25 Nov 74	40 <sup>0</sup> 59.74'	73 <sup>0</sup> 27.56'
94	25 Nov 74	41 <sup>0</sup> 00.24'	73 <sup>0</sup> 27.67'
95	25 Nov 74	41 <sup>0</sup> 00.37'	73 <sup>0</sup> 27.14'
96	25 Nov 74	41 <sup>0</sup> 00.72'	73 <sup>0</sup> 26.64'
97	25 Nov 74	41 <sup>0</sup> 00.83'	73 <sup>0</sup> 26.02'
98	25 Nov 74	41 <sup>0</sup> 01.06'	73 <sup>0</sup> 25.54'
99	27 Nov 74	40 <sup>0</sup> 59.77'	73 <sup>0</sup> 21.80'
100	27 Nov 74	40 <sup>0</sup> 59.52'	73 <sup>0</sup> 21.80'
101	27 Nov 74	40 <sup>0</sup> 59.77'	73 <sup>0</sup> 21.47'
102	27 Nov 74	41 <sup>0</sup> 00.02'	73 <sup>0</sup> 21.80'
103	27 Nov 74	40 <sup>0</sup> 59.77'	73 <sup>0</sup> 22.14'
104	27 Nov 74	41 <sup>0</sup> 01.14'	73 <sup>0</sup> 26.87'
105	27 Nov 74	41 <sup>0</sup> 00.81'	73 <sup>0</sup> 27.27'
106	27 Nov 74	41 <sup>0</sup> 00.46'	73 <sup>0</sup> 27.59'
107	27 Nov 74	41 <sup>0</sup> 01.39'	73 <sup>0</sup> 26.35'
108	27 Nov 74	41 <sup>0</sup> 01.51'	73 <sup>0</sup> 25.70'

---

SUMMARY OF LABORATORY TEST RESULTS											FILE NO 3515	
LONG ISLAND SOUND CORE SAMPLES TESTING											SHEET 1 OF 1	
EATON'S NECK POINT												
BORING & SAMPLE NUMBER	DESCRIPTION	DEPTH (FEET)	TEST NO	NATURAL WATER CONTENT %	ATTERBERG LIMITS %		UNIT WEIGHT LB/CU FT	UNCONFINED TEST		CONSOLIDATION		OTHER TESTS
					LL	PL		COMPRESSIVE STRENGTH PSF	STRAIN %	MAX PAST PRESSURE TON/SQ FT	C <sub>c</sub>	
16	Dark gray silty fine SAND, trace coarse to medium sand		SG-1									SG = 2.67
18	Dark gray medium to fine sandy SILT (trace shells)		SG-2									SG = 2.64
51	Dark gray gravelly coarse to fine SAND, trace silt		SG-3									SG = 2.62
54	Dark gray silty medium to fine SAND, little clay		SG-4									SG = 2.68
8	Dark gray SILT, little fine gravel, trace clay (trace shells)					134.0	43.3					
17	Dark gray fine sandy SILT (trace shells)					99.0	35.2					
25	Dark gray SILT, little fine sand (trace shells)					106.0	36.7					
45	Dark gray fine sandy SILT, trace clay (trace shells)					97.5	34.6					

Data sheet of summary of laboratory test results on core samples from Eatons Neck

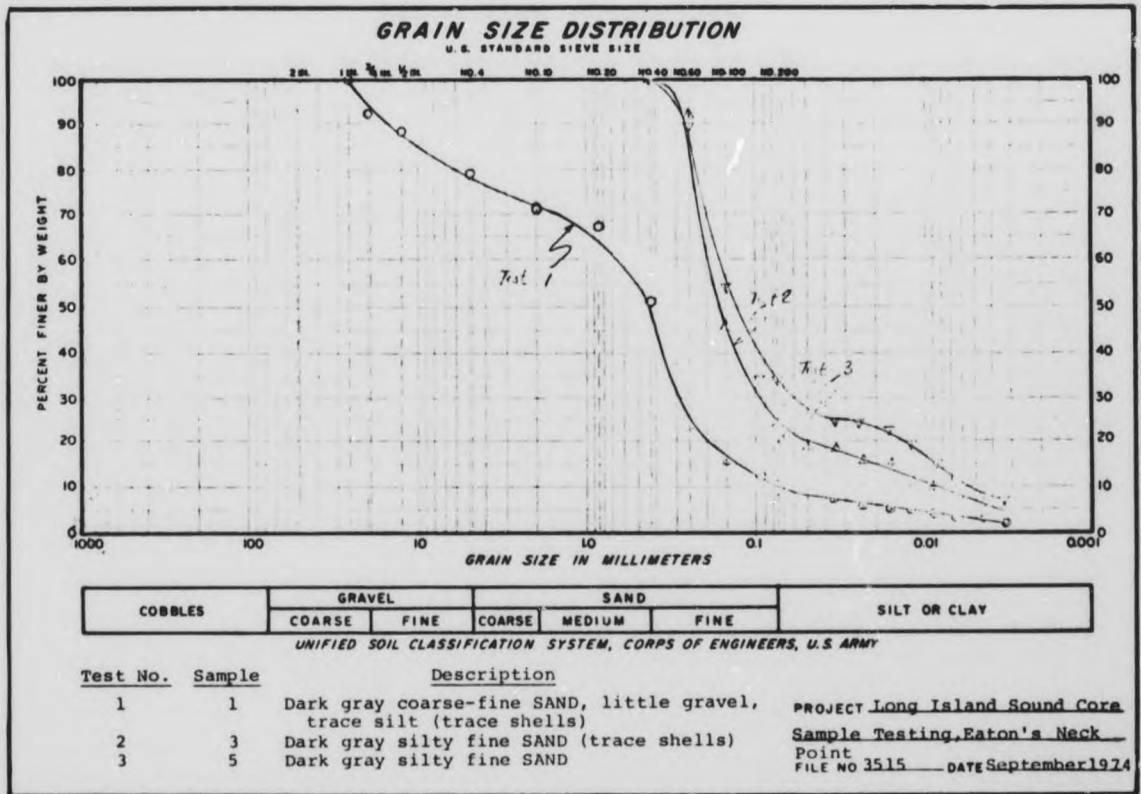
(Continued)

**SUMMARY OF LABORATORY TEST RESULTS**  
**LONG ISLAND SOUND CORE SAMPLES TESTING**  
**EATON'S NECK POINT**

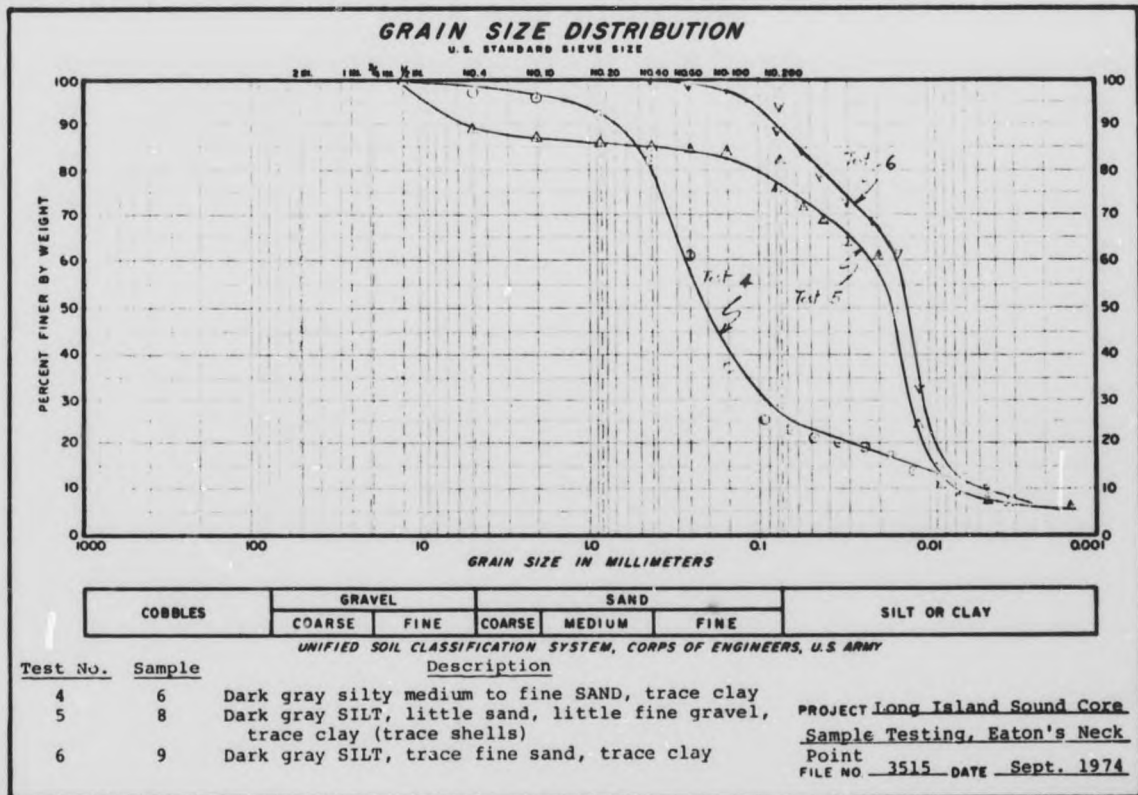
FILE NO 3515  
 SHEET 2 OF 2

BORING & SAMPLE NUMBER	DESCRIPTION	DEPTH (FEET)	TEST NO.	NATURAL WATER CONTENT %	ATTERBERG LIMITS		UNIT WEIGHT LB/CU FT	UNCONFINED TEST		CONSOLIDATION		OTHER TESTS
					LL	PL		COMPRESSIVE STRENGTH PSF	STRAIN %	MAX. PAST PRESSURE TON/SQ. FT.	C <sub>c</sub>	
90	Dark gray clayey medium to fine SAND, little silt (trace shells)				37.0	18.7						
93	Dark gray clayey SILT little sand (trace shells)				57.5	26.5						
99	Dark gray organic SILT, little clay, little fine sand				135.0	44.6						
107	Dark gray silty fine SAND, trace to little clay (trace shells)				49.2	21.4						

(Concluded)

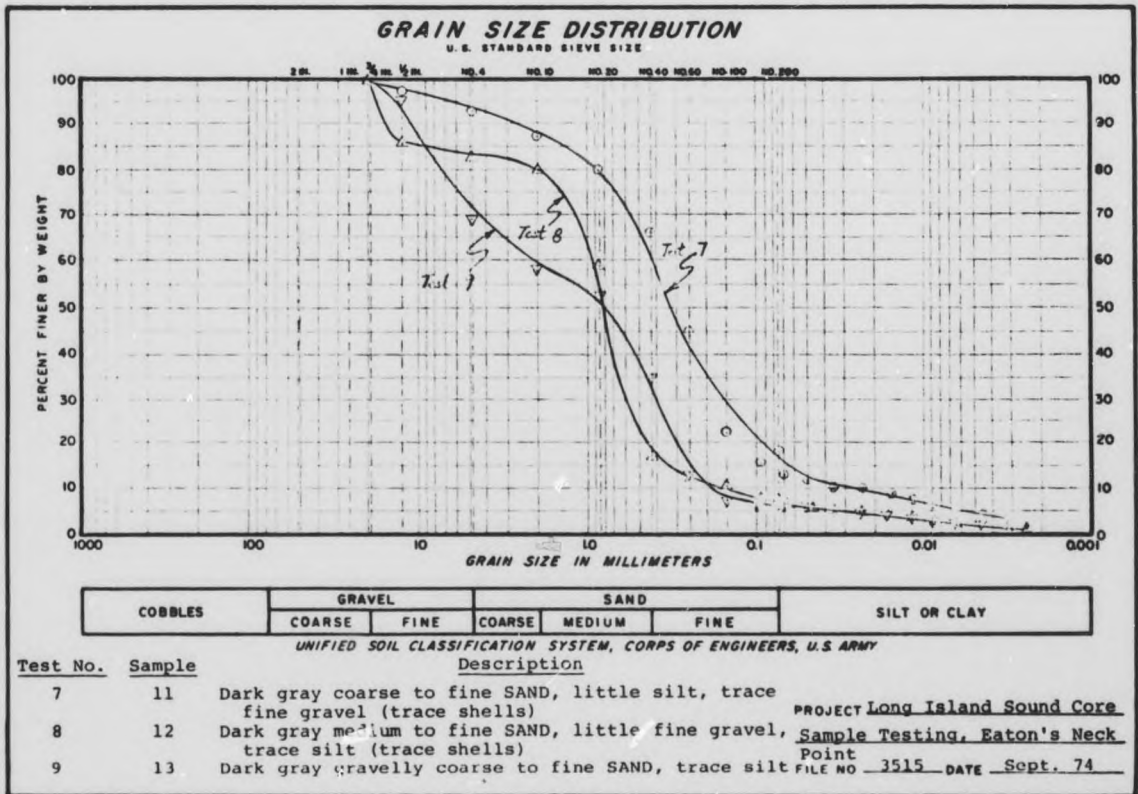


Data sheet of grain-size distribution analysis on core samples from Eatons Neck: tests 1, 2, and 3

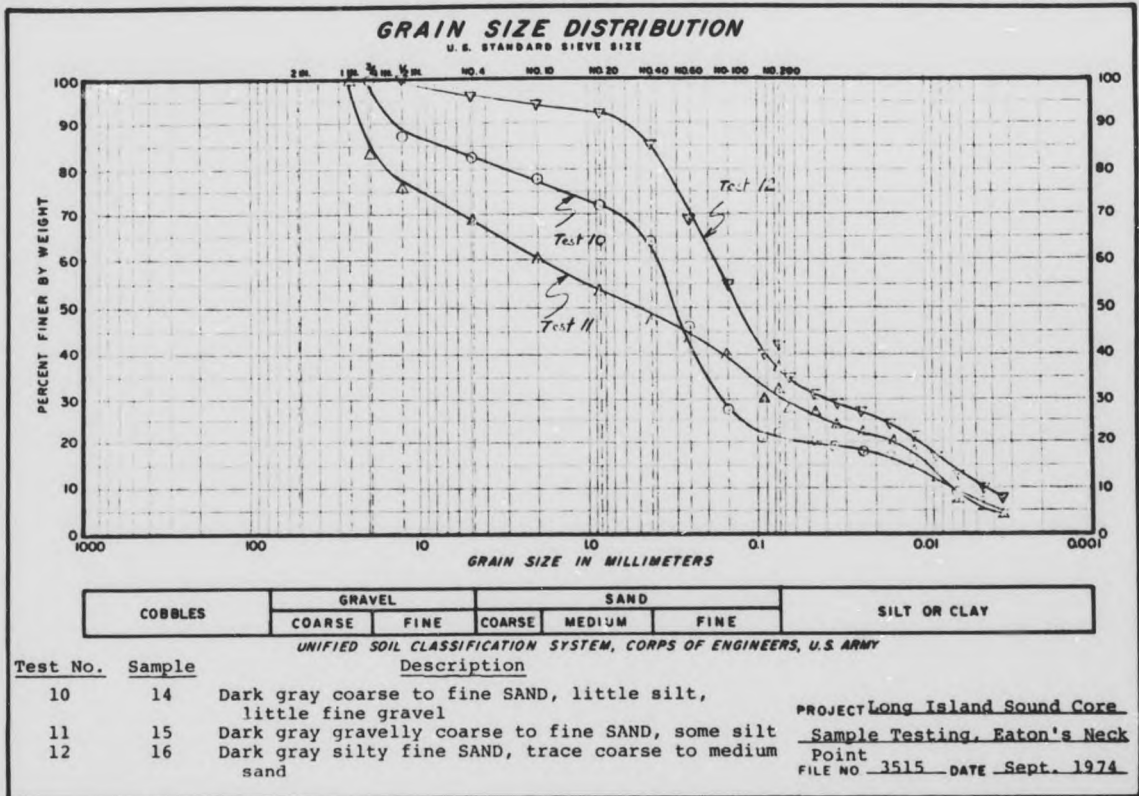


Data sheet of grain-size distribution analysis on core samples from Eatons Neck: tests 4, 5, and 6

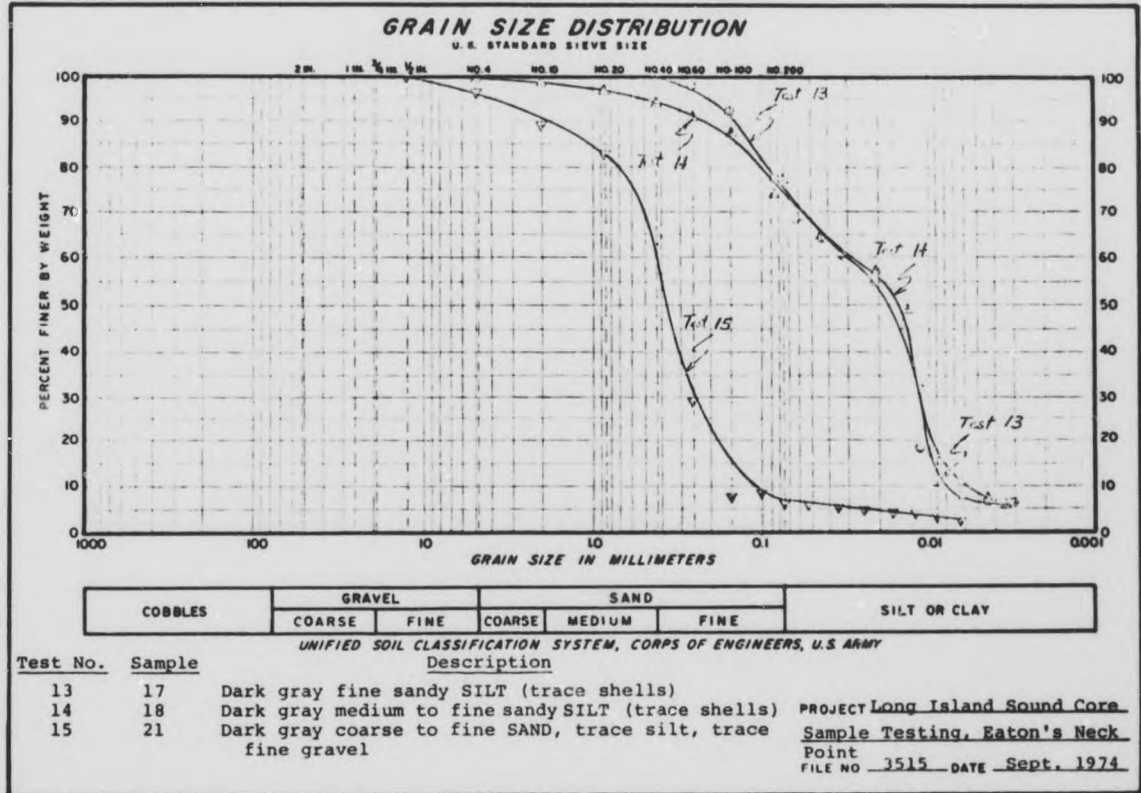




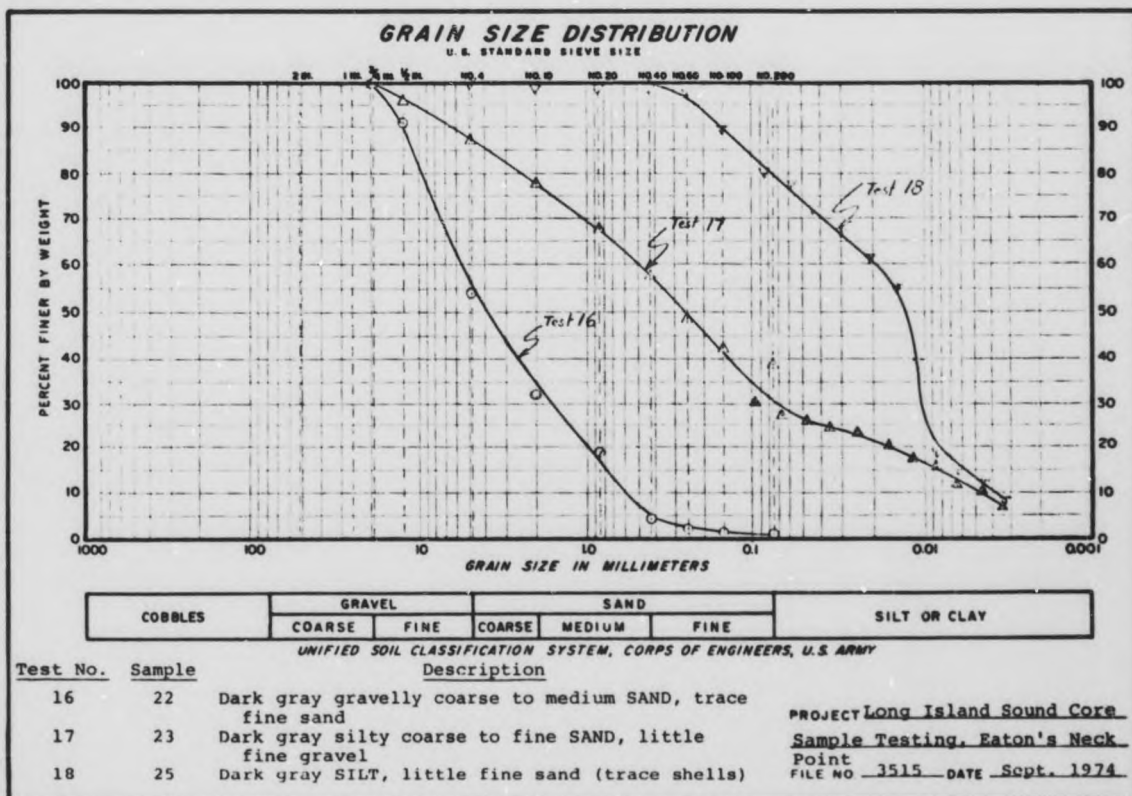
Data sheet of grain-size distribution analysis on core samples from Eatons Neck: tests 7, 8, and 9



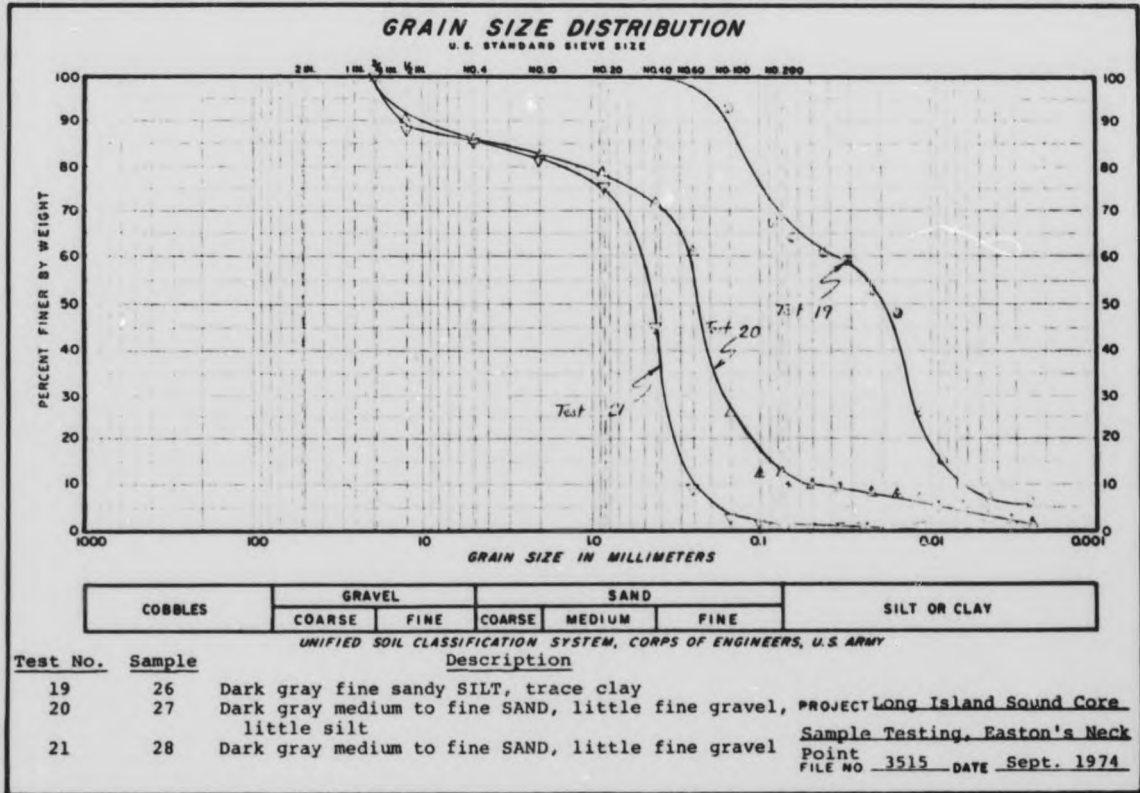
Data sheet of grain-size distribution analysis on core samples from Eatons Neck: tests 10, 11, and 12



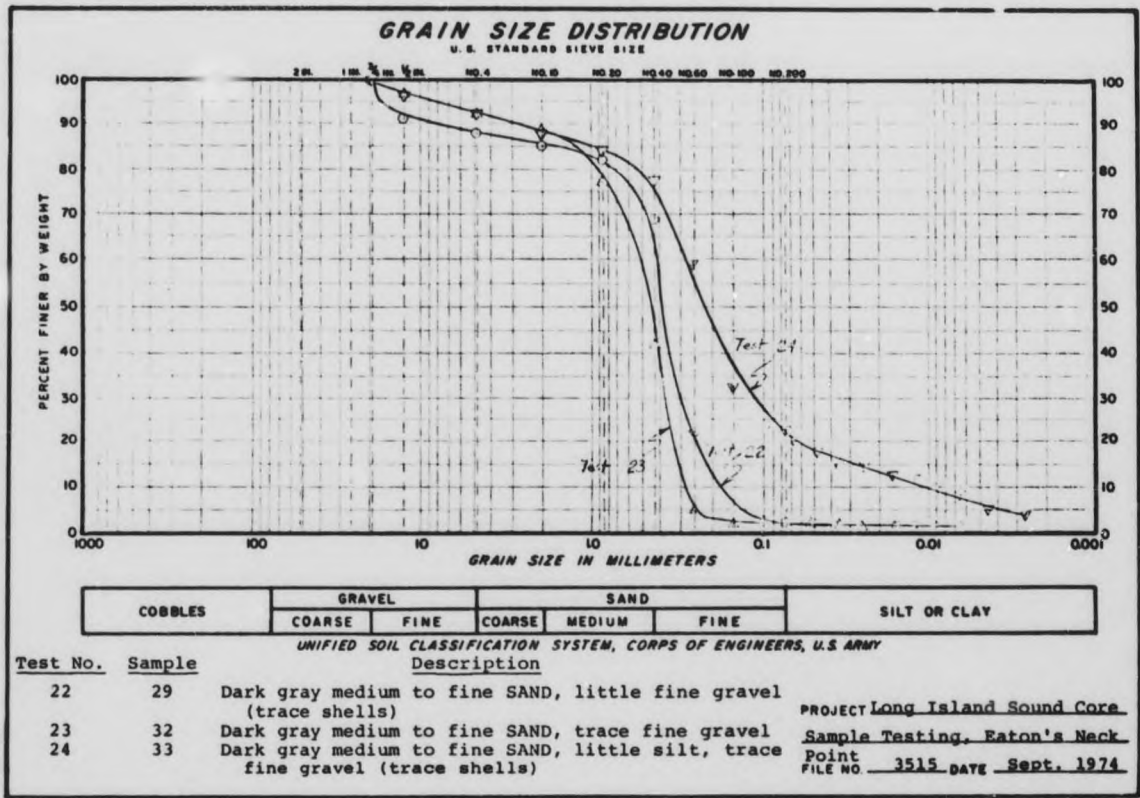
Data sheet of grain-size distribution analysis on core samples from Eatons Neck: tests 13, 14, and 15



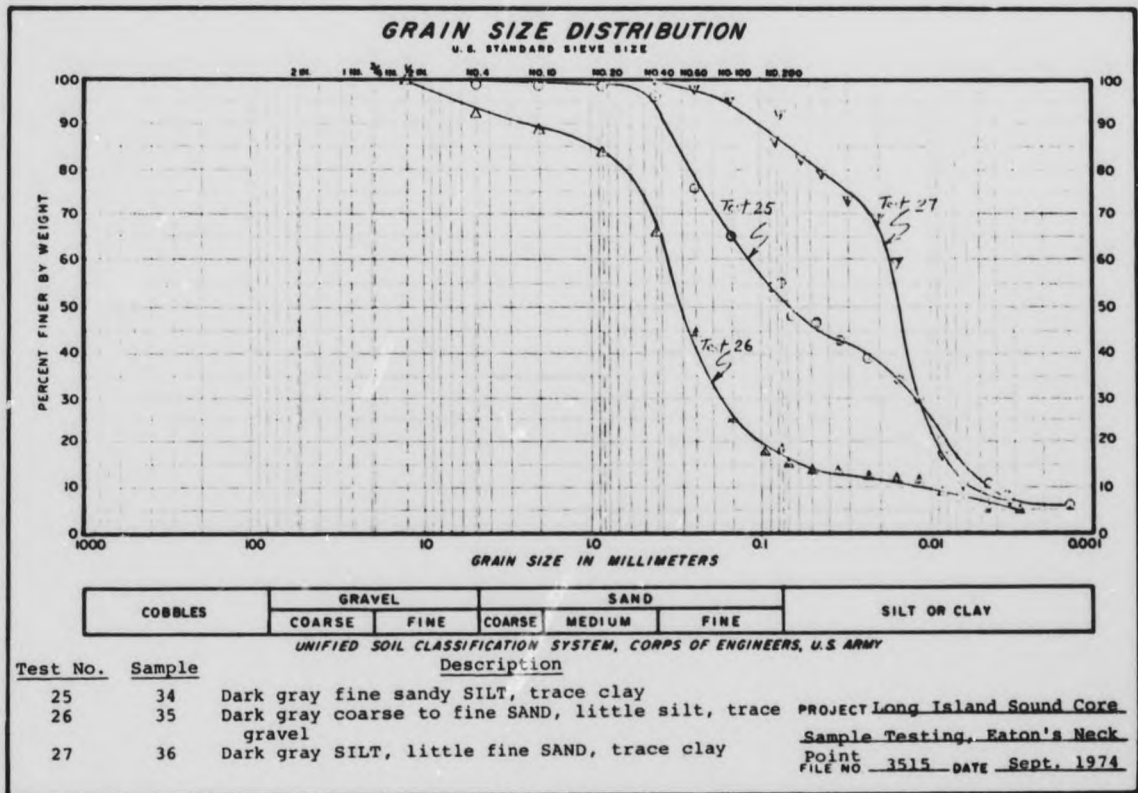
Data sheet of grain-size distribution analysis on core samples from Eatons Neck: tests 16, 17, and 18



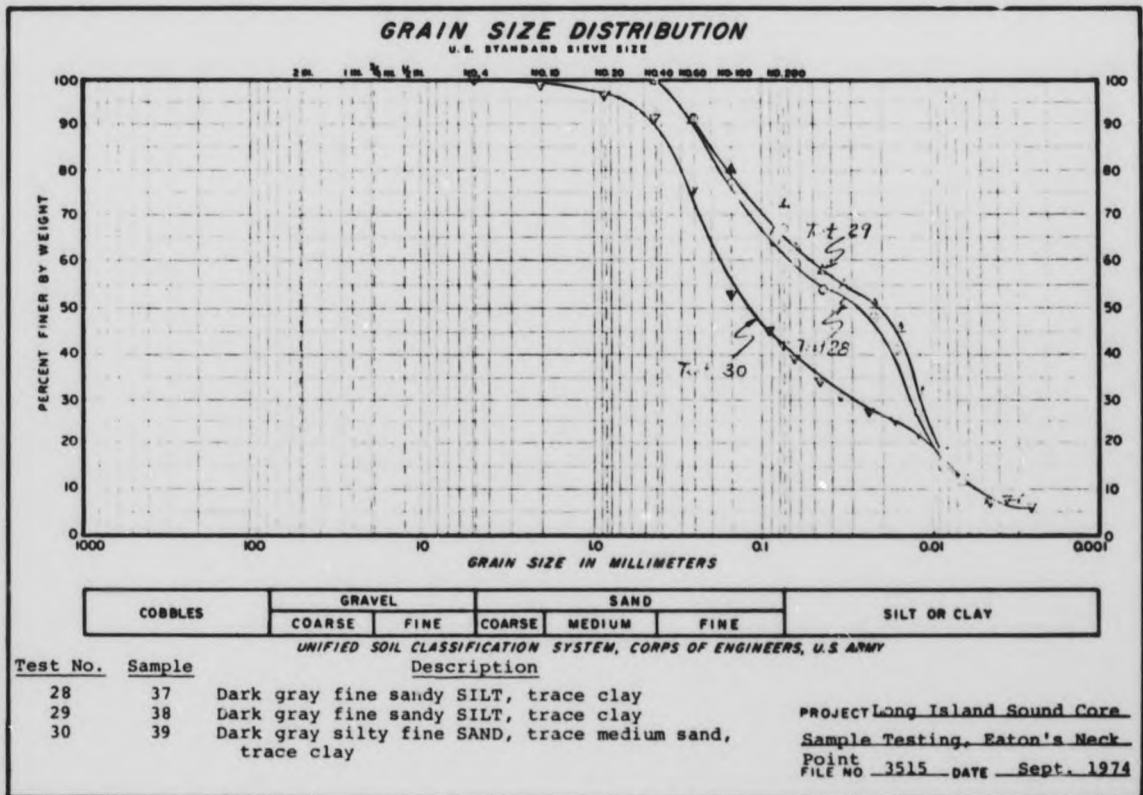
Data sheet of grain-size distribution analysis on core samples from Eatons Neck: tests 19, 20, and 21



Data sheet of grain-size distribution analysis on core samples from Eatons Neck: tests 22, 23, and 24

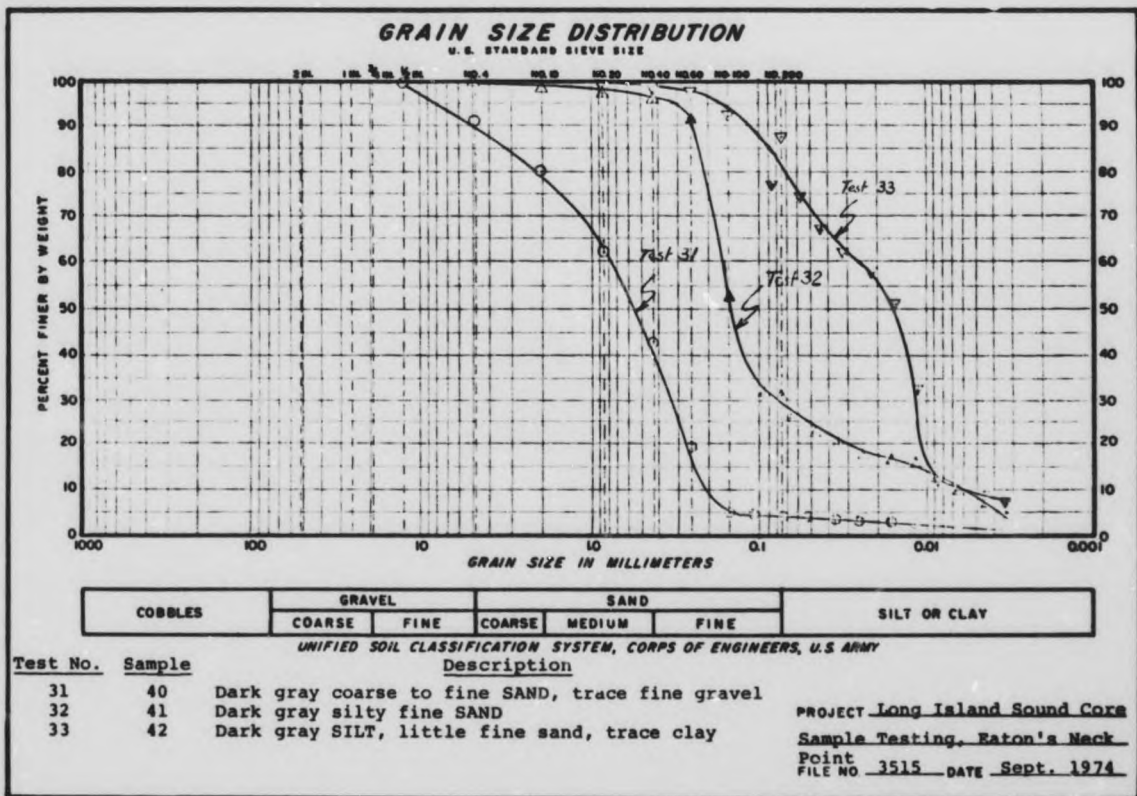


Data sheet of grain-size distribution analysis on core samples from Eatons Neck: tests 25, 26, and 27

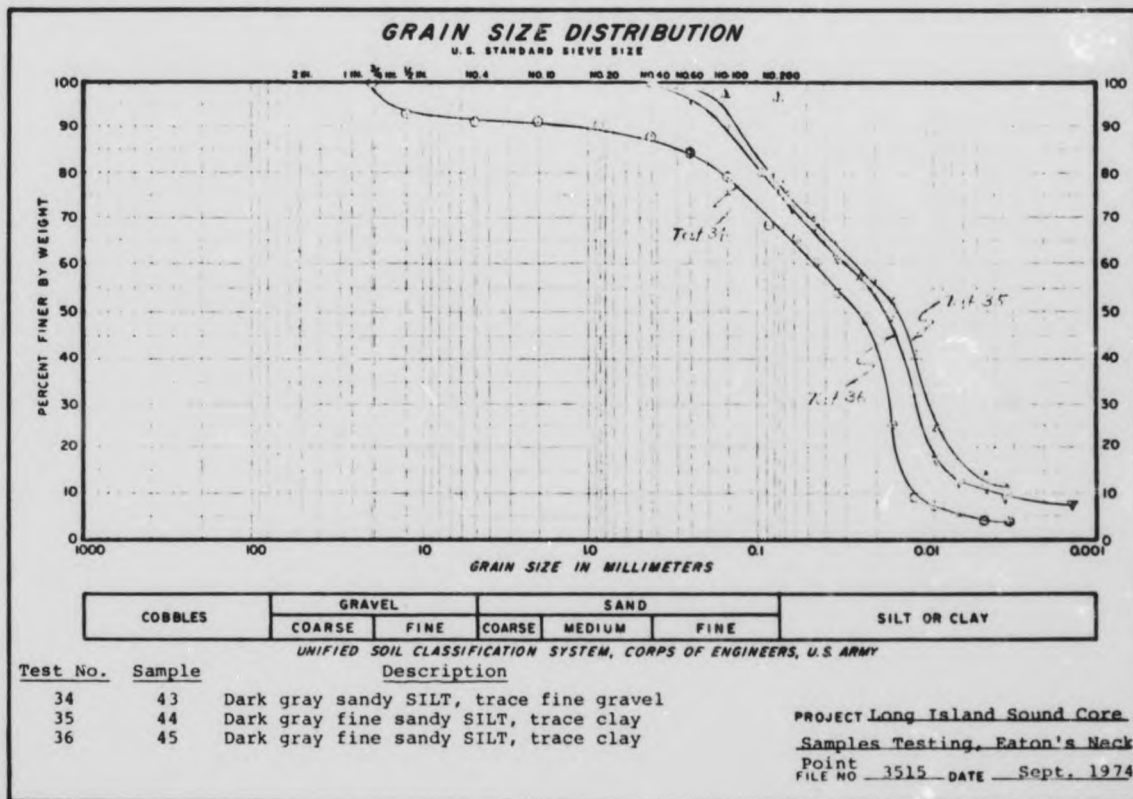


Data sheet of grain-size distribution analysis on core samples from Eaton's Neck: tests 28, 29, and 30

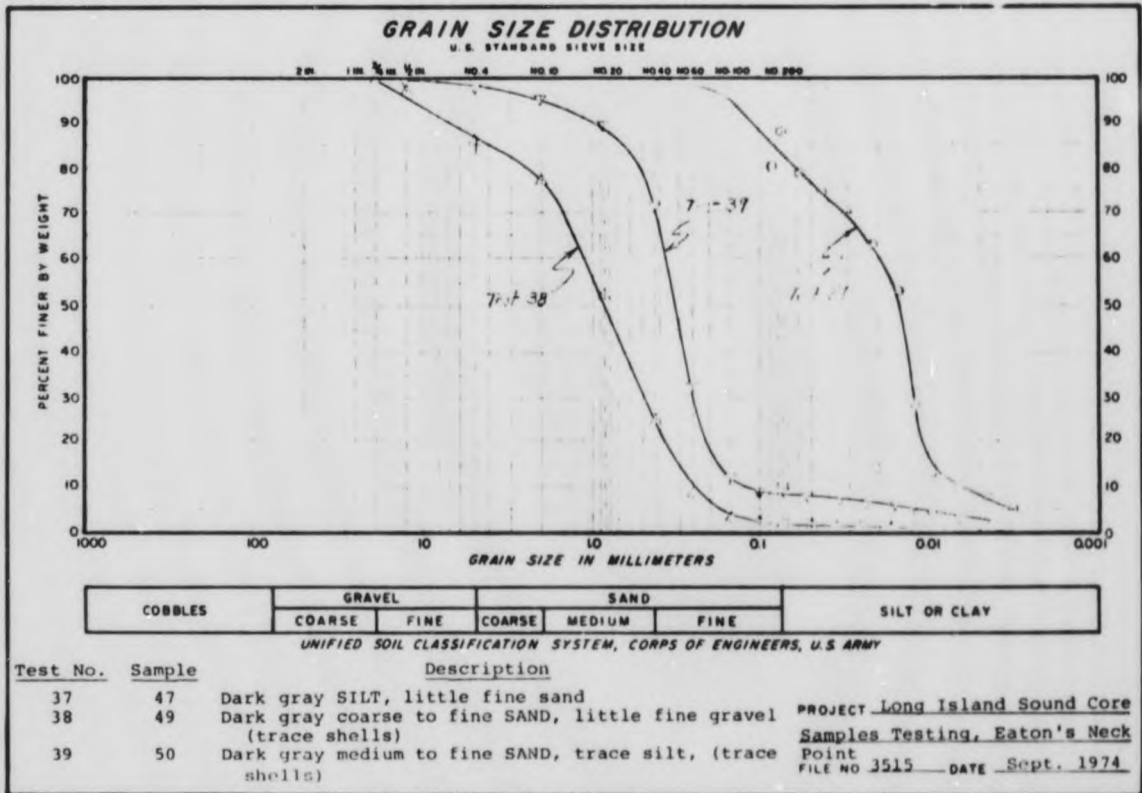




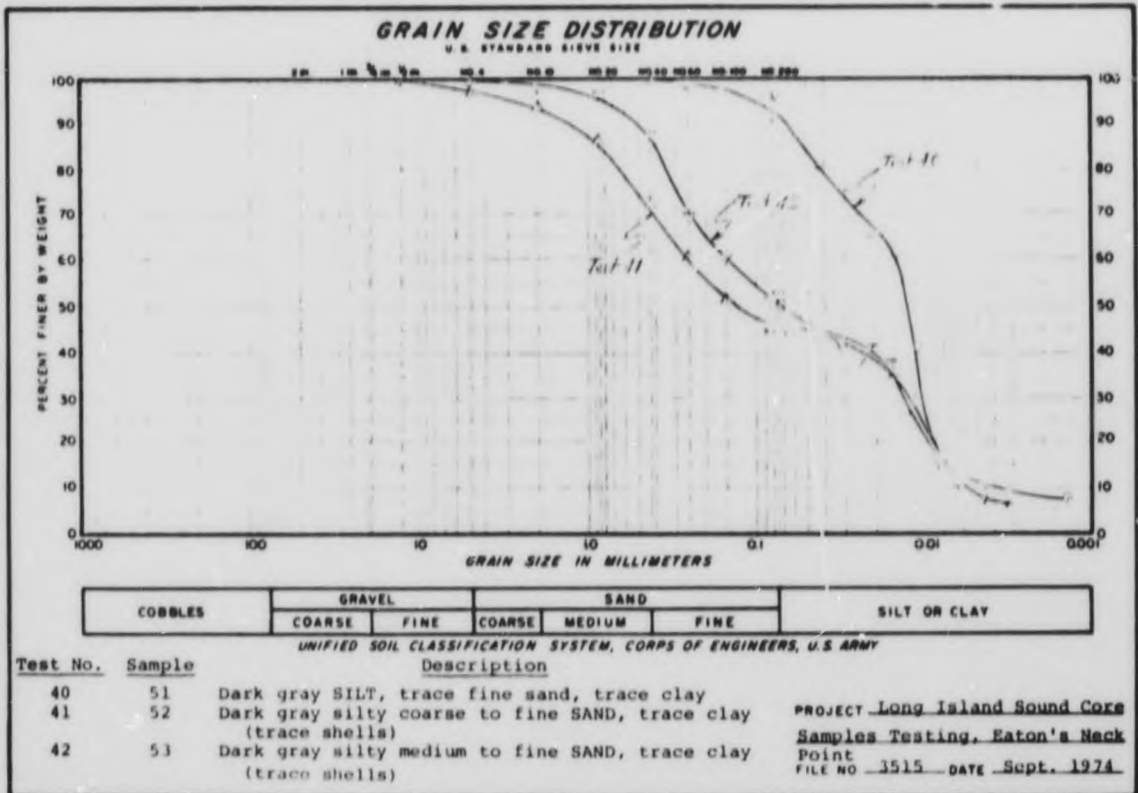
Data sheet of grain-size distribution analysis on core samples from Eatons Neck: tests 31, 32, and 33



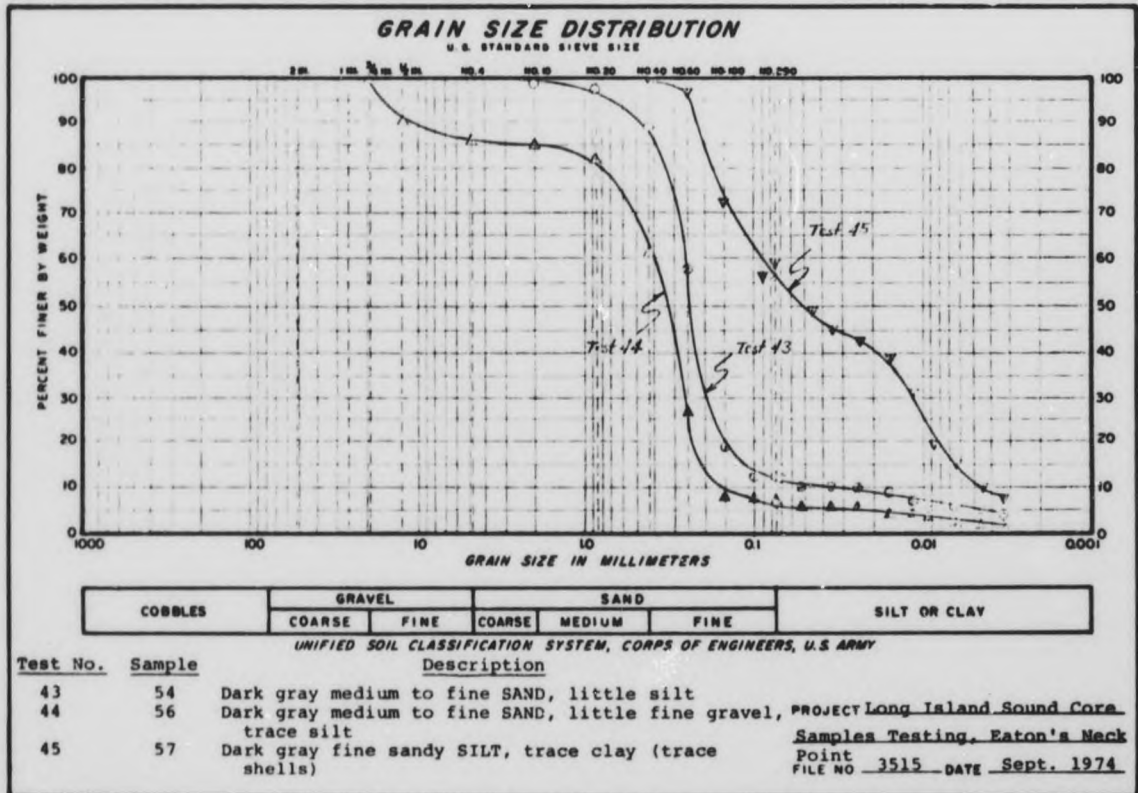
Data sheet of grain-size distribution analysis on core samples from Eaton's Neck: tests 34, 35, and 36



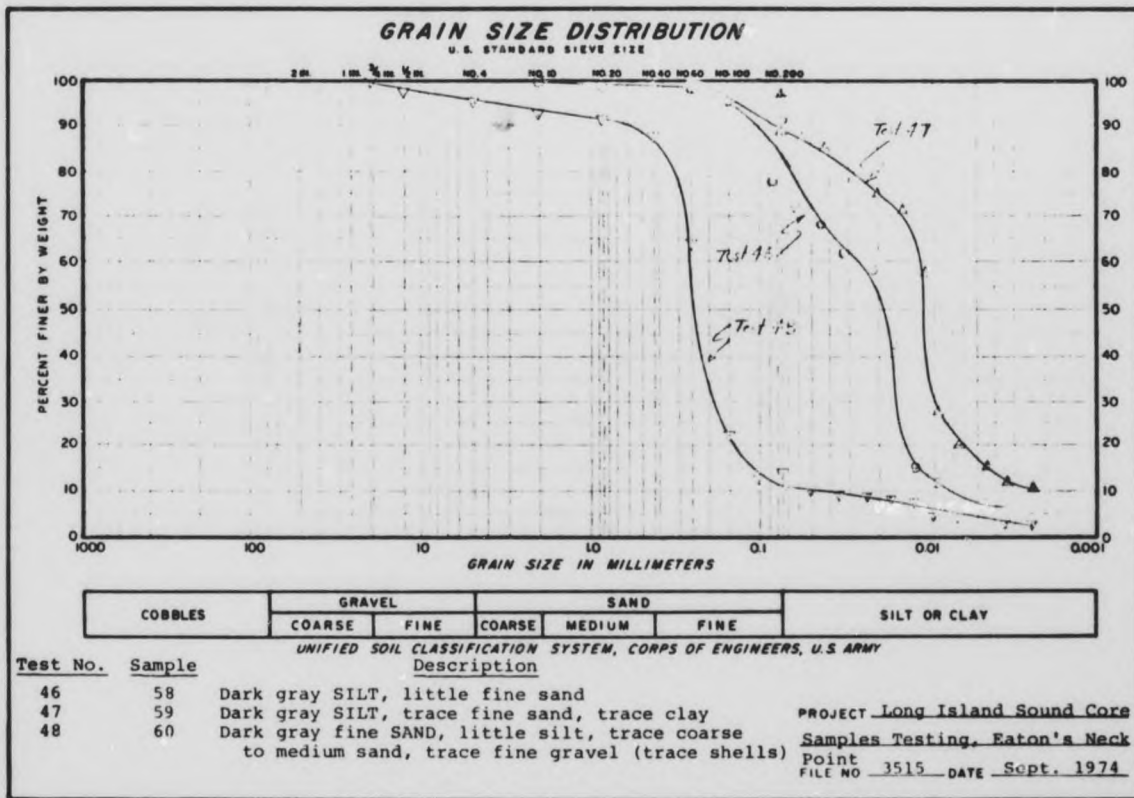
Data sheet of grain-size distribution analysis on core samples from Eatons Neck: tests 37, 38, and 39



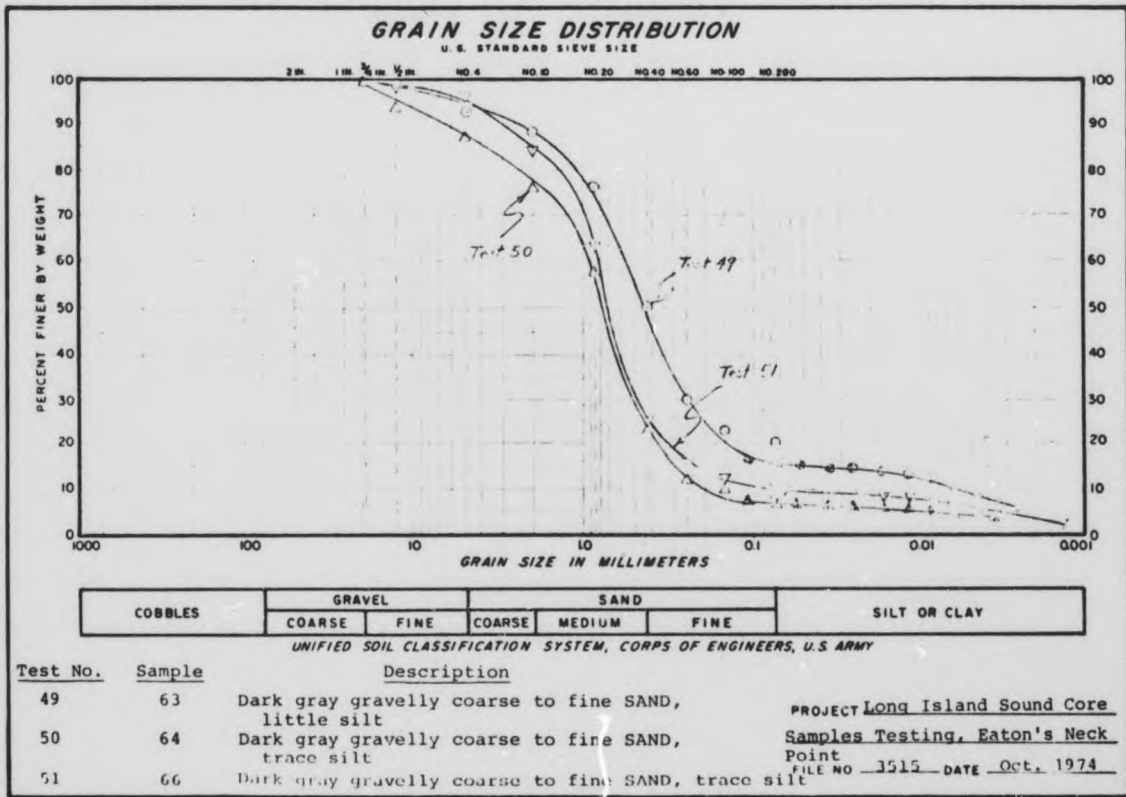
Data sheet of grain-size distribution analysis on core samples from Eatons Neck: tests 40, 41, and 42



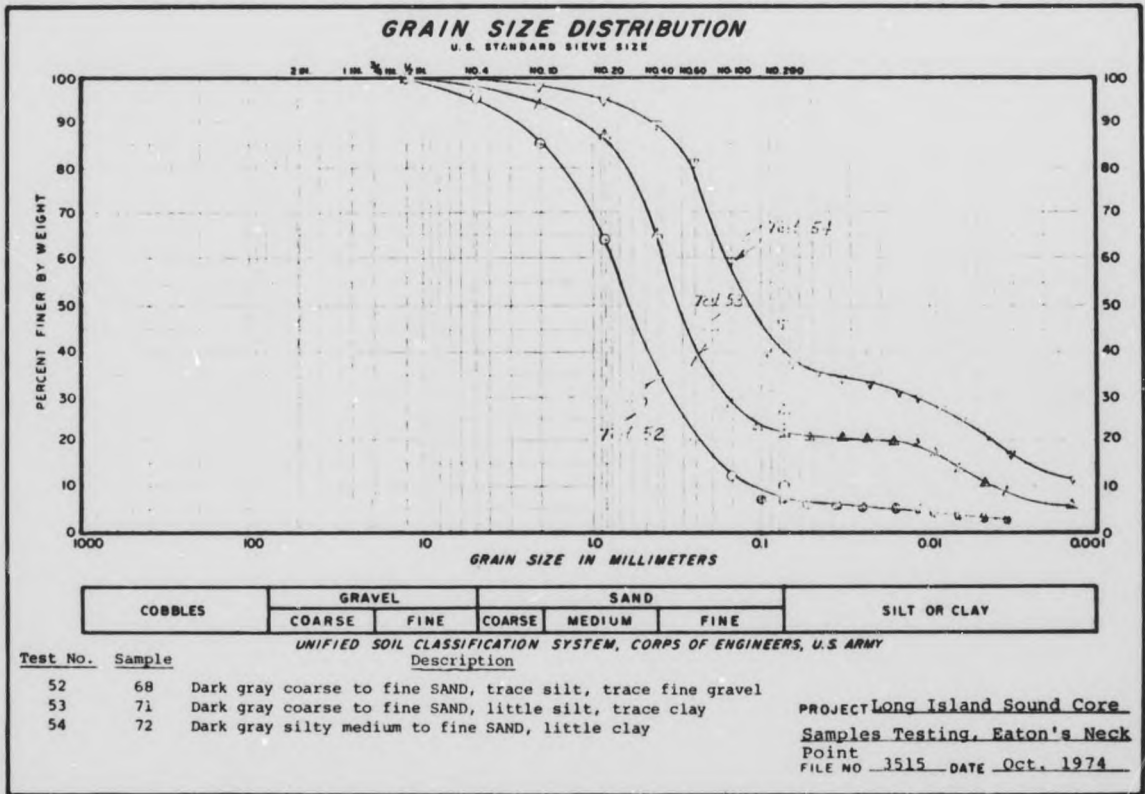
Data sheet of grain-size distribution analysis on core samples from Eatons Neck: tests 43, 44, and 45



Data sheet of grain size distribution analysis on core samples from Eatons Neck: tests 46, 47, and 48

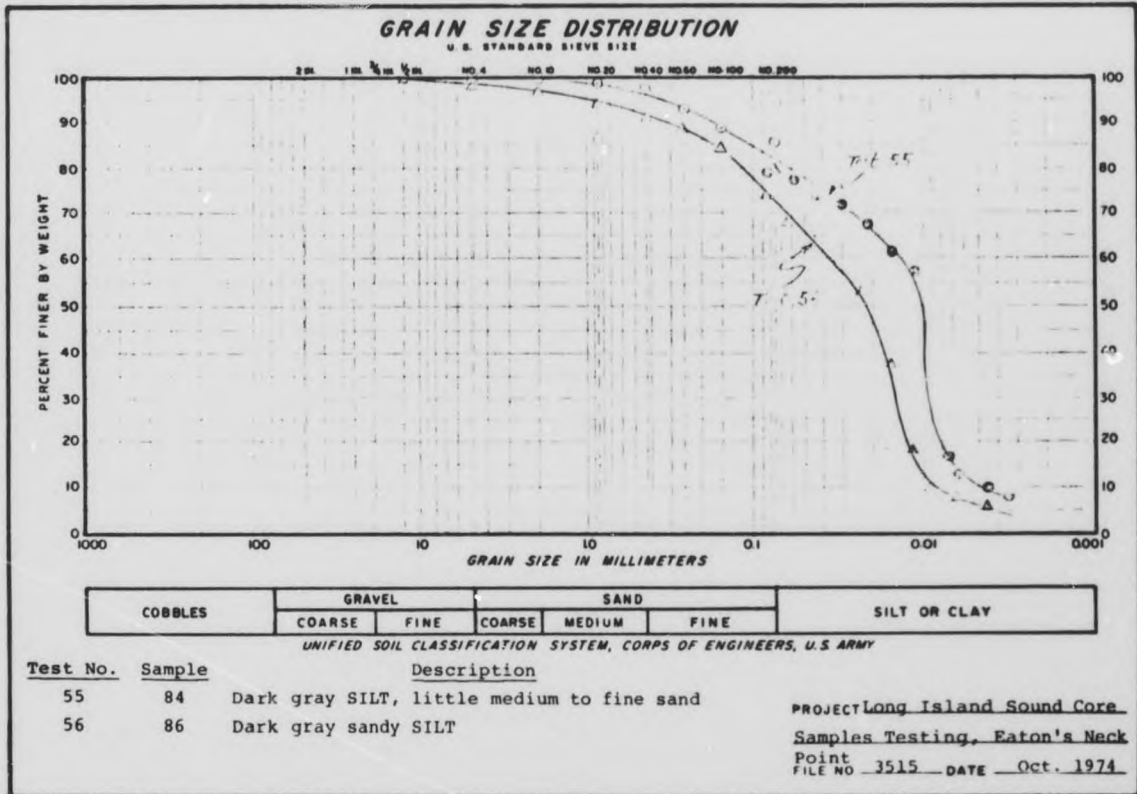


Data sheet of grain-size distribution analysis on core samples from Eatons Neck: tests 49, 50, and 51

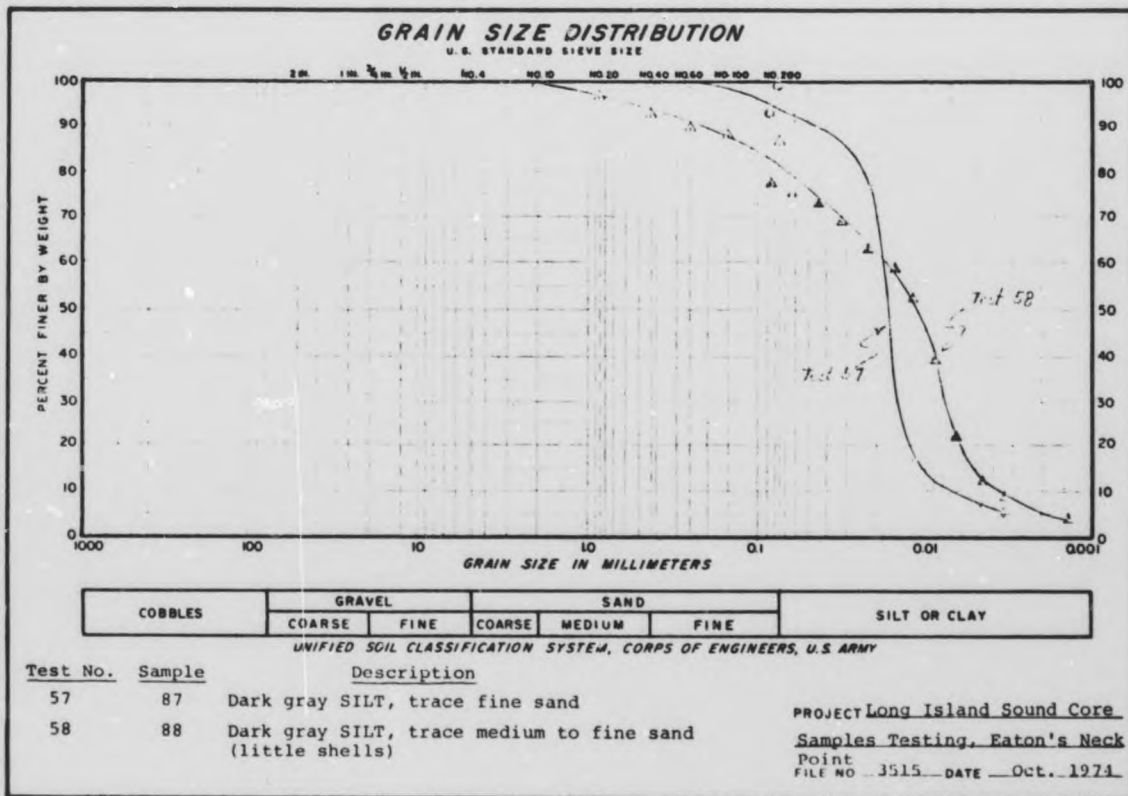


Data sheet of grain-size distribution analysis on core samples from Eatons Neck: tests 52, 53, and 54

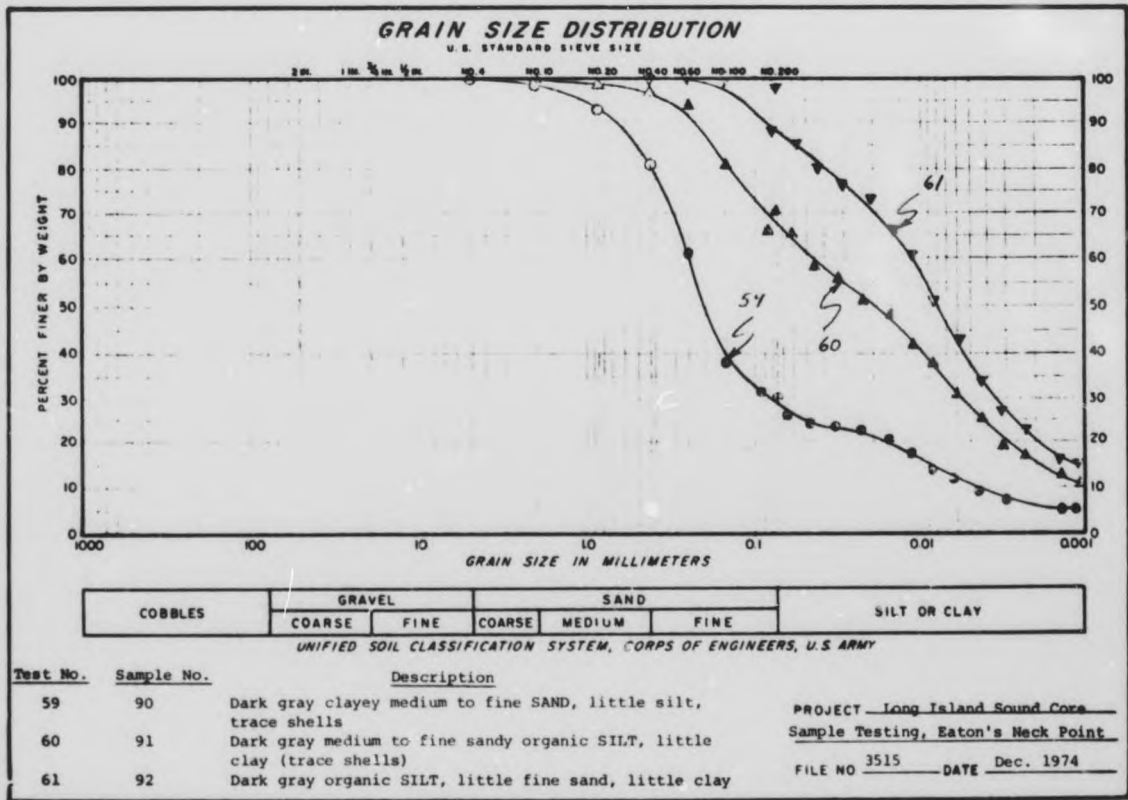




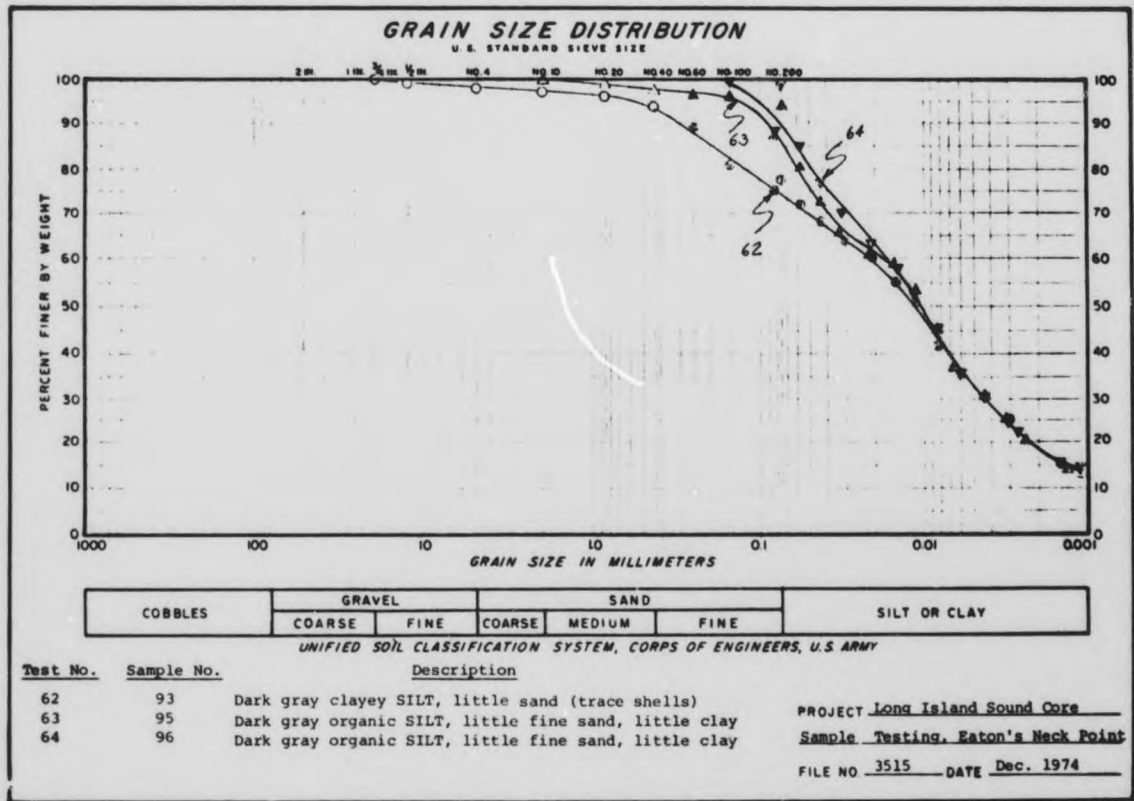
Data sheet of grain-size distribution analysis on core samples from Eaton's Neck: tests 55 and 56



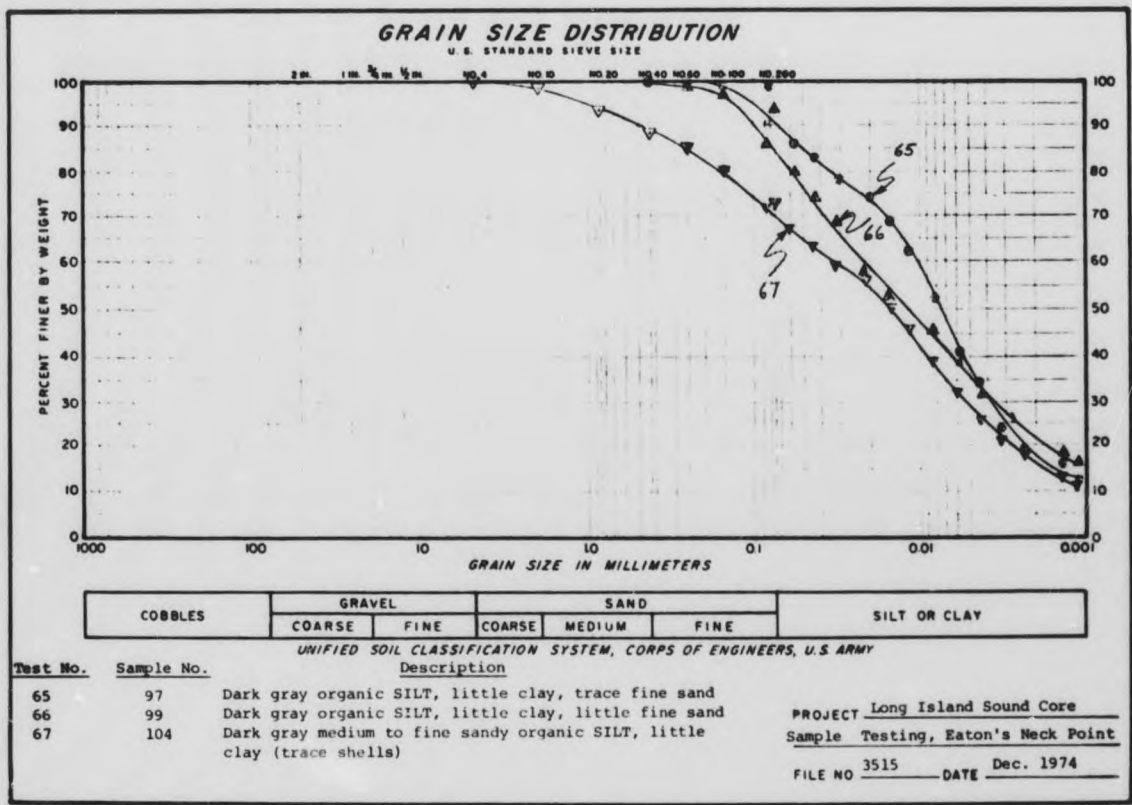
Data sheet of grain-size distribution analysis on core samples from Eatons Neck: tests 57 and 58



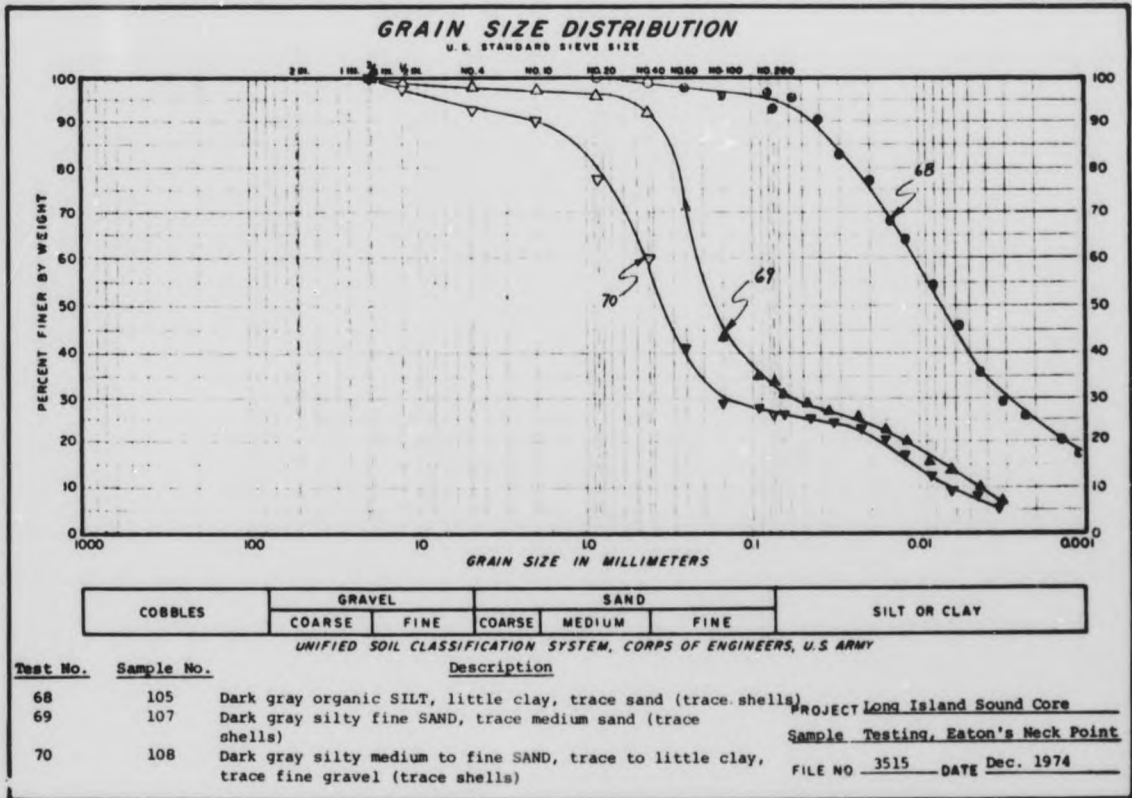
Data sheet of grain-size distribution analysis on core samples from Eatons Neck: tests 59, 60, and 61



Data sheet of grain-size distribution analysis on core samples from Eatons Neck: tests 62, 63, and 64



Data sheet of grain-size distribution analysis on core samples from Eaton's Neck: tests 65, 66, and 67



Data sheet of grain-size distribution analysis on core samples from Eatons Neck: tests 68, 69, and 70

APPENDIX D: PROFILE CAMERA PHOTOS



Photo D1. Interface photo taken at EN-S on 24 Mar 75 (see Figure 4 for location)





Photo D2. Interface photo taken at EN-N on 25 Mar 75 (see Figure 5 for location)



Photo D3. Interface photo taken at EN-N on 25 Mar 75 (see Figure 5 for location)



Photo D4. Interface photo taken at EN-S on 24 Mar 75; note similarity to D5, D6, and D7 (see Figure 4 for location)



Photo D5. Interface photo taken at EN-S on 24 Mar 75 (see Figure 4 for location)



Photo D6. Interface photo taken at EN-S on 24 Mar 75 (see Figure 4 for location)



Photo D7. Interface photo taken at EN-S 24 Mar 75 (see Figure 4 for location)



Photo D8. Interface photo taken at EN-N on 25 Mar 75 (see Figure 5 for location)



Photo D9. Interface photo taken at EN-S on 24 Mar 75 (see Figure 4 for location)



APPENDIX E: BOTTOM PHOTOS



Photo E1. Pebbles and coarse sand characteristic of a glacial lag deposit

E1



Photo E2. Material bound together by algae

E2

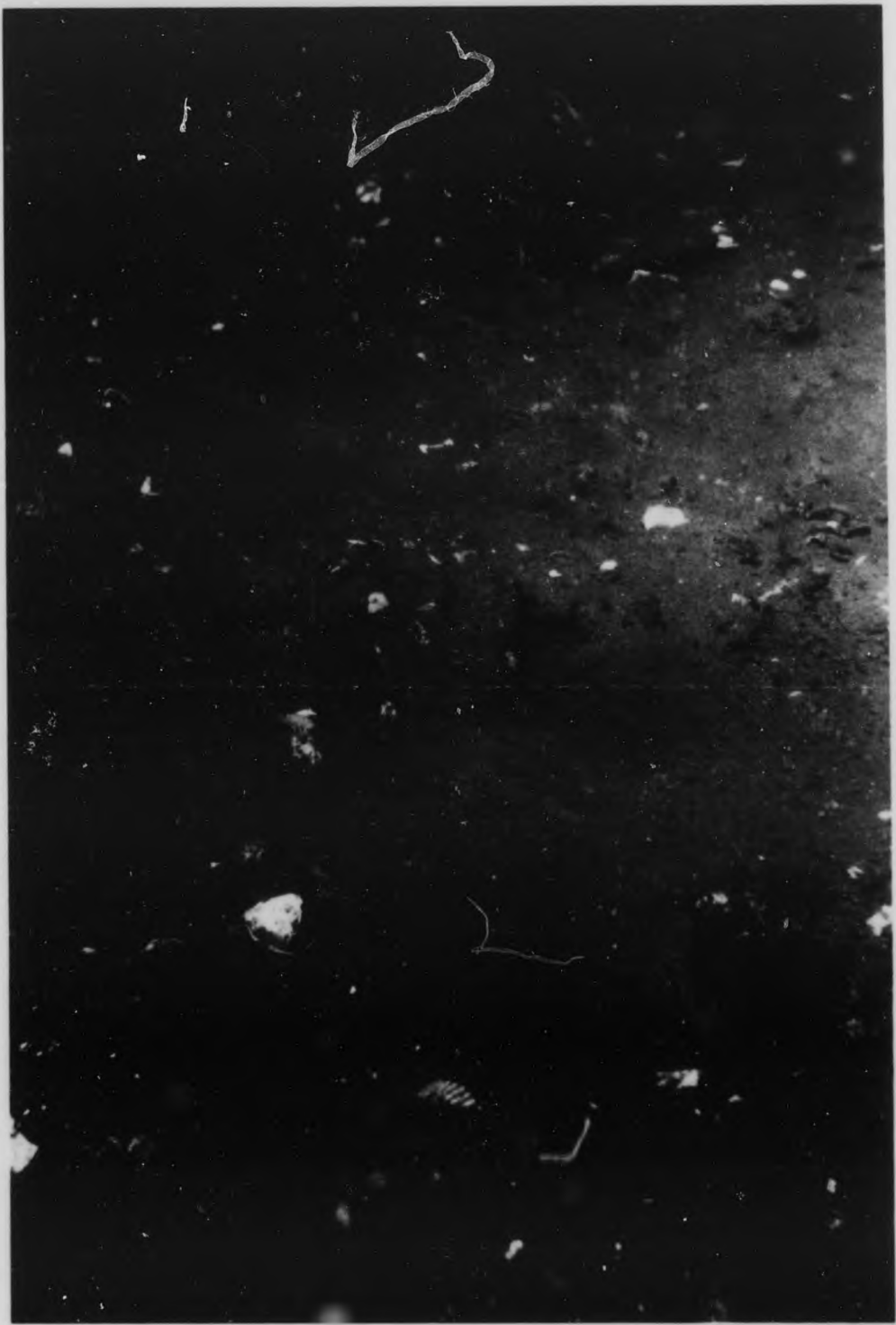


Photo E3. Diver photo showing top of mound of disposed material with evidence of deposit-feeding benthic organisms

E3



Photo E4. Diver photo showing closer look at sediment

E4



Photo E5. Diver photo showing hydroid



Photo E6. Diver photo showing sponges, hydroids, and polychaete tubes



Photo E7. Diver photo showing a sponge

E7





Photo E8. Diver photo showing cup corals

E8



Photo E9. Diver photo showing cup coral

E9

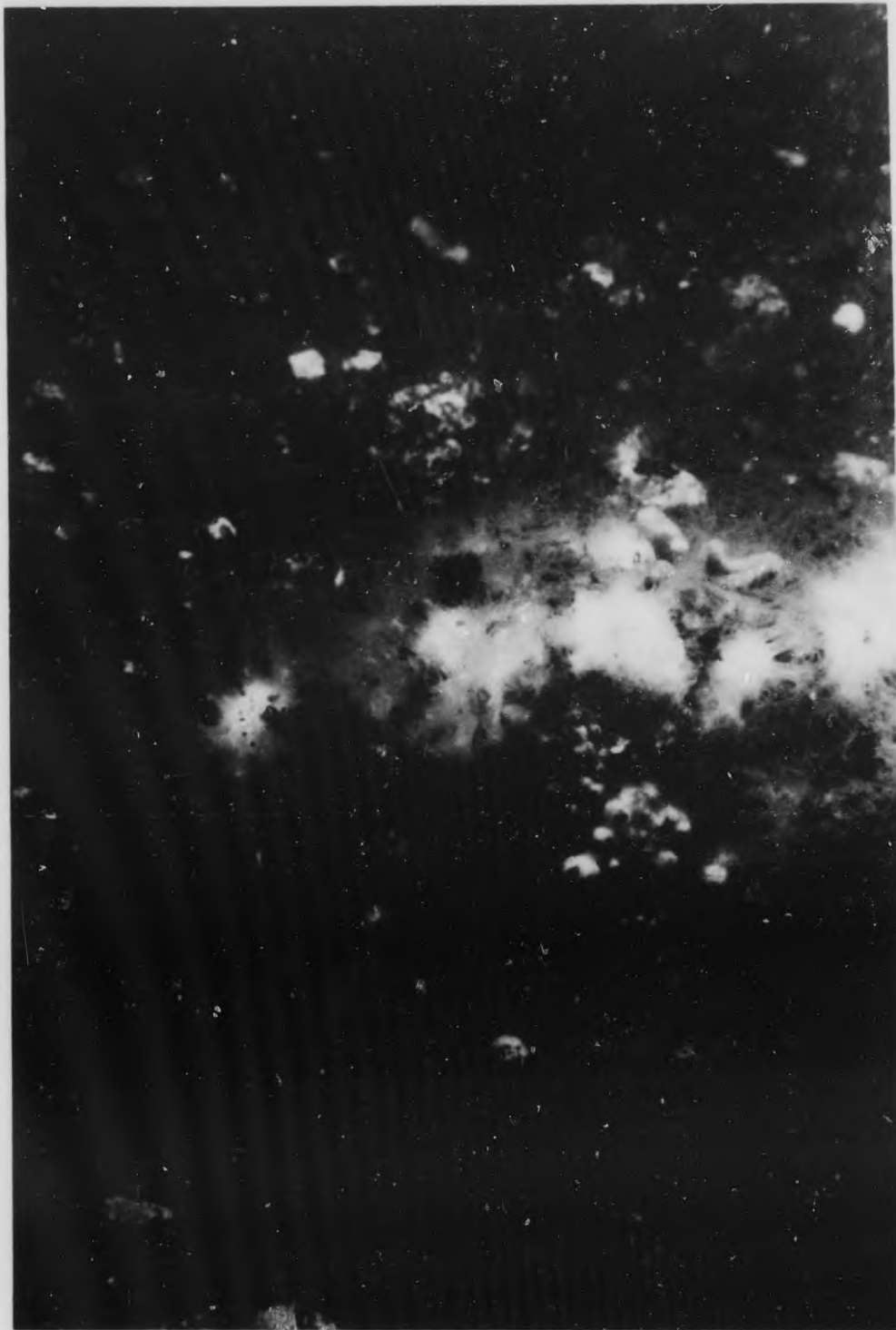


Photo E10. Diver photo showing cup coral with polyps extended

E10

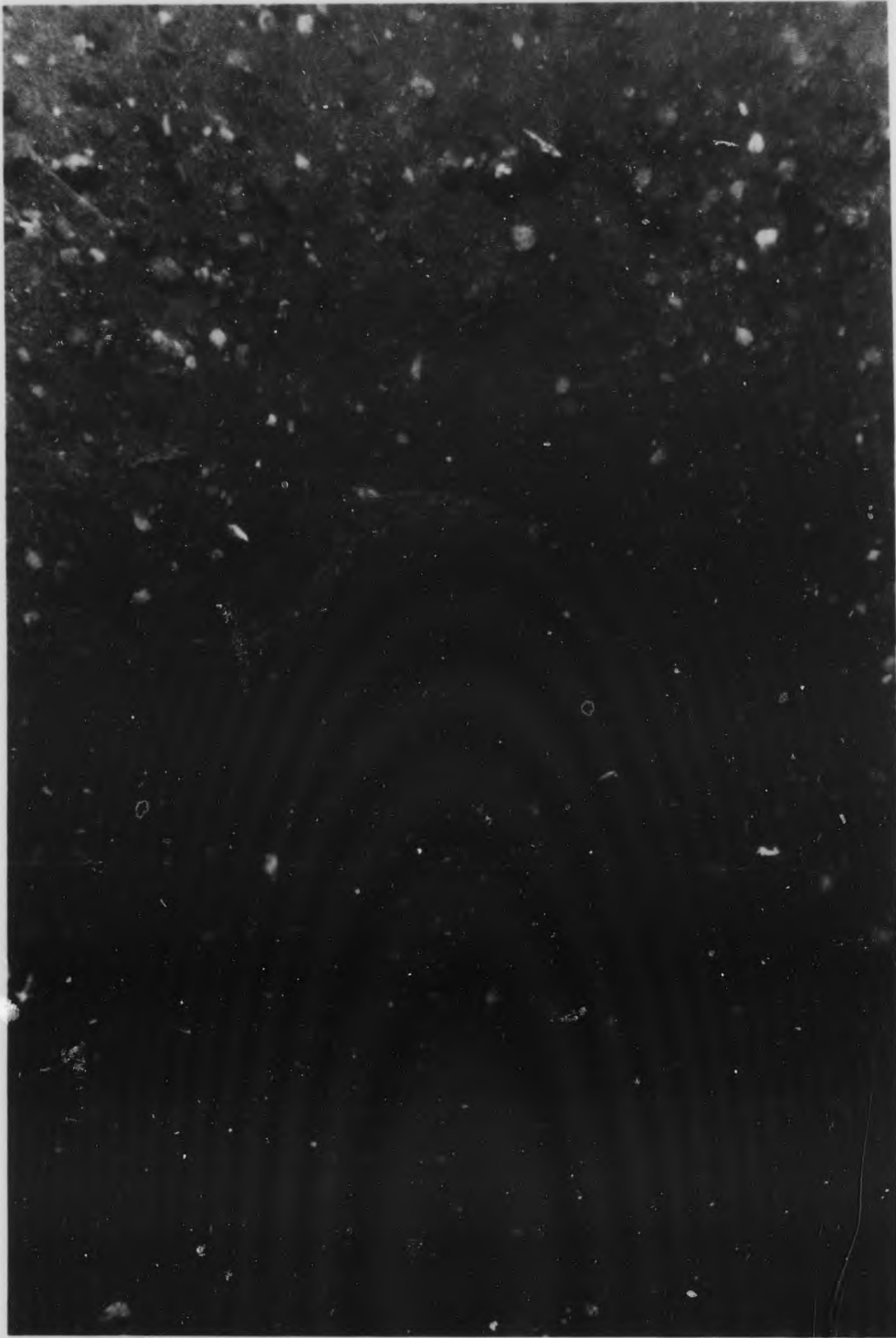


Photo E11. Diver photo of a demersal fish

E11



Photo E12. Diver photo showing starfish

E12



UNSPETCHED  
18 JUN 1978  
ENGINEERING  
DIVISION